Republic of Iraq
Ministry of Higher Education and Scientific Research
University of Misan/Collage of Engineering
Department of Civil Engineering

SHEAR STRENGTH OF REINFORCED CONCRETE DEEP BEAM USING RECYCLED BRICK AS COARSE AGGREGATE

Prepared By

Shams Al-Duha Dakhil Khalaf

B.Sc. civil engineering, 2016

A thesis submitted in partial fulfillment of the requirements for the Master of Science degree in Civil Engineering

The University of Misan

2024

Thesis Supervisor: Asst. Prof. Dr. Samir Mohammed Chassib

﴿ وَلَقَدْ آتَيْنَا دَاوُودَ وَسُلَيْمَانَ عِلْمًا ۖ وَقَالَا الْحَمْدُ لِلَّهِ الَّذِي فَضَّلَنَا عَلَىٰ كَثِيرٍ مِنْ عِبَادِهِ الْمُؤْمِنِينَ ﴾

سورة النمل الآية 15

صدق الله العلي العظيم

ABSTRACT

This research thesis presents a comprehensive investigation into the shear behavior of reinforced concrete (RC) deep beams. The study examines the effects of combining recycled bricks (RB) with normal concrete as a partial alternative to the coarse aggregate. Experimental and Numerical testing was conducted to analyze the factors influencing the behavior of these deep beams at failure. Experimental work was conducted on nine beams to evaluate the impact of various factors on deep beam behavior. The experimental specimens were divided into three series of beams designed to fails in shear with different parameters. The main parameters included replacement ratio of bricks aggregate, grading size, and shear span to depth ratio (a/d). The results of the analysis revealed several significant findings. For first series, when the replacement ratio was increased to 5% and 10%, there was a reduction in both the cracking and ultimate load capacities by 10.4% and 29.9%, respectively. These results indicated that as the replacement ratio increased, the shear strength capacity of the beams decreased. Regarding the maximum deflection, the replacement ratio reduced the maximum deflection which the reduction occurred for the 10% of replacement ratio higher than 5% due to several reasons such as bonding between recycled bricks and concrete matrix, particle packing and grading, and inhomogeneity and interface effects. While for beams with less grading size of RB the reduction in the cracking load reduced hugely with 18.5% and 38.5% for beams with 5% and 10% recycled bricks concrete respectively. The reduction in the ultimate load for beams with the same beams were 10.4% and 28.9% respectively. Regarding the effect of the a/d, the reduction of a/d (for two-point load instead of one point load) for the same grading size of the recycled bricks showed that the cracking load was enhanced and revealed higher increment in comparison with the a/d of 2. The displacement of this beam varied hugely which the replacement of the one-point load to two-point load decreased the average displacement from 6.23 mm to 4.88

mm with a decrement ratio of 21.7%. For the recycled concrete deep beams, the cracking load for these beams were with a variation of 13.3%. The ultimate load was comparable which the variation between the both beams were 7.1%.

The second part was numerical analysis to describe simply supported deep beam structural behavior based on experimental tests. Beams testing results from experiments is used to simulate deep beams for verification. In comparison to experimental data the verification specimens' anticipated load deflection curves were very similar, according to numerical analytical results. Parametric analysis was used to study the hybridization of concrete deep beams with recycled broken brick concrete layers. The numerical study has three series. The first series is a numerical deep beam specimen constructed and tested under one-point load to understand recycled brick shear reinforcement spacing. The second and third series used ANSYS APDL to model ten deep beams to study recycled brick layers and a/d. The numerical results demonstrated that transverse reinforcement strengthened concrete deep beams. Reinforcing the shear zones with steel rebar increased the final shear strength by 39.6%, 27.46%, and 21.2% compared to the shear plain concrete deep beam. Second numerical series tested three numerically produced RC deep beams with different recycled brick thicknesses in concrete deep beam. Top-of-cross section beams hybridized with 5, 10, 20, 30, and 40 cm recycled brick layers. Recycled bricks in hybridized cross-section regions affected deep beam ultimate shear strength and maximum displacement. As recycled bricks were inserted in cross-section regions at varying thicknesses (5 cm, 10 cm, 20 cm, 30 cm, and 40 cm), the final shear strength decreased compared to the ordinary concrete deep beam. Beams subjected to two-point loads with a shear span to depth ratio (a/d) decreased in ultimate shear strength by 4.1% for 5 cm and 9% for 40 cm.

SUPERVISOR CERTIFICATION

I certify that the preparation of this thesis entitled " **Shear Strength of Reinforced Concrete Deep Beam Using Recycled Brick as Coarse Aggregate**" was presented by " **Shams Al-Duha Dakhil Khalaf**", and prepared under my supervision at The University of Misan, Department of Civil Engineering, College of Engineering, as a partial fulfillment of the requirements for the degree of Master of Science in Civil Engineering (Structural Engineering).

Signature:

Asst. Prof. Dr. Samir Mohammed Chassib

Date:

Signature:

In view of the available recommendations, I forward this thesis for discussion by the examining committee.

Signature:

Assist Prof. Dr. Murtada Abass Abd Ali

(Head of Civil Eng. Department)

Date:

EXAMINING COMMITTTEE'S REPORT

We certify that we, the examining committee, have read the thesis titled **(Shear Strength of Reinforced Concrete Deep Beam Using Recycled Brick As Coarse Aggregate)** which is being submitted by (**Shams Al-Duha Dakhil Khalaf**), and examined the student in its content and in what is concerned with it, and that in our opinion, it meets the standard of a thesis for the degree of Master of Science in Civil Engineering (Structures).

Signature:

Name: Asst. Prof. Dr. Samir Mohammed Chassib

(Supervisor)

Date: / /2024

Signature:

Name:

(Chairman)

Date: / /2024

Signature:

Name:

(Member)

Date: / /2024

Signature:

Name:

(Member)

Date: / /2024

Approval of the College of Engineering:

Signature:

Name: Prof. Dr. Abbas Oda Dawood

Dean, College of Engineering

Date: / /2024

DEDICATION

❖ To whom stood beside me and took care of me over the years, to my parents, family, and close friend.

❖ To all those who supported and helped me, made the difficult easy, especially to my supervisor

I present my effort to them with all of my respect and appreciation

ACKNOWLEDGEMENTS

First of all, all my thanks for **Allah** who led me during my way to complete this work.

I would like to express my cordial thanks and deepest gratitude to my supervisor **Asst. Prof. Dr. Samir Mohammed Chassib**, whom I had the honor of being under his supervision, for his advice, help, and encouragement during the course of this study.

I would like to extend my thanks to **Prof. Dr. Abbas Oda Dawood** Dean of the college of engineering, and **Assist Prof. Dr. Murtada Abass Abd Ali**, the Head of Civil Engineering Department.

Special thanks go to **the soul of my dear father, my main supporter my mother and sisters, my special family my husband and daughter, and everyone who supported me on this journey.** Special thanks also go to **Assist. Lect. Haider Hassan,** for their effort in helping me in this thesis.

TABLE OF CONTENTS

Contents

LIST OF TABLES

LIST OF FIGURES

LIST OF SYMBOLES

σ Stress (MPa)

f_c' Cylinder concrete compressive strength in (MPa)

f_{cu} Cube Compressive Strength in (MPa)

$\emptyset$ Diameter of Reinforcement (mm)

ϵ_c Concrete Strain

E_c Concrete modulus of elasticity, (GPa)

DI Ductility Index

f_r Modulus of Rupture in (MPa)

f_t Tensile Strength in (MPa)

f_y Yield Strength in (MPa)

Δ_y Yield Deflection in (mm)

Δ_u Ultimate Deflection in (mm)

LIST OF ABBREVIATIONS

ASCE American Society of Civil Engineers

ASTM American Society of Testing and Material

BFRP Basalt fiber reinforced polymer

CBA crushed bricks aggregate

CFRP Carbon fiber reinforced polymer

EC Euro Code

ECC Engineering Cementitious Composite

FRP Fiber-reinforced polymer

GFRP Glass Fiber Reinforced Polymer

HSC High Strength Concrete

IQS Iraqi Standard

LWC Lightweight Concrete

NC Normal Concrete

NSC Normal strength concrete

R.C.A Recycled Concrete

R.C Reinforcement Concrete

R.O Reverse Osmosis

RB Recycled bricks

Rs Rectangular section

SF Steel fiber

CHAPTER ONE: INTRODUCTION

1.1 General

During the early part of the last century, there was a significant increase in factory productivity, partly driven by the growth of the world population and the migration of people from rural areas to cities. This expansion of cities necessitated the use of reusable materials as a means to preserve the environment and reduce construction costs. The increase in factory productivity during this time was a result of various factors, including advancements in technology, improved manufacturing processes, and a growing labor force. As factories became more efficient, they were able to produce goods at a faster rate, leading to increased productivity. The rise in population and urbanization created a demand for more buildings and infrastructure [1]. To address this demand, it became important to find ways to minimize construction costs. One approach was to utilize reusable materials. By reusing materials from existing structures, construction costs could be reduced, as there was no need to procure new materials. This approach also contributed to environmental preservation by minimizing waste and reducing the extraction of raw materials. The concept of using reusable materials aligns with the principles of sustainability and resource conservation. It offers economic benefits by reducing construction expenses, and it also helps mitigate the environmental impact associated with new material production. According to Franklin Associates [2], in the USA, the waste generated from construction operations amounted to 136 tons of building and demolition materials, and this amount increased until 2003 to 170 million tons. According to research studies, 39% of construction waste is generated from residential buildings and 61% is generated from non-residential buildings. Concrete has become the material that is utilized the most frequently in the field of construction all over the world as a result of the growing demand for its use in a variety of civil engineering applications, including the construction of

buildings, bridges, dams, and other structures. According to Ramtin Movassaghi [2], the construction over the world around the world requires ten billion tons of concrete annually, making it one of the largest industrial processes consuming earth resources around the world. On the other hand, the concrete industry requires a high cost in terms of mining raw materials and producing cement [2]. Although many countries have called for the need to preserve the environment and to recycle and reuse materials once, this does not mean providing facilities with low quality [3]. Reducing the consumption of the earth's natural resources is one of the most important goals that all countries call for, and it can be achieved through recycling and using materials and reducing the natural extraction of rubble, which leads to a positive impact on the environment [4]. One of the reasons why countries around the world call for the use of reusable materials or the recycling of waste and used materials is the economic crisis that many countries suffer from. Still, the used materials must provide performance and behaviour similar to the originally used materials and not less than them, even though the recycled materials need additional improvements that make them eligible to replace many construction materials [4].

1.2 Recycled Bricks Properties

The most essential properties of recycled bricks (RB) are briefly given in this chapter based on available experimental findings as revealed in Figure 1.1. The process of producing recycled bricks is by demolishing walls, crushing them, and removing the cement paste stuck to the bricks; therefore, their properties will differ from those of traditional bricks [5]. According to the results obtained by many researchers [5-8], concluded that there is a difference in mechanical properties of recycled aggregates comparative with the natural aggregates: Up to a 50% reduction in drying shrinkage, up to a 50% increased creep, The amount of water absorbed increased by 50%, Compressive strength has been reduced by

25%, Decrement in flexural and tensile strength by 10%, Reduced elasticity modulus by up to 45%, Reduced frost strength.

1.3 Recycled Bricks

Recycled bricks (RB) are the term used to describe the material produced crushed construction and demolition waste from bricks the reused bricks can be used as a total or partial substitute for the conventional fine or coarse aggregate. Since the aggregate makes up over 75% of the concrete volume, it is necessary to recycle and reuse it or find a substitute to achieve economic and environmental advantages. This needs a pre-examination of recycled aggregate quality and advanced treatment processes with the use of special facilities. Recycled bricks aggregate is usually extracted by demolishing walls with the use of advanced processing techniques and special facilities to control the quality of the extracted bricks. Refining and replacing recycled bricks aggregates are a closed-loop bricks recycling system [6, 7]. It is important to note that completely removing cement from recycled bricks aggregate requires high energy and additional cost. It should be noted that recycled bricks aggregate has advantages that you prefer over natural aggregate, which is that it does not contain cracks or a high percentage of voids, such as those found in natural aggregates [8]. In the refining process of recycled bricks aggregates, several steps are typically taken to improve their quality and ensure their suitability for reuse. One common step is the secondary crushing of walls using an impact crusher. Once the bricks have been crushed, they undergo a segregation process. crushed bricks are separated to create distinct fractions that can be used for different purposes. This segregation is important as it allows for better control over the grading and composition of the recycled bricks aggregates, which can affect the properties of the resulting concrete or other construction materials. Additionally, impurities present in the recycled bricks aggregates are removed during the refining process. These impurities can include debris, contaminants, or any unwanted materials that may have been mixed with

the concrete mixtures component. Removing these impurities helps ensure the quality and performance of the recycled bricks aggregates. According to the desired building criteria, the relative quality value approach is used to calculate the ratio of replacement by coarse recycled aggregate original coarse. Fine-recycled aggregate can be used in the production of precast concrete products [9]. One of the most important mechanical properties that differ between the natural and recycled aggregate is workability. As a result of the presence of cement sticking to the bricks when the wall is crushed, the ability of the bricks to absorb water becomes significantly larger, and this makes the workability of recycled concrete less, which requires adding more water before or during mixing, and sometimes there is a need to use some additives.

Figure 1- 1 Recycled bricks production and treatment.

1.4 Applications of Recycled Bricks Aggregate

One of the most important applications of using recycled aggregates is road construction. Road construction is the first consumer of recycled materials, especially aggregates. The use of recycled bricks aggregates in soils is more than concrete structures, as it requires less treatment when used on soils, unlike concrete that requires high treatment of recycled bricks aggregates as it affects the workability of concrete, water absorption, and concrete resistance and other mechanical properties. Etc. The percentage of recycled aggregate used on soils is 72% due to its availability and good properties. It is also used in sidewalks, bridges, infrastructure, and structures, but in lower percentages. More than half

of the recycled bricks are often found in the granular base material. The fine proportion of recycled bricks infill applications, particularly in soils, road sub-base applications, may limit drainage [10]. Figure (1.2) shows the recycled bricks. Indeed, crushed clay brick is generally not recognized as a recyclable material in the Middle East, unlike recycled concrete aggregate. The initial utilization of crushed brick with Portland cement dates back to 1860 in Germany, primarily for producing concrete products. However, the notable application of crushed brick as aggregates in fresh concrete was observed during post-World War II reconstruction efforts [3].

Figure 1- 2 Collecting of Recycled bricks.

1.5 Burned bricks

Burned cricks are the result of exposing the bricks to high oven temperatures; this method offers numerous benefits over the old one. They are resistant to corrosion, keep their shape erratically, are dense and low porosity, and can be either pale or dark green in colour. Used in foundation work and building below the moisture arrester level. The increased exposure to high heat beyond the necessary duration causes the clay to undergo a vitreous phase, which imparts durability to the bricks; this is one of the type's advantages.

1.6 Effect of Recycled Bricks Aggregate on Fresh and Hardened Concrete

The aggregate usually occupies 70-75% of the total concrete volume and 75-85% of the mass of concrete. Reused and recycled bricks are characterized by the presence of cement mortar adhered to their surfaces, so their physical and mechanical properties differ from natural aggregates. One of the most important effects caused by recycled bricks is their effect on the workability of concrete. By increasing the percentage of recycled bricks, the workability decreases unless the ratio of water to cement is increased or some additives are used. The surface area of the used aggregate is influenced by the recycled brick type and the curing method [11]. The use of recycled bricks aggregates can have a direct effect on the mechanical properties and homogeneity of the concrete mix, in addition to its impact on porosity and durability. The appropriate aggregate grade for recycled concrete is determined based on the workability and the concrete's tensile and compressive strength. Regarding the bricks type of the concrete component, as well as the amount and distribution of reinforcing steel, all of these variables determine the mechanism for selecting the maximum ratio of crushed bricks. Recycled bricks vary in their absorption of water and specific gravity by age, size, strength, and cement content. As the particle size decreases, the specific gravity gradually reduces. It is important to note caution when choosing the appropriate gradation of recycled bricks for the concrete mix, as the incorrect choice of grading can cause a relatively higher demand for water in addition to the possibility of segregation. Also, due to the high porosity of the recycled bricks, the water absorption will be higher compared to the natural fine aggregate. Choosing recycled bricks provides lower performance than the natural aggregate [11]. When recycled bricks are produced by crushing bricks, the result of this crushing is rough-surfaced bricks that have a bigger surface area than round aggregate and hence may give greater interlock and adhesive strength between concrete particles than round aggregate, but it causes an increase in the voids between the particles of the concrete. Therefore, the concrete mixture containing

recycled bricks requires more care in terms of increasing the water content and an increase in cementitious materials compared to normal concrete [11].

1.7 Advantages and Disadvantages of Bricks

Many advantages can be gotten with use of recycled bricks as alternative aggregates, include the reduction of concrete density, decreased consumption of natural aggregates, and the environmentally friendly nature of this approach. Recycled concrete offers a lower construction cost than its normal counterpart. Recycled concrete usually has good resistance to freezing and thawing, which makes it suitable for use in areas with variable temperatures. This is because the process of crushing and recycling concrete can create a more durable and less porous material. The volume response, in terms of thermal expansion, contraction, and moisture-induced swelling or shrinkage, is generally comparable between concrete made with recycled aggregates and concrete made with natural aggregates [12]. In the other side, these advantages can also pose significant disadvantages such as the high porosity, high absorption rate, and variation in the quality of crushed brick aggregates. Inadequate specifications, uncertainties surrounding regular supply, and a lack of confidence and experience in utilizing these materials are additional obstacles that are encountered. When the recycled bricks are obtained through demolishing, the bricks may be contaminated with gypsum plaster, and this causes a high sulfate content within the recycled concrete. The possibility of interaction with alkaline water and the result of this reaction can cause cracks and partial damage to the concrete. Depending on the bricks content, the strength of concrete with bricks decreases by 15 to 25%. When recycled bricks are used in cold areas, a reaction will occur between concrete additives and chlorides, and this will cause changes in the hardening behaviour of the first stages of concrete. Elastic and plastic energy capacity and toughness decrease with the increase in the proportion of recycled bricks in a concrete mixture. The use of recycled bricks causes an increase in creep and a decrease in

the modulus of elasticity, and this change is not considered a negative in general, especially in the projects of water channels and drainage channels [12].

1.8 Deep Beams

Reinforced concrete deep beams are widely used in many structural engineering applications, such as transfer girders, pile caps, offshore structures (caisson), shear walls, wall footings, floor diaphragms, and complex foundation system [2]. When the a/d of simply supported beams is less than 2, or less than 2.5 for any span of a continuous beam, it is customary to define these beams as deep [3]. The ACI building code 318R-08 [4] defines deep beams as members loaded on one face and supported on the opposite face so that compression struts can develop between the loads and the supports, and have either with clear span equal to or less than four times the overall member depth, or regions of beams loaded with concentrated loads within twice the member depth. Simply supported deep beams may be classified according to loading and supporting conditions as directly loaded deep beams (forces applied on the top and reactions on the underside), and indirectly loaded deep beams (forces applied through adjacent framing members) as shown in Figure (1.1). The behavior of deep beams differs from that of slender beams, and as a result, it is indicated that the difference between the shear strength for deep beams and slender one is different.

1.8.1 Behavior of Deep Beams

The behavior of deep beams is different from that of common flexural members; the behavior is governed by shear rather than flexure. Since large portion of compressive force is directly transferred to support by the arch action, and the shear strength is much greater than that predicted by ordinary shear equation. Figure (1.3) illustrate the arch action in a deep beam [5]. The shear strength of deep beams is a function of many factors such as concrete compressive

strength, main and web reinforcement, slenderness (a/d), loading and supporting conditions [6]. The ACI building code 318R-08 [4] recommends taking into account the nonlinearity of strain distribution in the design of deep beams. Also, it is based on D-region behavior, (D-region is defined as the portion of a member within a distance equal to the member height or effective depth from a force discontinuity or a geometric discontinuity) as shown in Figure (1.3).

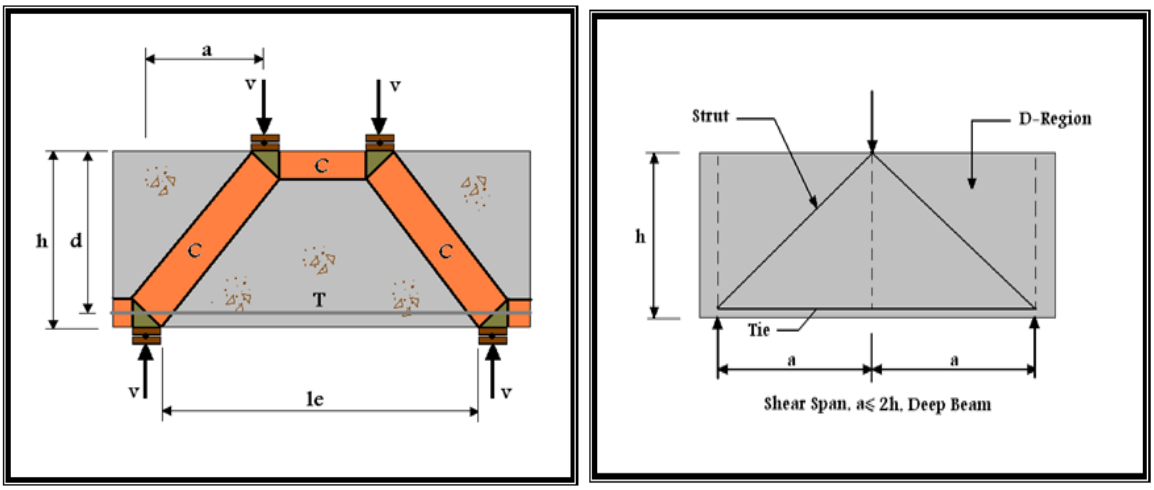

Figure 1- 3 Deep beam design characteristics

1.7 Research Objectives

The purpose of this research is to study the shear behavior of concrete deep beams made with recycled crushed bricks at different replacement ratios. The investigation includes experimental and numerical investigations involving the testing of nine and thirteen beams, respectively. The beam variables are the recycled bricks replacement ratio, curing method, and brick type, in addition to the hybridization with recycled bricks aggregate. In the second part of the study, the tested specimens are to be analyzed by using the three-dimensional nonlinear finite element method.

1.8 Thesis Layout

This thesis is organized in six chapters as follows:

[1] **Chapter One** presents a general introduction to recycled bricks aggregate, the properties of recycled bricks and its advantages and applications, in addition to the deep beam's properties and behavior.

[2] **Chapter Two**: The relevant theoretical and experimental studies are presented as a literature review.

[3] **Chapter Three**: The experimental program and the material's properties, in addition to the laboratory tests, are presented in this chapter.

[4] **Chapter Four:** This chapter shows numerical modelling by ANSYS as well as finite element equations

[5] **Chapter Five** includes the obtained experimental and analytical results and a discussion.

[6] **Chapter Six:** The conclusions and recommendations are presented in this section.

CHAPTER TWO: LITERATURE REVIEW

2.1 Introduction

A brief summary of previous experimental studies on the structural behavior of deep beams built from recycled materials is the goal of this chapter. In the first part of this chapter include review of the researchers works who have looked into this topic and offered several approaches to analysis and design in the hopes of improving the performance of these concrete components and determining their maximum capacity. Research pertaining to reinforced concrete deep beams is the subject of the second part.

2.2 Previous Studies of Recycled Bricks

In 2008, Debieb and Kenai [11] conducted a study to investigate the effects of using crushed bricks as a replacement for coarse and fine aggregates in concrete. The researchers partially replaced fine, coarse aggregates, or both of them, with crushed brick aggregates at varying percentages (25%, 50%, 75%, and 100%). They compared the compressive and flexural strengths of the concrete at different ages (up to three months) with those of concrete made solely with natural aggregates. Experimental investigations were conducted to assess the properties of concrete containing crushed brick aggregates, focusing on porosity, shrinkage, water permeability, and water absorption. The test outcomes indicated that it is feasible to produce concrete incorporating crushed brick aggregates, both coarse and fine, which exhibit comparable characteristics to concrete made with natural aggregates. However, it was noted that to maintain desired performance, the percentage of recycled aggregates should be restricted to 25% for coarse aggregates and 50% for fine aggregates. In comparison to natural aggregates, the recycled brick aggregates demonstrated relatively lower bulk density and higher water absorption. Concrete made with crushed bricks exhibited lower densities,

with reductions of up to 17% when compared to concrete made with natural aggregates. However, it is worth noting that concrete containing 100% recycled coarse and fine aggregates exhibited some segregation, leading to a delayed demolding process that occurred 56 hours after casting. The study revealed a decline in compressive strength at 28 days of age, with reductions of approximately 35%, 30%, and 40% observed when coarse aggregates, fine aggregates, or both coarse and fine aggregates were replaced, respectively. Interestingly, the relationships between compressive strength and nondestructive tests were found to be highly similar to those established for concrete made with natural aggregates. The researchers suggested the utilization of water-reducing and plasticizer admixtures to mitigate the water content in the concrete. Additionally, the study indicated a decrease in flexural strength of approximately 15% and up to 40% when incorporating recycled coarse and fine aggregates in the concrete. The ratio of compressive strength to flexural strength ranged from 8.1 to 11.8. Similarly, the modulus of elasticity followed a similar trend as the compressive strength, with reductions of 30%, 40%, and 50% observed for concrete containing crushed bricks in the coarse aggregates, fine aggregates, and both coarse and fine aggregates, respectively.

In 2010, Yang et al. [13] conducted a study to investigate the behaviour of concrete containing recycled bricks and aggregates as an alternative to coarse natural aggregate. The study explored various replacement ratios of recycled materials for the coarse natural aggregate. The replacement ratios were categorized into four cases: the first one was the natural aggregate, whereas the remaining three used 20, 50, and 50% recycled bricks, corresponding to 80, 50, and 0% recycled aggregate. The results of the study revealed that even after undergoing proper cleaning procedures at the recycled aggregate treatment plant, a small amount of waste impurities (approximately 1.4%) remained present after manual sorting processes. The use of fine recycled concrete aggregate as a mixing

material and pre-wetting methods before mixing significantly improved the fresh concrete properties. A 50% replacement ratio of recycled bricks in the recycled aggregate resulted in low workability, making it difficult to compact and finish the fresh concrete. The recycled bricks displayed higher water absorption percentages in comparison to recycled aggregate and natural aggregates. The presence of cement mortar on the attached aggregate and recycled bricks within the recycled aggregate had a notable impact on the physical and mechanical properties of both fresh and hardened concrete. The variation in the content of recycled bricks (0-50%) had a notable impact on physical and mechanical properties, particularly on compressive and cylinder-splitting strengths. However, the effect on flexural strength was relatively limited. The inclusion of recycled bricks also increased the permeability of the concrete. However, with up to 20% inclusion of recycled bricks in the recycled aggregate, the resulting concrete still exhibited a "very good" level of protective quality. When the inclusion reached 50%, the concrete fell into the "good" level of protective quality.

Figure 2- 1 Specimens tested by Yang et al.

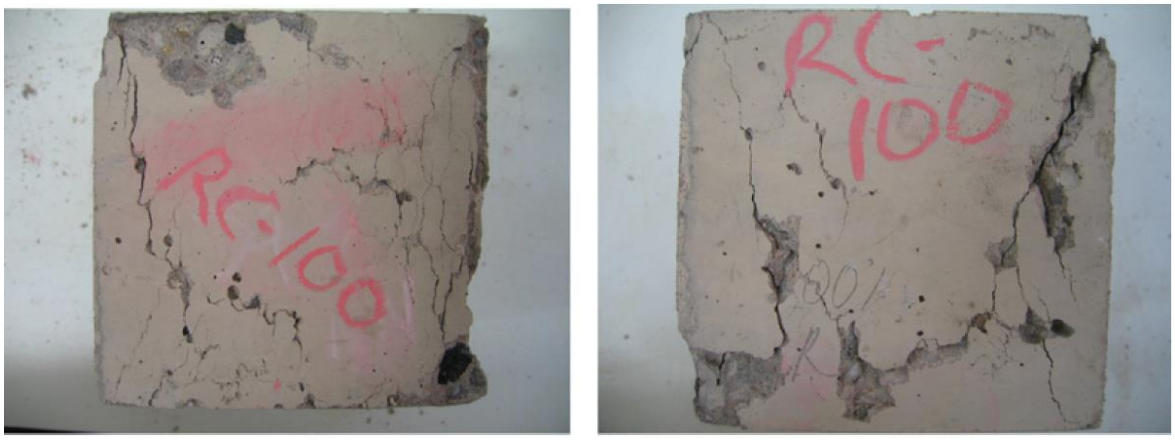

Figure 2.1 Cont. [13].

In 2017, Kumar et al. [14] conducted an experimental investigation focusing on the analysis of concrete made from recycled bricks. The study aimed to directly replace the coarse aggregate with recycled bricks with replacement ratio of 10, 20, and 30% in addition to the modifying the mixture components to minimize any significant loss in the mechanical properties of the concrete. This research aimed to contribute to the sustainable utilization of available waste materials at construction sites. The strength of the concrete made from recycled bricks was determined in this experimental study. The researchers examined the substitution of coarse aggregates with 10%, 20%, and 30% of bricks at different concrete strength grades mixtures (C25, C30, and C35). The effects of these replacement percentages were analyzed at different curing durations, specifically 7, 14, 28, and 50 days. The investigation revealed that as the percentage of brick replacement increased in the concrete, the workability of the mixture decreased due to the high absorption of water of the recycled bricks. However, the compressive strength showed an increase with 10% and 20% brick replacement. However, when the replacement percentage reached 30%, the compressive strength began to decrease. These findings suggest that while a partial replacement of coarse aggregates with recycled bricks can lead to improvements in compressive strength at lower replacement percentages, a higher replacement percentage (30%) can result in a decline in compressive strength. It is important

to carefully optimize the percentage of brick replacement to achieve the desired balance between workability and compressive strength in concrete made from recycled bricks.

Table 2- 1 Test results of Kumar et al.

Compressive strength of concrete mixes of M-25 grade				
Days/%	0 %	10%	20 %	30 %
7	19.06	16.96	18.04	17.13
14	26.40	21.41	23.38	22.03
28	30.61	25.45	26.44	23.66
50	31.47	27.73	28.52	25.17

Compressive strength of concrete mixes of M-30 grade				
Days/%	0 %	10%	20 %	`30 %
7	26.152	21.44	23.349	22.047
14	29.811	26.50	27.991	26.777
28	39.795	34.71	36.777	32.149
50	40.471	35.76	38.918	34.266

Compressive strength of concrete mixes of m-35 grade				
Days/%	0 %	10%	20 %	30 %
7	30.195	25.388	28.13	26.346
14	32.531	29.419	30.52	29.666
28	44.299	36.488	37.32	32.377
50	45.4	37.577	38.17	33.12

In 2020, Zhu and Zhu [16] conducted a study to explore the potential use of clay brick waste in mortar and concrete applications. The crushed recycled bricks exhibited pozzolanic activity, allowing for the partial replacement of cement in mortar production. Additionally, the recycled bricks were used to produce recycled brick concrete, although the mechanical properties of this concrete were inferior to those of normal concrete. The addition of recycled bricks in concrete improved the durability of the material in certain cases. Furthermore, the use of recycled brick concrete offered advantages such as reduced transportation costs

and dead loads. It was suitable for the production of various structural elements, including units, beams, and columns. The study demonstrated the feasibility of completely replacing natural aggregates with recycled brick aggregates (RBAs). This substitution not only reduced the consumption of natural resources but also promoted the reuse of construction waste.

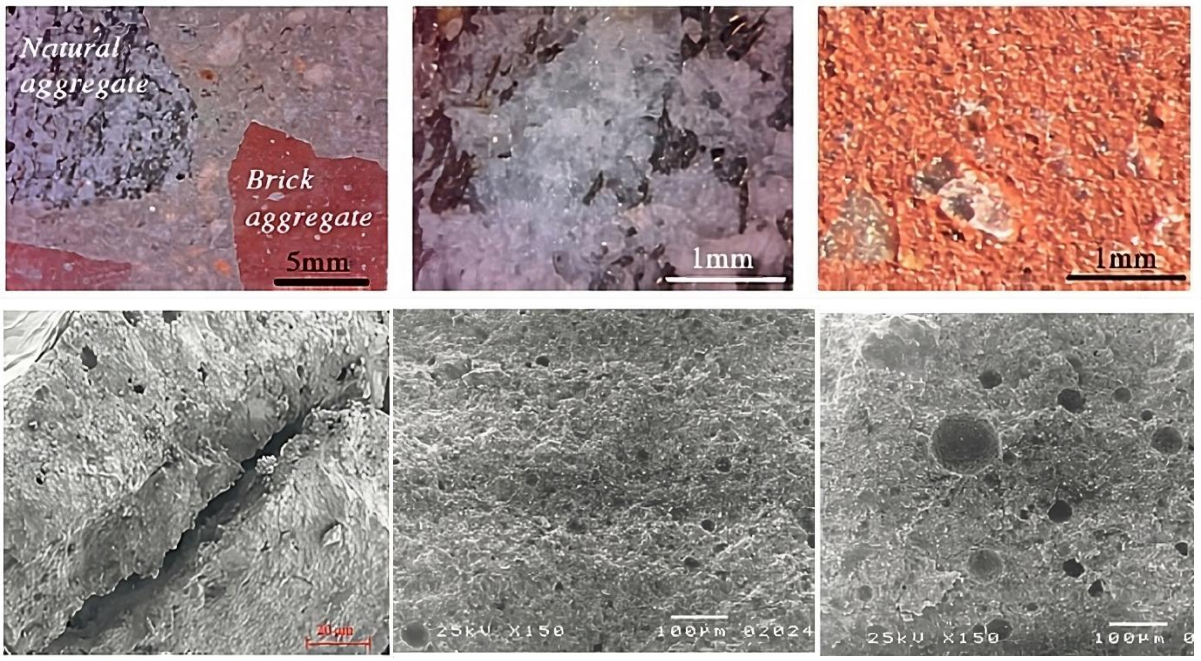

Figure 2- 2 Specimens tested by Zhu and Zhu

In 2021, Tarek et al. [15] conducted an extended study to investigate the feasibility of recycling concrete made with brick aggregate as the coarse aggregate. The brick aggregates were collected from demolished concrete blocks from six building demolition sites and manually crushed to obtain coarse aggregate. The physical properties of the collected coarse aggregate were evaluated. Samples of 100 mm x 200 mm cylindrical concrete were made using the recycled concrete. In the concrete mixtures, various water-to-cement (W/C) ratios of 0.40, 0.45, and 0.50 were employed. The specimens underwent testing for compressive strength, tensile strength, and Young's modulus of concrete at 7, 14, and 28 days. Control specimens were also prepared using virgin brick aggregate to facilitate a comparison with the outcomes attained from the recycled

aggregate. According to the experimental findings, the recycled brick aggregates exhibited a lower absorption capacity than the virgin brick aggregate. The average strength of the concrete incorporating recycled brick aggregate was measured at 29 MPa for W/C ratio of 0.45 and 23.5 MPa for a W/C ratio of 0.55. These findings suggested that concrete produced with recycled brick aggregate could achieve satisfactory strength properties. The lower absorption capacity of the recycled brick aggregate indicated its potential for producing durable concrete. However, it was important to note that the concrete strength varied depending on the water-to-cement ratio used in the mixture.

Figure 2- 3 Specimens tested by Tarek et al.

In 2021, Abdullah et al. [17] conducted a review focusing on the use of recycled bricks as an alternative to coarse aggregate in the production of environmentally friendly concrete. The review highlighted several key findings: the first one was that the clay brick powder exhibited pozzolanic activity, enabling its use as a cement substitute at replacement levels of up to 10%. Recycled brick aggregate can be used as a substitute for natural coarse aggregate, but with limitations on the replacement level. Concrete produced using recycled aggregate has the potential to attain sufficient strength and is suitable for manufacturing medium or low-strength concrete. The incorporation of fine recycled brick waste as aggregate in concrete production enhances the properties of the concrete. In certain cases, it has been observed to improve the durability of concrete when used as a replacement for up to 10% by weight of fine aggregates. The use of waste brick as a partial substitute for cement or aggregate (coarse or fine) in concrete production offered several sustainability benefits. It saves natural resources, reduces energy consumption, and lowers carbon dioxide (CO_2) emissions associated with cement and concrete production processes. By incorporating waste brick powder into concrete, the density of the concrete increases, leading to lower porosity and a more compacted structure. This densification can help minimize the corrosion of steel reinforcement. Furthermore, the inclusion of fine brick aggregate can enhance the strength of concrete and reduce chloride penetration as long as the replacement level does not exceed 10%. When waste brick was used as coarse aggregate in concrete, it often led to a decrease in compressive strength as the replacement level increased. Additionally, the workability of concrete containing crushed brick aggregate was lower compared to conventional concrete due to the high absorption capacity of the brick aggregate. Waste brick aggregate could reduce transportation costs and dead loads. Additionally, it enhanced the durability of concrete in certain cases.

In 2021, Monawar and Alawi [18] conducted a study to investigate the influence of recycled bricks on concrete behaviour. The objective of the study was to explore the feasibility of using building waste materials, specifically crushed clay bricks and cement blocks, as recycled aggregates in concrete manufacturing. The study involved the experimental evaluation of three concrete mix designs, incorporating 15%, 20%, and 30% of cement. Several tests were conducted, including the slump test, air content measurement, and compressive strength testing. The findings of the study indicated that the reuse of crushed clay bricks and cement blocks as recycled aggregates in concrete was feasible. This was particularly applicable to non-structural concrete elements such as barriers and temporary constructions. Moreover, the reuse of these materials had several positive impacts. It contributed to the reduction in the consumption of natural resources, saved energy, and minimized the disturbance of the natural environment. This was because these waste materials are widely available in new construction projects or as by-products of demolishing buildings. Overall, the study concluded that incorporating crushed clay bricks and cement blocks as recycled aggregates in concrete manufacturing could be a viable and sustainable approach, particularly for non-structural applications.

Figure 2- 4 Concrete mix with recycled construction demolition waste

In 2021, Rasheed et al. [19] investigated the behavior of the concrete beam made with recycled clay bricks. This research focused on investigating the long-term potential for cracking in normal concrete by utilizing clay brick waste as an internal curing agent, thereby promoting a sustainable approach. To enhance cement hydration and improve the properties of the concrete, 10% and 15% of the sand volume were replaced with an equivalent volume of pre-saturated clay brick waste. Four cured beams were compared with two control beams that did not incorporate any internal curing agent. The objective was to evaluate the impact of the clay brick waste on the compressive and splitting tensile strength of the concrete, as well as its ability to reduce crack formation. The results indicated that the inclusion of clay brick waste led to improvements in both compressive and splitting tensile strength. Furthermore, a significant reduction in cracks was observed in the internally cured beams compared to the control beams. Based on the recorded results, it was determined that an exemplary percentage of 15% clay brick waste to natural fine aggregate resulted in the highest compressive and splitting tensile strength. Additionally, this composition demonstrated a reduction in cracks during flexural testing. The utilization of saturated surface dry clay brick waste, with a replacement ratio of 15% of the fine aggregate, could be

considered as the optimal proportion for incorporating it into concrete mixes to enhance the concrete properties. This ratio has been found to result in significant improvements in the desired characteristics of the concrete. By using this specific ratio, the concrete can achieved an enhanced properties and performance.

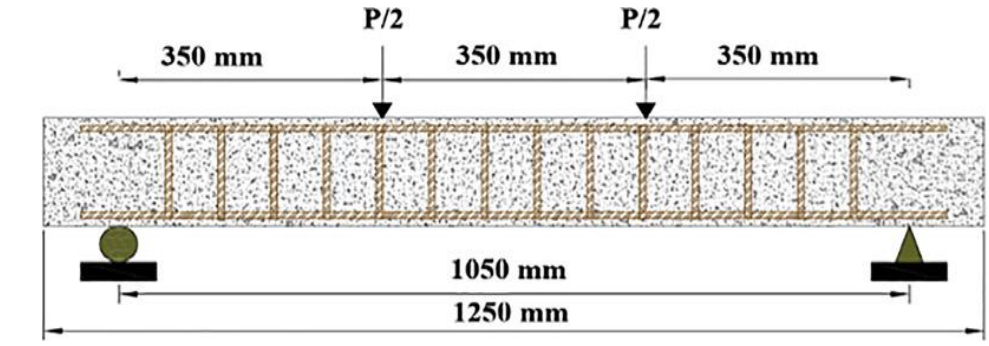

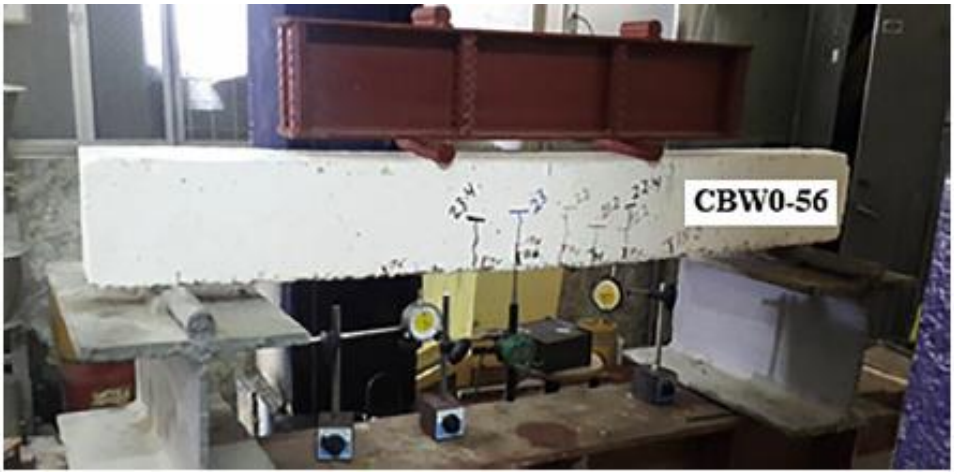

Figure 2- 5 Concrete beam made by Rasheed et al

The study by Janotka et al. in 2021 [20] focused on the design of concrete using recycled brick waste (RBW) and its environmental performance. The researchers found that RBW can effectively replace natural aggregates in concrete, and RBW powder, also known as TERRAMENT, was suitable for use as an industrially made type II addition. RBW powder showed similar pozzolanic reactivity to pozzolan-fly ash, suggesting it can enhance concrete properties. Both

RBW and RBW powder were suitable for the production of industrially made TRITECH Eco-designed ready-mixed concrete. The researchers concluded that the powdered RBW, along with the 0/4 mm fraction, could partially replace a portion of cement and natural aggregate in a specified concrete mixture composition. This combination was declared suitable for the production of industrially made TRITECH Eco-designed ready-mixed concrete with a strength class of C 25/30. The k-value factor that used in the calculation of the equivalent w/c was found equal to 0.5, which applied to a wide range of w/c ratios, except for ratios of 0.65 and higher. The study also found that experimental cement mortar (EXP-2) made with CEM II/B-S 42.5 and TERRAMENT demonstrated resistance to the influence of aggressive CO2 in the XC2 environment, as specified by STN EN 206 + A1. Concrete incorporating TERRAMENT exhibited durability against carbonation in the XC2 environment. In conclusion, the study found that RBW, both as an aggregate and as a powder addition, can be effectively utilized in the production of industrially made ready-mixed concrete. The specific k-value of TERRAMENT allowed for its use according to relevant standards.

In 2022, Ali and Abdelaleem [21] examined the influence of silica fumes on the lightweight RC deep beam made with crushed clay bricks. Fifteen RC deep beams were constructed and tested until failure. The experimental program consisted of five groups. The first one served as the control and fabricated normal weight concrete (NWC), while the remaining groups were cast using lightweight concrete (LWC). The purpose of the study was to compare the structural behavior and performance of the RC beams constructed with NWC and LWC. By examining the differences between the control group and the LWC groups, the researchers aimed to assess the impact of using lightweight concrete on the

beams' load-carrying capacity, deflection, and other relevant structural characteristics. The study involved various tests, including bending tests and load tests, to evaluate the beams' response under different loading conditions. The beams were monitored for factors such as ultimate strength, cracking behaviour, and overall structural integrity. In the experimental program, several parameters were considered to evaluate the behaviour of the beams, including the type of concrete, reinforcement ratio, repalcement ratio of crushed bricks (5% and 10%) and the content of silica fume (SF). These factors were varied to investigate their influence on the performance of the beams. The evaluation of the beams focused on various aspects such as crack patterns, failure modes, ultimate deflection, and ductility. By analyzing these parameters, the researchers aimed to understand how the different concrete types, reinforcement ratios, and SF content affected the overall behaviour and performance of the beams. The experimental results indicated that the resulting concrete satisfied the requirements of LWC in terms of unit weight and strength. This suggests that the chosen combination of concrete type, reinforcement ratio, and SF content was successful in achieving the desired properties of LWC. Furthermore, the crack patterns, failure modes, ultimate deflection, and ductility of the beams were assessed to characterize their structural behaviour. In the experimental program, it was observed that increasing the reinforcement ratio and SF content had a positive impact on the overall performance of the beams. This suggested that higher reinforcement ratios and SF content resulted in improved structural behaviour and performance. The addition of SF in the concrete mix led to measurable enhancements in the majority of the performance characteristics of the LWC beams. This indicated that the inclusion of SF contributed to improved crack resistance, increased ultimate capacity, and reduced mid-span deflection.

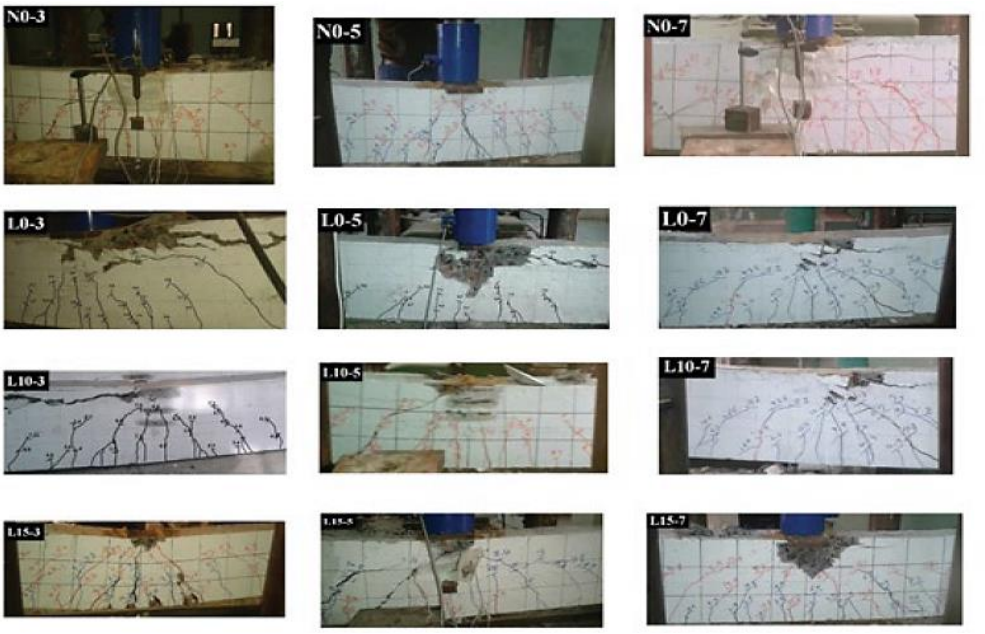

Figure 2- 6 Specimens tested by Ali and Abdelaleem

In 2023, an experimental investigation was presented by Alam and Ahmad [22] regarding the torsional behaviour of concrete beams made with crushed clay bricks. Partial replacement of coarse aggregate was performed with crushed bricks (at replacement ratio of 17%, and 24%) to make concrete beams under torsional loads. In this study, different types of aggregates were employed as partial alternatives to the coarse aggregate in concrete mixtures. The mixtures included natural stone aggregate concrete (NSAC), crushed virgin clay brick aggregate concrete (VBAC), crushed recycled brick aggregate concrete (RBAC), and crushed recycled stone concrete aggregate concrete (RSAC). These variations in aggregate types aimed to explore the effects of using different materials on the properties and performance of the concrete. In this study, a comprehensive testing program was carried out to examine and compare the torsional behaviour of concrete using crushed clay bricks and recycled brick concrete as coarse aggregates. Concrete specimens were prepared with target strengths of 18.9, 20.7, 22.4, and 24.1 MPa, utilizing four different types of coarse aggregate: natural stone, crushed clay brick, recycled stone, and recycled brick aggregate concrete. The purpose was to assess the torsional properties and

performance of the concrete specimens when different types of coarse aggregates were utilized. In this research, cylinder samples were utilized to evaluate various properties of the concrete, including compressive strength, splitting tensile strength, density, porosity, and absorption. These tests provided insights into the mechanical properties and durability characteristics of the respective concrete mixtures. Furthermore, beam samples were subjected to pure torsion until failure to investigate the torsional behaviour of the concrete. The objective was to observe the ultimate torque and maximum twisting angle achieved by the beams, as well as to analyze the torque versus twisting angle relationship. These tests helped to assess the structural performance and resistance to torsional loads of the concrete specimens. For the evaluation of torsional capacity, angle of twist, crack pattern, and other parameters, beam specimens measuring 150mm × 150mm × 400mm were prepared. These beams were used to test concrete with different types of coarse aggregates and different strength levels. The size of the beams was kept constant across all concrete types to eliminate the size effect. The results of the study revealed that the ultimate torque of crushed virgin VBAC was approximately 95% of that of NSAC, while RBAC had an ultimate torque of around 90% of NSAC. The torsional toughness of VBAC was found to be in the range of 68% to 72% of NSAC. Furthermore, the experimental torques were compared with predictions of torsional strength using five commonly used models. It was observed that for VBAC, the closest prediction to the experimental findings was made by the skew bending theory, which is a commonly used approach for estimating torsional strength.

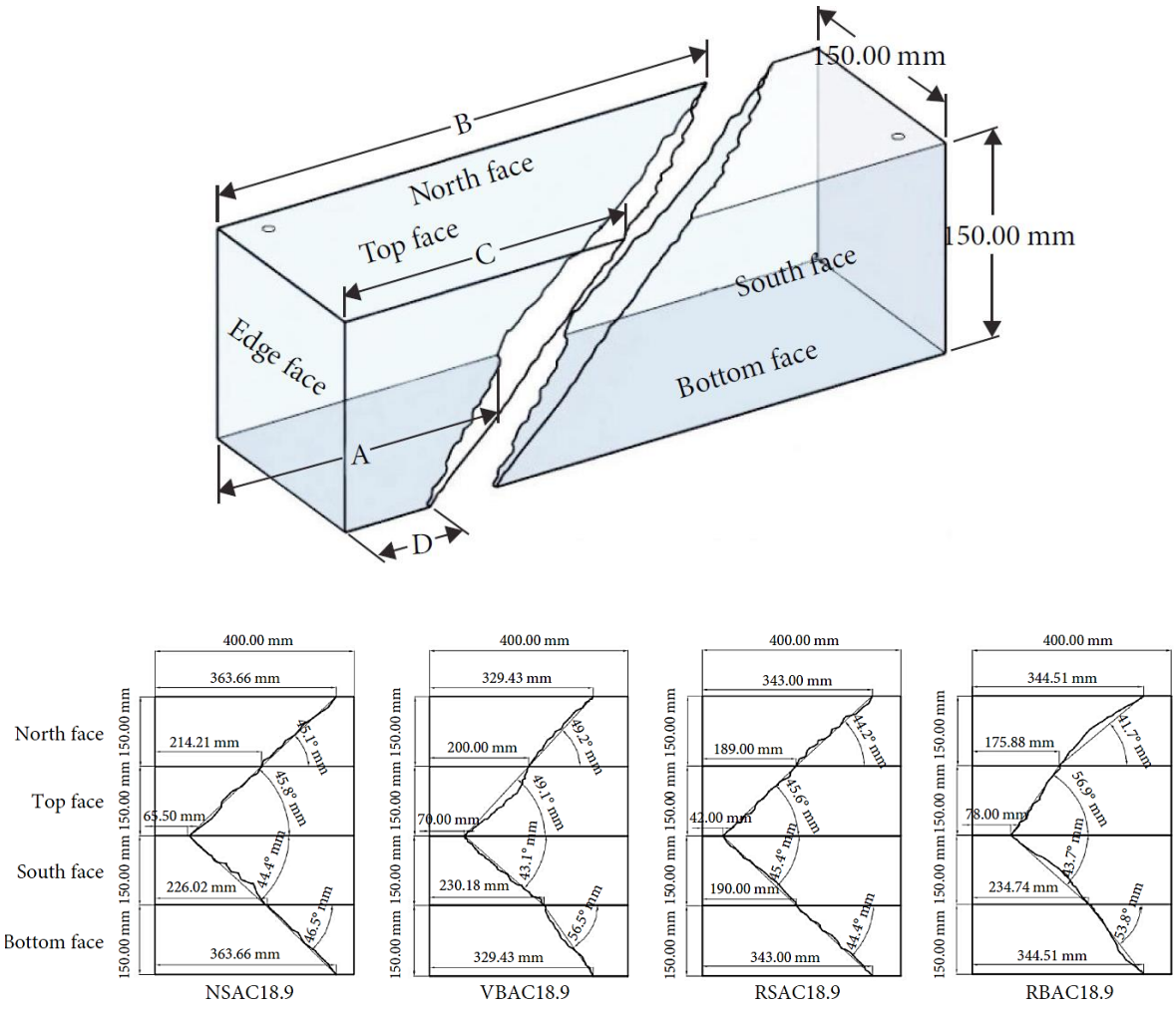

Figure 2- 7 Specimens tested by Alam and Ahmad

Figure 2.7 Cont. [22].

2.3 Previous Studies of Deep Beams

The study conducted by Kong and Robins in 1971 [23] investigated the behaviour of simply supported deep beams. They tested 38 deep beams with effective span-depth ratios (L/D) ranging from 1 to 3 and clear-shear-span/depth ratios (a/D) ranging from 0.23 to 0.7. The study specifically focused on examining the effects of eight types of web reinforcement on the behaviour of these deep beams. One of the key findings of their research was that the ultimate strength formulas that are suitable for normal-weight concrete deep beams may not necessarily be applicable to deep beams made with lightweight aggregate concretes. This suggests that the behaviour and strength characteristics of deep beams can vary depending on the type of concrete used. The study highlights the importance of considering the specific properties and characteristics of lightweight aggregate concrete when designing and analyzing deep beams. It indicates that the traditional formulas and design approaches developed for normal-weight concrete may not accurately predict the behaviour and ultimate strength of deep beams made with lightweight aggregate concretes. These findings emphasize the need for further research and development of design guidelines specifically tailored to deep beams made with lightweight aggregate concretes. Such guidelines would enable engineers to accurately assess the structural behaviour and strength of deep beams in lightweight construction applications, ensuring safe and efficient design practices.

In 1996, Kong and Teng [24] conducted a study involving the testing of 24 deep beams made with LWC. The objective of the study was to investigate whether the behaviour of these beams was influenced by the embedment lengths used for the end-anchorage of the main tension reinforcement, with a specific focus on the ultimate load range. In their tests, Kong and Teng closely examined

the ultimate behaviour of the beams as they varied the embedment length of the tension reinforcement. They specifically considered the design recommendations for deep beams outlined by ACI (American Concrete Institute) and other relevant sources. By reducing the embedment length, the authors aimed to investigate the impact on the ultimate load-carrying capacity and failure modes of the deep beams, comparing the results with existing design guidelines. This study is the first known attempt to directly validate the beneficial effect of normal pressure on bond strength in deep beams.

In 2010, a study was conducted by Yang [25], which aimed to compare the behaviour of deep beam specimens made of sand-lightweight concrete (SLWC), ALWC, and NWC. Sixteen specimens were carefully selected for testing, encompassing shear span-to-overall depth ratios of 0.5 and 1.0. Additionally, the section overall depths of the specimens ranged from 400 mm to 1000 mm. The purpose of this study was to investigate and analyze the structural performance and load-carrying capacity of deep beams constructed using different types of concrete, namely SLWC, ALWC, and NWC. The research findings revealed that the size effect in LWC deep beam behaviour was more pronounced than that of NWC deep beams. This suggests that the size (dimensions) of the deep beams had a more significant influence on the behaviour and performance of LWC deep beams. Additionally, the study observed that the influence of section overall depth on the ultimate shear stress was slightly greater in ALWC deep beams compared to SLWC deep beams. This implies that the overall depth of the section had a slightly stronger impact on the ultimate shear stress of ALWC deep beams compared to SLWC deep beams. The study also revealed that the strut-and-tie models (STMs) proposed by ACI 318-08, CSA, and EC2 demonstrated conservative behaviour when applied to LWC and NWC deep beams without shear reinforcement. Notably, the ratio between predicted and measured shear strengths for LWC deep beams was found to be higher than that for NWC deep

beams across all four STMs considered. This suggests that the current STMs might overestimate the shear strength of LWC deep beams. In conclusion, the study by Yang highlighted the significance of considering the material properties and section geometry in the design and analysis of deep beams. The size effect was more pronounced in lightweight concrete deep beams, indicating the need for careful consideration when using LWC in such structural elements. The findings also indicated that the impact of section overall depth on shear behaviour differs between SLWC and ALWC deep beams. Additionally, the study raised concerns about the conservatism of current strut-and-tie models, particularly in predicting the shear strength of LWC deep beams. These insights contribute to a better understanding of the behaviour of LWC and NWC deep beams, providing valuable guidance for their design and structural analysis.

In 2011, a study was conducted by Gedik and Nakamura [26] to explore the three-dimensional effects in short deep beams that lacked stirrups and experienced shear failure. The investigation employed a combination of experimental and analytical methods. Specifically, two deep beams were selected for testing, both having a/d of 0.5. The beams differed in terms of their widths, which were varied for the purpose of the study. The objective was to analyze and understand the three-dimensional behaviour and failure mechanisms of these short deep beams under shear loading conditions. The analysis of the deep beams was carried out using a three-dimensional rigid-body-spring model (RBSM). The study involved a comparison between the analytical results, which included load-displacement curves and crack patterns, and the experimental findings. Additionally, the research delved into the analysis of three-dimensional deformations, strut widths, and cross-sectional stress distribution in order to gain a comprehensive understanding of three-dimensional behavior. These analytical

results were then compared with the experimental results to elucidate the 3-D effects in short deep beams.

In 2012, Mazin Deewan [27] conducted a study to investigate the shear behavior of deep beams and the effectiveness of strengthening and repairing techniques using carbon fiber reinforced polymer (CFRP) strips. The research focused on three types of concrete: normal-strength concrete, high strength concrete, and lightweight concrete. The experimental work involved fabricating and testing twenty-seven simply supported reinforced concrete deep beams, which were divided into three groups. The results of the experimental work demonstrated a significant improvement in the behavior and load-carrying capacity of the reinforced concrete deep beams when strengthened or repaired with CFRP strips. The deep beams strengthened with CFRP strips exhibited an increase in ultimate load ranging from 17% to 52% for indirectly loaded flanged deep beams and from 12% to 67% for directly loaded rectangular deep beams, compared to the control deep beams. The deep beams repaired with CFRP strips achieved an increase in ultimate load of 54% to 58% compared to the control deep beams. Additionally, the strengthened deep beams displayed a stiffer load-deflection response compared to the corresponding control deep beams. The effectiveness of CFRP with lightweight concrete was found to be lower than that with normal strength concrete and high strength concrete. For the nonlinear finite element analysis in the study, the researchers utilized the ANSYS finite element program (Version 13). By employing this software, they were able to simulate and analyze the behavior of the deep beams under investigation. The results obtained from the finite element analysis were then compared to the experimental findings. It was observed that there was good agreement between the predicted load-deflection behavior from the finite element analysis and the actual behavior

observed in the experiments. However, the finite element models exhibited a slightly stiffer response compared to the experimental results. In conclusion, the study demonstrated that strengthening and repairing deep beams with CFRP strips could significantly improve their behavior and load-carrying capacity. The effectiveness of CFRP varied depending on the type of concrete used. The finite element analysis provided a reliable approximation of the experimental results, although a slight discrepancy was observed in the stiffness of the response.

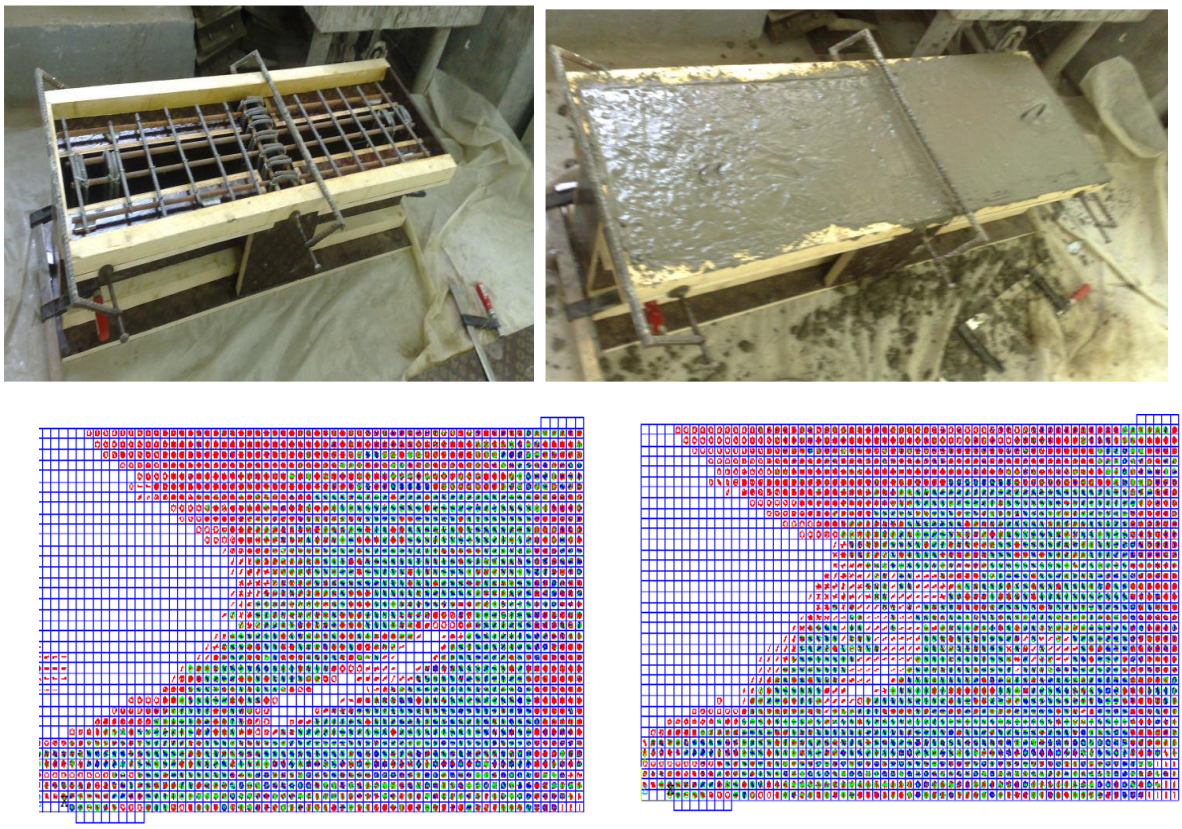

Figure 2- 8 Specimens tested by Mazin

In 2020, Alhussein and Khudhair [28] conducted a study to investigate the impact of replacing coarse aggregate with recycled concrete debris on reinforced concrete rectangular deep beams. These deep beams were cast using self-compacted concrete (SCC) that incorporated recycled concrete as coarse aggregate (RCA). The beams were subjected to both direct and indirect loading

conditions. The experimental work involved testing fifteen deep beams, with two main parameters being studied. The first parameter was the a/d ratio, which determines the geometric proportions of the beam. The second variable was the replacement ratio, which indicated the extent to which the normal coarse aggregate was replaced with RCA. It's important to note that no shear reinforcement was used in the casting of the beams. During the testing process, several aspects of the beam behavior were carefully recorded and analyzed. These included the cracking load, ultimate load, concrete strain, and mid-span deflection. Upon analyzing the test results, it was observed that the inclusion of RCA had a notable effect on the beam behavior. Specifically, the values of both the cracking load and ultimate load were reduced when RCA was incorporated into the concrete mixture. This suggested that the presence of RCA influenced the load-carrying capacity and strength of the beams, leading to a decrease in their overall performance. As the RCA replacement increased by 25%, 50%, and 75%, the cracking load decreased by 9%, 23%, and 50% respectively. Similarly, the ultimate load decreased by 2%, 23%, and 25%, with the corresponding increase in RCA replacement for a fixed a/d ratio of 1.0. Furthermore, it was observed that increasing the (a/d) ratio resulted in a decrease in the ultimate load. This was attributed to a lower contribution of arch action shear transfer in beams with higher a/d ratios. In conclusion, the study by Alhussein and Khudhair demonstrated that the presence of RCA in deep beams cast with self-compacted concrete (SCC) had a detrimental effect on the cracking load and ultimate load. The reduction in load-carrying capacity was more pronounced with higher replacement ratios of RCA. Additionally, increasing the shear span to the (a/d) ratio led to a decrease in the ultimate load, primarily due to diminished arch action shear transfer. These findings provide valuable insights for the design and assessment of deep beams incorporating recycled concrete debris.

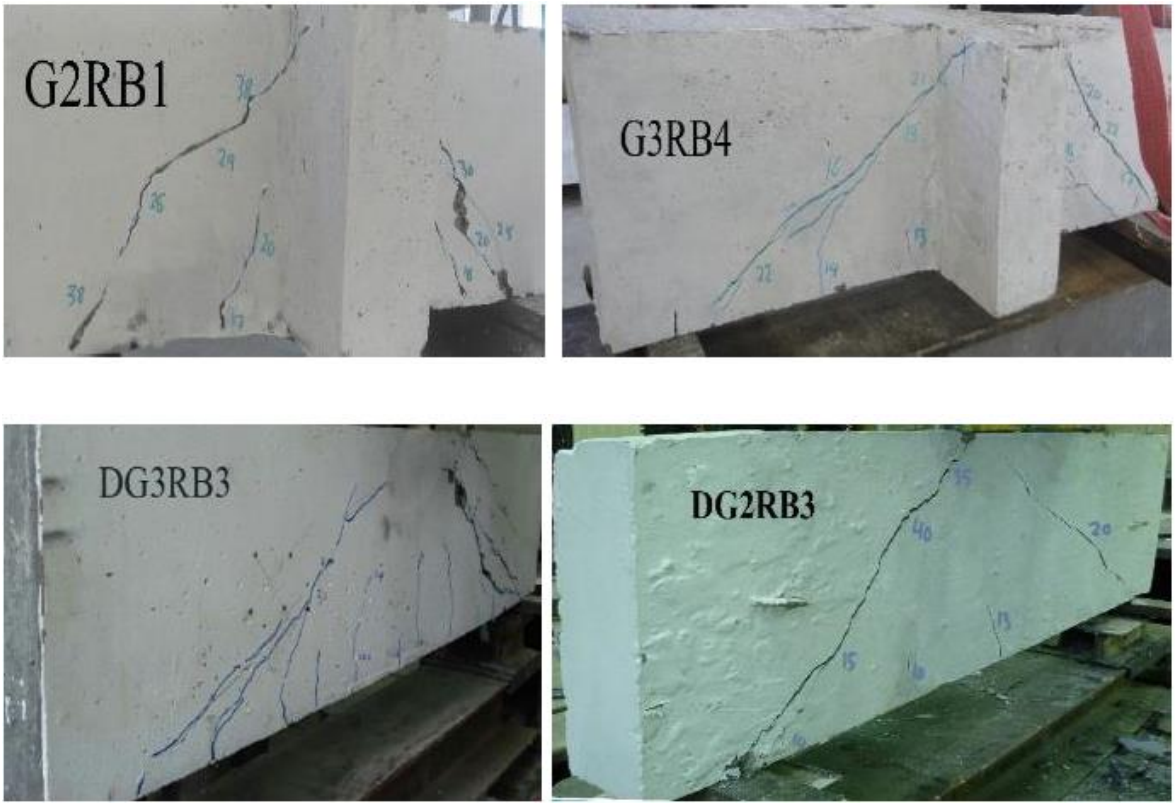

Figure 2- 9 Specimens tested by Alhussein and Khudhair

In 2022, Kachouh et al. [29] examined the effect of recycled aggregate on the shear behavior of steel fibers reinforced concrete with the opening. The research aimed to investigate the shear response of RC deep beams with openings, particularly those constructed using 100% RCA. The main aim of the study was to assess the potential efficacy of substituting steel fibers for the minimum conventional steel stirrups in deep beams with web openings, which were constructed using RCA. The presence of web openings and the incorporation of RCA in the concrete mix contributed to the complexity of the beams' structural behavior. The experimental investigation involved testing RC deep beams with web openings that were constructed using 100% RCA. The beams were subjected to shear loading to evaluate their shear response. The presence of web openings in the beams allowed for the examination of the behavior and performance of RCA-based deep beams under shear forces. Seven RC deep beams were constructed and tested in the study, all having a/d of 0.8.

Each beam featured a circular opening positioned at the midpoint of the shear span, with an opening height-to-depth ratio of 0.3. Several test parameters were considered, including the type of coarse aggregate NA and RCAs, the volume fraction of steel fibers (vf = 1%, 2%, and 3%), and the presence of minimum conventional steel stirrups. The experimental results indicated that the RC deep beam specimens with web openings made entirely with RCAs experienced reductions in shear capacity ranging from 13% to 18% compared to their counterparts constructed with NAs. When 100% RCA were incorporated into RC deep beams with openings, the effectiveness of conventional steel stirrups in enhancing the shear response was found to be limited. In contrast to the limited effectiveness of conventional steel stirrups, the study found that the inclusion of steel fibers had a significant positive impact on the shear response of the tested beams made with RCA. By incorporating steel fibers into the mix, the shear capacity of the RCA-based beams was notably enhanced. Specifically, the study observed an increase in shear capacity ranging from 39% to 84% when steel fibers were added to the RCA-based beams. This improvement in shear capacity demonstrated the effectiveness of steel fibers in reinforcing the beams and enhancing their resistance to shear forces. Comparatively, the use of conventional steel stirrups resulted in a more modest increase in strength, with an observed improvement of 18% in shear capacity. n the absence of conventional steel stirrups. It was found that this level of steel fiber reinforcement was capable of restoring 96% of the original shear capacity observed in the NA-based (non-aggregate) beam with conventional steel stirrups. This indicates that the addition of steel fibers at a volume fraction of 1% was highly effective in improving the shear capacity of the RCA-based beams, bringing them close to the performance of the NA-based beam with conventional steel stirrups. The ratio of the predicted shear capacity to the measured shear capacity fell within the range of 0.71 to 1.49, indicating that the analytical models provided reasonably accurate estimations of

the shear capacity. In summary, the study revealed that RC deep beams with openings constructed using 100% RCA experienced reduced shear capacities compared to those made with NAs. The inclusion of steel fibers proved to be an effective means of enhancing the shear response of RCA-based beams. The study's findings contribute to the understanding of the behavior and reinforcement techniques for RC deep beams with web openings made with RCA, providing valuable insights for sustainable construction practices.

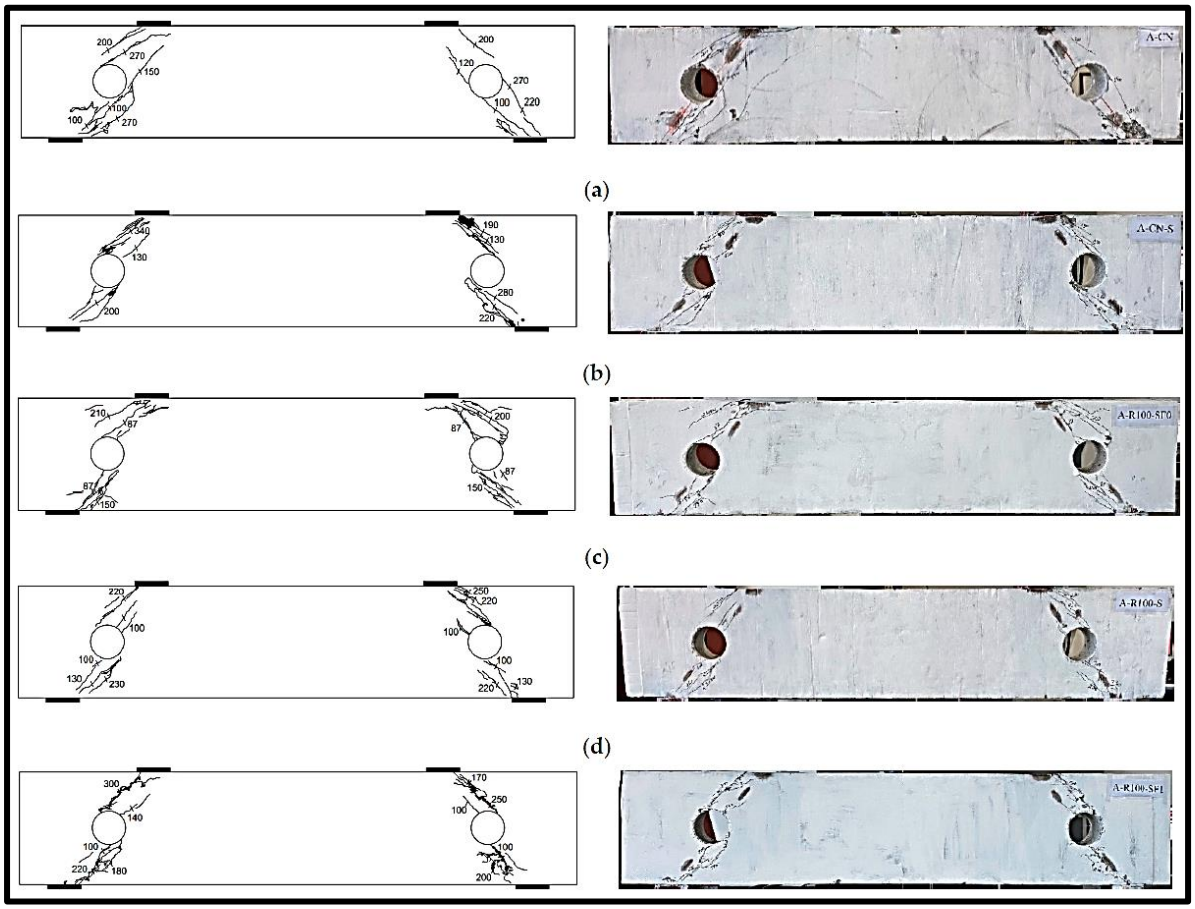

Figure 2- 10 Specimens tested by Kachouh et al

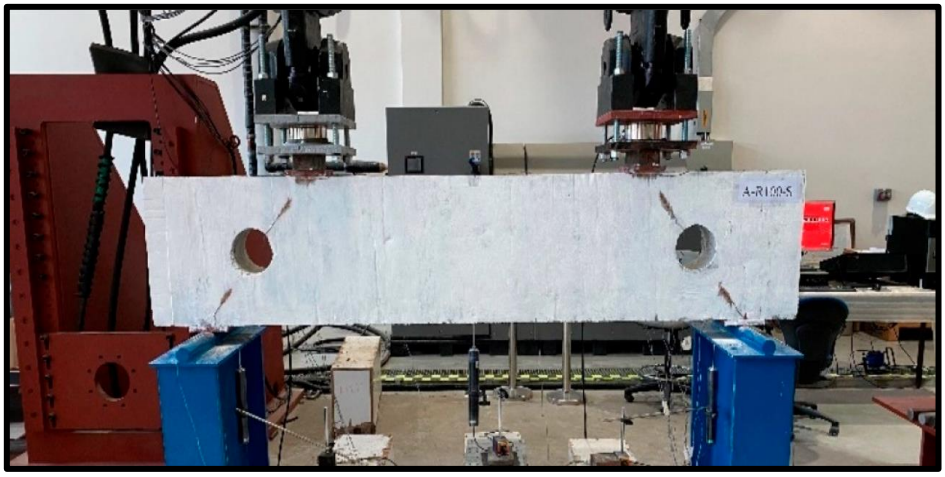

Figure 2.10 Cont. [29].

In 2023, Sagheer and Tabsh [30] conducted an experimental study focusing on the shear behavior of deep beams. The study involved an experimental program in which fifteen half-scale beams were tested in shear without the use of stirrups. A theoretical component was also included, along with the experimental program. The results of the study revealed that the shear strength of recycled concrete beams utilizing 50% recycled coarse aggregate was approximately 27% lower on average compared to beams made with natural aggregate. These findings were obtained when the beams were tested at a shear span-to-depth ratio of 1.15. Interestingly, when the beams were subjected to a higher shear span-to-depth ratio of 2.5, the shear strength of the recycled concrete beams became nearly equal to that of beams made with natural aggregate. This suggests that the influence of the recycled coarse aggregate on shear strength diminishes as the shear span-to-depth ratio increases. On the other hand, beams utilizing 100% recycled aggregate had an average shear strength approximately 5% lower than their natural aggregate counterparts, regardless of the shear span-to-depth ratio.

Figure 2- 11 Specimens tested by Sagheer and Tabsh

2.4 Summary

The use of recycled and alternative materials in concrete has been an area of extensive research in recent years, driven by the need for more sustainable and environmentally-friendly construction practices. One such material that has gained attention is recycled bricks aggregate. Several studies have investigated the properties and performance of concrete containing recycled bricks but these studies were limited in providing a wide range of parameters offers fully understand to the concrete made with recycled bricks such as:

1- The studies didn't used methods for curing the recycled bricks to avoid the defects and the negative effect of the recycled bricks impurities.
2- The replacement ratio didn't exceed high replacement ratio without failing in the mechanical properties.
3- The previous studies lack in use the concrete made with recycled bricks in RC members such as beams, column, slabs. Etc.
4- Modifying the concrete mixtures made with recycled bricks to improve the properties of fresh and hardened concrete was limited in previous studies.
5- Previous investigations were limited in use of many types of recycled bricks.

CHAPTER THREE: EXPERIMENTAL PROGRAM

3.1 Introduction

Laboratory tests were conducted on the materials used, and the casting and testing of specimens took place in the laboratories of the Faculty of Engineering at the University of Misan. The experimental work involved the testing of nine deep beams with utilizing of several parameters. Table 3.1 presents the parameters that were considered in this study.

Table 3- 1 Deep beams parameters.

No.	Beams Variables
1	Replacement ratio of recycled bricks
2	Use of burned crushed recycled bricks
3	Curing Method

3.2 Testing Program

The first stage of the process involves selecting the construction materials and conducting physical and chemical tests on them. This helps in determining the optimal and most suitable proportions of the concrete mixtures by specifying the quantity and ratio of each material, including additives. In the second stage, experimental models are tested to obtain the mechanical properties of the mixtures. Subsequently, beams are cast and subjected to test until failure occurs. This allows for a comprehensive evaluation of the structural performance and strength characteristics of the beams.

3.3 Materials

The selection of samples, including their quantity, type, and quality, was meticulously carried out based on an extensive study. This careful selection

process was conducted before the casting of concrete beams. The materials utilized in this investigation were commercially available and included cement, both natural and recycled aggregates, natural sand, water, and a superplasticizer. These materials were chosen to represent real-world construction scenarios and to ensure the validity and relevance of the study's findings.

3.3.1 Cement

In this investigation, Portland Iraqi cement manufactured by the Cresta factory was exclusively used. The testing of materials was conducted at Misan University. To preserve its properties, all the cement was carefully transported and stored in a dry and moderate-temperature environment. A comprehensive set of laboratory tests, encompassing both chemical and physical analyses, were performed. The specific tests conducted can be found in Tables (3.2) and (3.3). These tests were carried out following the ASTM C191[31] standard, and the results complied with the Iraqi standard 5/2019 [32]. The selection of cement as a material in this study hinged on the outcomes of the laboratory tests, which were crucial in determining its quality and suitability for research purposes.

Table 3- 2 Physical properties of ordinary Portland cement

Physical Properties	Test Results	Limit of Iraqi specification
Setting time using Vicats Method		
Initial (hrs: min)	2:00	≥45 min
Final (hrs: min)	3:45	≤10 hrs
Compressive strength of mortar		
3 day (Mpa)	21.2	≥15
7day (Mpa)	27.8	≥23
28day (Mpa)	34.7	-

Table 3- 3 Chemical composition of cement.

Compound Composite	Chemical Composite	% by Weight	Limits of Iraqi specification No.5/1984 [32]
Lime	Cao	63.96	-
Silica	Sio2	21.32	-
Alumina	Al2o3	4.58	-
Iron oxide	Fe2o3	3.25	-
Magnesia	MgO	2.44	≤5%
Sulfate	So3	2.32	≤2.8%
Loss on ignition	L.O.I	3.61	≤4%
Insoluble residue	I.R	1.17	≤1.5%
Lime saturation factor	L.S.F	0.75	(0.66-1.02)%
Tricalcium silicate	C3S	50.69	-
Dicalcium silicate	C2S	18.28	-
Tricalcium aluminate	C3A	8.14	-
Tetracalcium alumminoferrite	C4AF	9.89	-

3.3.2 Aggregate

A. Fine Aggregate (Sand):

In this investigation, the normal sand was specifically sourced from the Al-Zubair region in Basra, chosen for its availability and relevance to the study's geographical context. The sand tests were conducted at Misan University, specifically within the College of Engineering, which possesses the necessary facilities and expertise for conducting such tests. To evaluate the particle size distribution of the sand, the sieve analysis test was performed according to ASTM C-136 [33]. This test method involves passing the sand through a series of sieves with different mesh sizes to separate and measure the different particle sizes present in the sample. The results of the sieve analysis help determine the gradation and suitability of the sand for use in concrete. Tables 3.4 & 3.5 and Figure 3.1 showcase the sand grading used for normal concrete in the study. These tables provide detailed information about the particle sizes and their corresponding percentages within the sand sample. It is worth noting that the sand

used in this investigation complies with Iraqi Specifications Iraqi standard 5/2019 [32]., indicating that it meets the required standards and specifications outlined by the Iraqi authorities. By conducting these tests and ensuring compliance with relevant standards, the study authors aimed to ensure the quality and appropriateness of the sand as a crucial component in the concrete mixture. This meticulous approach enhances the reliability and validity of the research findings and supports the overall integrity of the study.

Table 3- 4 Grading of the fine Aggregate.

No.	**Sieve size (mm)**	**% Passing by weight**	
		Fine Aggregate	**Limits of IOS No. 45/1984-Zone 2 [32]**
1	10	100	100
2	4.75	99	90-100
3	2.36	90	75-100
4	1.18	75	55-90
5	0.60	53	35-59
6	0.30	17	8-30
7	0.15	2	0-10

Table 3- 5 Physical properties of the fine Aggregate.

Physical Properties	Test results	Limits of IOS No.45/1984
Specific gravity	2.65	-
Sulfate content(SO3) %	0.33	≤ 0.5
Absorption %	1.1	-
Loose bulk density kg/m3	1645	-

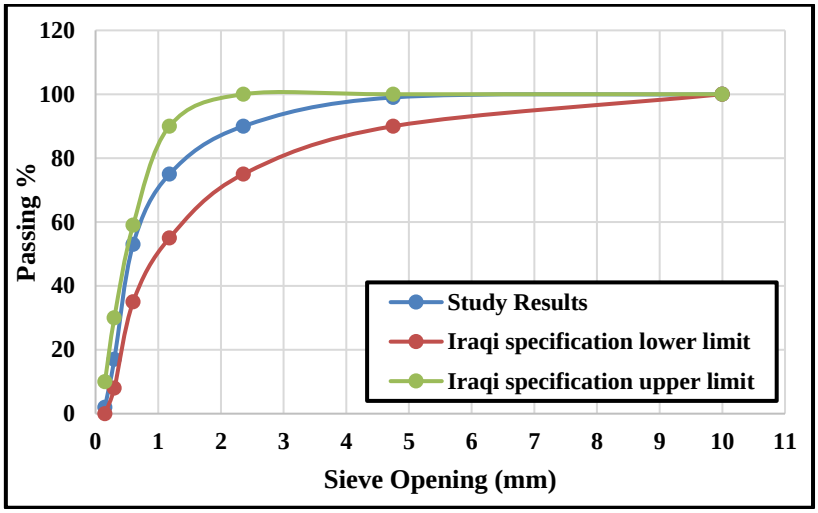

Figure 3- 1 Grading graph of fine Aggregate.

3.3.3. Coarse Aggregate (Gravel):

Crushed gravel was included in the concrete mix used for this investigation. The grading of the crushed gravel was carefully selected to meet the requirements outlined in the Iraqi Specification No. 45/1984 [32] for graded gravel, as seen in Figure 3.2. This specification ensures that the gravel meets the necessary standards for use in construction applications. To assess the particle size distribution of the crushed gravel, the sieve analysis test was performed following the ASTM C136 guidelines [33]. This test method involves passing the gravel through a series of sieves with different mesh sizes to separate and determine the particle sizes present in the sample. The results of the sieve analysis help verify the compliance of the crushed gravel with the specified grading requirements. By satisfying the Iraqi specification and conducting the sieve analysis test, the researchers ensured that the crushed gravel used in the concrete mix met the necessary standards and provided the desired characteristics for the study. This attention to detail in material selection and testing contributes to the reliability and accuracy of the research outcomes.

Table 3- 6 Grading of the coarse Aggregate.

No.	Sieve size	Cumulative passing%	Limits according to IQS 45/1984	Iraqi specification lower limit	Iraqi specification upper limit
1	37.5	100	100	100	100
2	20	100	97.5	95	100
3	14	84.63	85	80	90
4	10	46.64	45	30	60
5	5	2.92	5	0	10

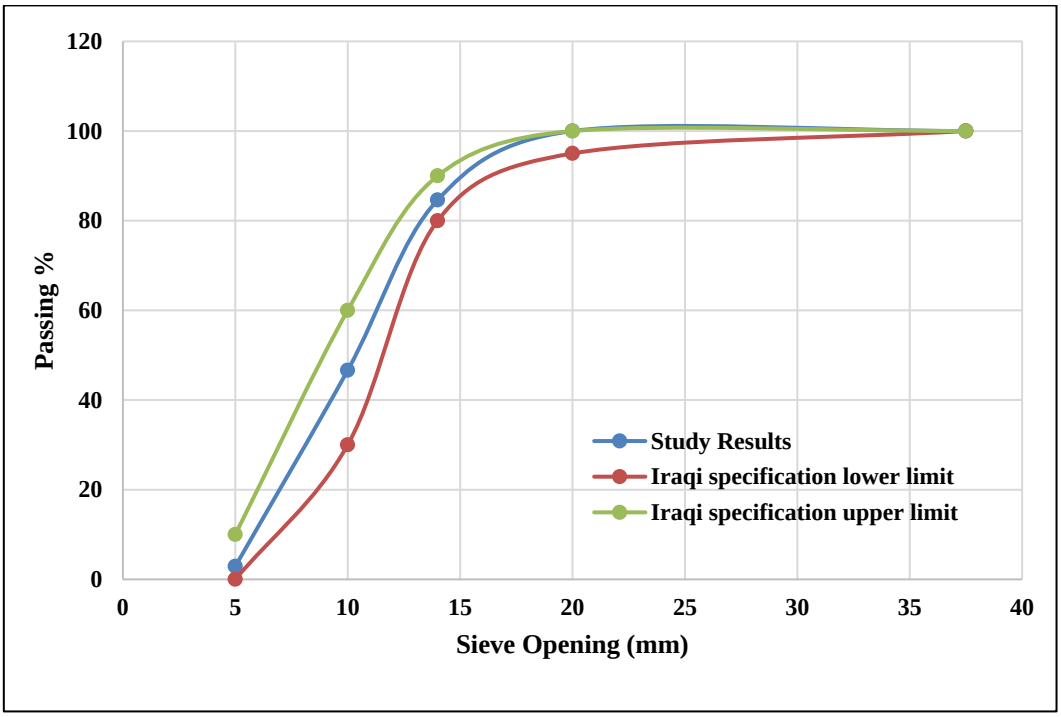

Figure 3- 2 Grading graph of coarse Aggregate.

3.3.4. Recycled bricks:

The recycled bricks used in this investigation were obtained from the demolition of walls. These bricks were carefully collected and brought to the laboratory for testing purposes. By utilizing recycled bricks, the study aimed to explore the feasibility and potential benefits of incorporating sustainable construction materials into the concrete mix. Once in the laboratory, the recycled bricks underwent testing to assess their properties and suitability for use in the

study. These tests likely included evaluations of strength, durability, and other relevant characteristics to ensure that the recycled bricks met the necessary standards and could effectively contribute to the desired concrete mixture. In this investigation, Recycled bricks were crushed using both hand hammers to produce aggregates with a required size range of (5-20) mm. This size range was chosen to meet the project's specifications and requirements. To ensure the quality of the crushed aggregate, it was screened using a standard sieve series that complied with the I.Q.S. 45/1985 limits. The sieve analysis results, outlining the particle sizes within the Aggregate is presented in Table (3-6). By adhering to the specified limits, the researchers ensured that the crushed aggregate met the required grading standards. The burnt aggregate, obtained from the recycled bricks, underwent a treatment process using a Sodium Hypochlorite solution. This treatment process, which lasted for 24 hours, was based on previous work. The purpose of this treatment was to modify the properties of the burnt Aggregate. After the treatment, the aggregates were thoroughly rinsed with tap water and dried for subsequent use in the study. All of these processes, including the crushing, screening, treatment, rinsing, and drying, were conducted at the Structural Laboratories of Misan University/ Engineering College. The laboratory facilities and equipment provided a suitable environment for carrying out these operations. Figure (3.3) depicts the rehabilitation of recycled bricks.

Figure 3- 3 Recycled bricks production.

3.3.5 Water

In this investigation, R.O. water was utilized for both the Preparation and curing of the specimens. R.O. water is a purified form of Water obtained through

the reverse osmosis process, which removes impurities and contaminants from the Water. The use of R.O. water in concrete specimen preparation ensures that the Water does not introduce any unwanted impurities or chemicals that could potentially affect the properties or performance of the specimens. It helps maintain the purity and consistency of the Water used in the concrete mixture. Additionally, R.O. water was employed to cure the specimens.

3.3.6 Superplasticizer

Additives play a major role in controlling the mechanical properties of concrete in addition to its workability and other properties. The most important of these additives are water reducers, which are the main factor in improving the workability of the concrete mixture, making the mixture more workable and less Water needed. One of the fastest-growing chemical additives on the cement market and on the concrete additives market are superplasticizers, also known as high-range water reduction agents. In the production of free-flowing concrete, the Superplasticizer was used to obtain self-compacting concrete with desired workability and resistance to segregation. In the present study, Glenium 51 superplasticizer is compliant with ASTM C494-99 [34]. Table 3.6 illustrates the properties and testing results of the Glenium 51 superplasticizer.

Table 3.6 Types, appearances and relative density of superplasticizers.

Superplasticizer	Company	Relative density	Appearance
Glenium 51	MBCC	1.05	Light yellow liquid

3.3.7 Silica Fume

In this study, Silica fume, also known as microsilica, is used in concrete mixture. The specific gravity of silica fume utilized in this study is reported as 2.2. In this study, a sieve with a mesh size of 0.125 mm was used. The silica fume

was passed through this sieve to obtain a powder with particle sizes smaller than 0.125 mm. The choice of a particle size less than 0.125 mm for the silica fume powder in this study aligns with the guidelines provided by EFNARC (European Federation for Specialist Construction Chemicals and Concrete Systems) in 2005 [35]. This replacement helps improve various properties of the concrete, such as workability, flowability, and durability.

3.3.8 Steel Reinforcement

In this study, steel reinforcement rebar was employed as both transverse and longitudinal reinforcement in the concrete specimens. The rebar used had three different sizes: Ø10 mm, Ø12 mm, and Ø16 mm, indicating their respective diameters. A tensile test was performed to verify the quality and applicability of the steel reinforcement, following the guidelines outlined in the ASTM A615 specification [36]. ASTM A615 is a globally acknowledged standard that offers requirements for the mechanical characteristics and excellence of deformed steel bars employed in reinforcing concrete. Table 3.7 displays the findings from the tensile test conducted on the steel reinforcement.

These results were obtained by subjecting the steel reinforcement samples to tension until fracture and measuring various mechanical properties, such as yield strength, ultimate tensile strength, and elongation. The values obtained from the tensile test were then compared to the limitations and criteria outlined in the ASTM A615 specification [36]. By ensuring that the results conform to the limitations specified in the ASTM A615 specification, the study confirms that the steel reinforcement used in the concrete specimens meets the required mechanical properties and quality standards. This verification is essential to ensure the reliability and performance of the reinforced concrete structures under investigation.

Table 3- 7 Properties of reinforcing bars.

Bar size (mm)	Test results			ASTM A615/A615M-06b [36] limits		
	Yield stress (N/mm^2)	Ultimate Strength (N/mm^2)	Elongation (%)	Yield stress Min.(N/mm^2)	Ultimate strength Min.(N/mm^2)	Elongation Min. (%)
10	500	650	14	420	620	9
12	480	630	13	420	620	9

3.4 Mixing procedure for Natural Aggregate and Recycled bricks

In the study, the mixed design of the concrete was a significant aspect that influenced the overall properties and performance of the beams. The process of creating a concrete mixture involves considering the characteristics of the materials used and determining the appropriate mix proportions. In this particular study, four trial concrete mixes were prepared to achieve two types of concrete. The first type of concrete utilized natural coarse aggregate, while the second type incorporated recycled concrete bricks as a partial replacement for the natural coarse aggregate. By replacing a portion of the natural coarse aggregate with recycled concrete bricks, the study aimed to investigate the effects of incorporating recycled materials on the properties and behavior of the concrete mixture. The replacements were 0%, 5%, 10%, 20% and 40% at curing time with (7 & 28 days). Concerning the mixing procedure, the mixing preparation is important to obtain the required workability and homogeneity of the concrete mix. In the research conducted, high speed mixer was used to mix the concrete component. Before initiating the mixing process, it was crucial to ensure that the mixer was clean, moist, and free from any excess water. This step is necessary to create an optimal environment for the mixing process. Based on previous work, a fixed mixing procedure was adopted and followed consistently throughout the research. This procedure was specifically designed to achieve two objectives: maximize the efficiency of the superplasticizer and ensure the complete

dispersion of its particles within the mortar or concrete mixture. Concrete mixing is implemented in several stages, which include first adding the cement and then sand. water and Superplasticizer were added to the mix. Then, then the coarse aggregate was added. To avoid the conglomerate in the mix and offer higher workability and a good consistency for the concrete mix, the materials are added gradually in small amounts. It should be noted that the mixing time is 10 min.

For concrete mixes with the replacement of aggregate, mixing took longer than expected. A quick mixing process of the components must be taken into account to ensure a more uniform distribution of the concrete components, especially the recycled bricks. For the splitting test, a cylinder with dimensions of (100x200) mm was cast. A (100x100x100) mm cube mould for a compressive strength test and (a 100x100x500) mm prism mould for a flexure strength test were implemented. The trial mixes are presented in Tables 3.8, while the results are shown in Table 3.9. At the end of 24 h after casting, the concrete was removed from the moulds and was put in the curing basin underwater until the age of 28 days. As illustrated in Figure 3.4, three mixed designs were carried out for recycled bricks concrete for each trial, which included using a different ratio of recycled bricks and addition.

For the experimental investigation, four different concrete mixes are prepared, and the reference mixture serves as a baseline and does not include crushed bricks (normal concrete (NC)). The proportions of the components are in a ratio of 1:1.5:3. The second one is crushed brick (CBC) treated with cement solution, which involves utilizing various weights of crushed bricks, based on a percentage of the natural coarse aggregate (NA) weight, are incorporated into the mix and treated with a cement solution. The third type is burned brick mixture (B-CBAC), which is made using burned bricks treated with cement. The last one (B-CBAC HCL) is crushed brick treated with hydrochloric acid (HCL) at concentrations of 5% and 10%.

Table 3- 8 Proportions of constituent materials in R.B.C. mixes.

Material /(kg/m3)	NC	CBC	B-CBAC	B-CBAC HCL
Cement.	500	500	500	667.125
Sand.	750	750	750	667.125
Coarse aggregate kg/m$^{3.}$	1500	1350	1350	1267.53
Super P.S.	0.5%	0.5%	0.5%	0.5%
C.B.C. Kg/m^3	-	150	150	126.753
Silica fume.	-	-	-	10%
w/c.	0.42%	0.38%	0.38	0.35

Figure 3- 4 Concrete specimens' fabrication.

3.5 Fresh Concrete Tests

In the experimental program, an important aspect was the selection of appropriate concrete mixtures to achieve the desired concrete properties. This involved carefully choosing the proportions of various ingredients, such as cement, aggregates, Water, and any additional admixtures or fillers, based on the specific objectives of the study. The fresh concrete mixtures investigate the consistency of concrete during the casting. Once the concrete mixtures were prepared, then the hardened tests were performed such as casting cubes and cylinders ..etc.

3.5.1 Slump Flow Test

As per EFNARC [15], it is necessary to conduct the essential tests to assess the flowability of mixtures. These tests can be conducted as follows:

1. Positioning the boards with the ring on the ground by placing them in a horizontal orientation.

2. Cleansing and smoothing the surfaces of the materials.

The next stage involves identifying the central position of the cone board.

4. Pouring concrete into the cone without applying pressure and letting it rest for about one minute after filling.

5. The timing commenced when the slump cone was raised and documented, and the concrete was given time to attain a diameter of 50 m (this is known as the m50 m time).

In order to ascertain the slump flow, the maximum breadth of the flow, represented by $dmVx$, and the width perpendicular to it, represented by $dperp$, were measured.

$$\text{Slump Flow} = \frac{(d_{max.} + d_{perp.})}{2} \qquad \text{..... (3.1)}$$

Figure 3.4 Continues

3.6 Hardened Testing

In the laboratory, the majority of specimens for hardened state tests are cast in moulds. After casting, the specimens are left undisturbed in the moulds for a specific period, typically 24 hours. During this time, the concrete undergoes initial setting and early strength development. After 24 hours, the specimens are demoulded, carefully removed from the moulds. To ensure proper curing and development of strength, the moulded specimens are then placed in water for the designated curing duration until they reach the desired testing age. Water curing involves submerging the specimens in water, typically in tanks or containers, to maintain a consistent and moist environment. This moist curing process facilitates hydration and further strength gain in the concrete. By following this curing procedure, the specimens are allowed to achieve the desired level of hydration and strength development before they are tested in the hardened state.

3.6.1 Compressive Strength Test

Three cubes of (150*150*150) mm for normal concrete and six cubes for R.C.B and cylinders (100 x 200) mm with the same number of specimens were cast to determine the compressive strength. All specimens are cured in the water basin for the full hardening period (28 days). According to Table 3.9, three specimens were used for each mixture to test the compressive strength of concrete; compressive strength was (54.03, 41.79, 39.51, 31.45, 19.74, and 13.63) MPa for the replacement ratios (0%, 5%, 10%, 20% and 40%) respectively.

Table 3- 9 Compressive strength test at 28 days.

Mix	Mix	RA%	*f'c* - Cube (MPa)	*fcu* - Cylinder (MPa)
NSC	S1	0%	58.00	39.30
	S2	0%	49.20	37.50
	S3	0%	54.90	38.47
RBC-5% (CBC)	S4	5%	41.30	33.04
	S5	5%	43.12	34.50
	S6	5%	38.77	31.02
RBC-5% (B-CBAC)	S7	5%	36.37	32.37
	S8	5%	32.78	26.46
	S9	5%	34.19	32.89
RBC-5% (B-CBAC-HCL)	S10	5%	45.00	36.45
	S11	5%	52.80	39.48
	S12	5%	53.40	40.76
RBC-10% (CBC)	S13	10%	36.35	28.76
	S14	10%	37.90	18.40
	S15	10%	35.20	26.80
RBC-10% (B-CBAC)	S16	10%	33.40	31.80
	S17	10%	30.10	24.30
	S18	10%	31.40	30.20
RBC-10% (B-CBAC-HCL)	S19	10%	45.00	33.55
	S20	10%	43.00	33.02
	S21	10%	42.00	30.88
RBC-20% (CBC)	S22	20%	19.32	13.49
	S23	20%	20.14	15.06
	S24	20%	18.71	14.28
RBC-20% (B-CBAC)	S25	20%	17.75	13.63
	S26	20%	16.00	11.41
	S27	20%	16.69	11.66
RBC-20% (B-CBAC-HCL)	S28	20%	23.91	19.37
	S29	20%	22.85	17.09
	S30	20%	22.32	17.04
RBC-40% (CBC)	S31	40%	13.43	10.31
	S32	40%	11.84	8.45
	S33	40%	15.63	10.92

3.6.2 Splitting Tensile Strength

In the investigation of tensile strength capacity, three cylindrical specimens were cast and tested for each replacement ratio. The dimensions of each cylinder were 100 mm in diameter and 200 mm in height. These dimensions adhere to the

specified requirements for conducting the tensile strength test. The testing procedure followed the guidelines outlined in the ASTM C496 specification [37]. ASTM C496 [37] provides standardized procedures for determining the tensile strength of concrete cylinders using a splitting tensile test method. During the test, a tensile stress was applied to the cylindrical specimens. This stress caused a longitudinal crack to occur in the cylinders. The crack, resulting from the tensile stress, led to a splitting or separation of the cylinder along the plane of the crack. Figure 3.5 illustrates the occurrence of the longitudinal crack and the subsequent splitting in the cylinder. This visual representation helps to depict the failure mode and the effect of the applied tensile stress on the specimen.

Figure 3- 5 splitting tensile test.

3.6.3 Flexural Strength

In the study, the flexural strength of the concrete specimens for each replacement ratio was evaluated using the results obtained from testing prisms. The flexural strength testing followed the ASTM C78-02 [38] standard, which provides guidelines for conducting third-point loading tests on concrete beams.

Test prisms with dimensions of 100 mm x 100 mm x 500 mm were cast and cured under the same conditions as the specimens used for the compressive strength tests. The curing conditions typically involve maintaining a specified temperature and moisture level to promote proper hydration and the development of strength in the concrete. For the flexural strength testing, a testing machine with a capacity of 2000 kN (kilonewtons) was used. This loading configuration induces bending stresses within the beam, allowing for the determination of its flexural strength. Flexural strength (MPa) is obtained by Three simply supported prisms with dimensions of (100x100x500) mm tested as revealed in Figure 3.6. The prism specimen was fabricated and tested after 28 days. The flexural tests were carried out according to the American specification ASTM C78 [38].

Figure 3- 6 Flexural test.

3.6.4 Static Modulus of Elasticity Test (E_c)

Tests of specimens for modulus of elasticity were carried out according to the ASTM C469 [39]. The testing specimens of the modulus of elasticity or the Young modulus have dimensions of (150x300) mm, as shown in Figure 3.7, where three samples were examined for each concrete mix.

Figure 3- 7 Modulus of Elasticity Test.

Table 3.9 Compressive strength test at 28 days.

Mix	Mix	RA%	Tensile Strength (MPa)	Flexural Strength (MPa)	*Modulus of Elasticity* (MPa)
NSC	S1	0%	5.96	8.75	31466.50
	S2	0%	6.04	8.87	31875.56
	S3	0%	6.12	8.98	32162.44
RBC-5% (CBC)	S4	5%	3.66	5.37	26431.86
	S5	5%	3.70	5.44	26775.47
	S6	5%	3.75	5.51	27016.45
RBC-5% (B-CBAC)	S7	5%	3.69	5.41	27671.51
	S8	5%	3.73	5.48	28031.24
	S9	5%	3.78	5.55	28283.53
RBC-5% (B-CBAC-HCL)	S10	5%	4.18	6.14	28324.56
	S11	5%	4.24	6.22	28692.78
	S12	5%	4.25	6.30	28951.02
RBC-10% (CBC)	S13	10%	2.22	3.25	23044.86
	S14	10%	2.25	3.30	23344.45
	S15	10%	2.27	3.34	23554.55
RBC-10% (B-CBAC)	S16	10%	2.75	4.03	24171.76
	S17	10%	2.78	4.09	24485.99
	S18	10%	2.82	4.14	24706.36
RBC-10% (B-CBAC-HCL)	S19	10%	3.16	4.64	26105.50
	S20	10%	3.20	4.70	26444.87
	S21	10%	3.24	4.76	26682.87
RBC-20% (CBC)	S22	20%	1.52	2.23	19396.39
	S23	20%	1.54	2.26	20177.44
	S24	20%	1.56	2.29	21468.13
RBC-20% (B-CBAC)	S25	20%	1.63	2.40	19997.67
	S26	20%	1.65	2.43	20802.94
	S27	20%	1.68	2.46	21489.60
RBC-20% (B-CBAC-HCL)	S28	20%	1.74	2.55	20057.67
	S29	20%	1.78	2.59	20865.34
	S30	20%	1.79	2.62	21704.49
RBC-40% (CBC)	S31	40%	0.54	0.79	13258.12
	S32	40%	0.48	0.48	13791.99
	S33	40%	0.44	0.44	14346.67

3.7 Beams details

This study encompassed a comprehensive investigation involving the casting and testing of concrete deep beams. A total of nine concrete beams were experimentally designed and fabricated, incorporating various parameters, as revealed in Figure Table 3.10. The rectangular beams had dimensions of (150 x 500 x 1300) mm and were reinforced with bottom steel rebar of (2 ϕ 16) and (3 ϕ 12) as the main reinforcement. Regarding the shear reinforcement, the deep beams are reinforced with Ǿ10 @ 10 cm. Figure 3.8 illustrates all the beam specimens used in the study.

Table 3-10 Details of beams.

Beam Status/Var.		Beam ID	Beam Dim.	a/d	Grading Size of recycled bricks (mm)	Loading Points
Experimental Shear Beams	Grading Size (19—20) mm	GA-N	150 x 500 x 1300	2	20	One-point load
		GA-5	150 x 500 x 1300	2	20	One-point load
		GA-10	150 x 500 x 1300	2	20	One-point load
	Grading Size (10—12) mm	GB-N	150 x 500 x 1300	2	12	One-point load
		GB-5	150 x 500 x 1300	2	12	One-point load
		GB-10	150 x 500 x 1300	2	12	One-point load
	Shear-to-depth ratio	GC-N	150 x 500 x 1300	1	20	Two-point load
		GC-5	150 x 500 x 1300	1	20	Two-point load
		GC-10	150 x 500 x 1300	1	20	Two-point load

a/d = 1, a/d= 1.444
a/d = 2, a/d=0.962

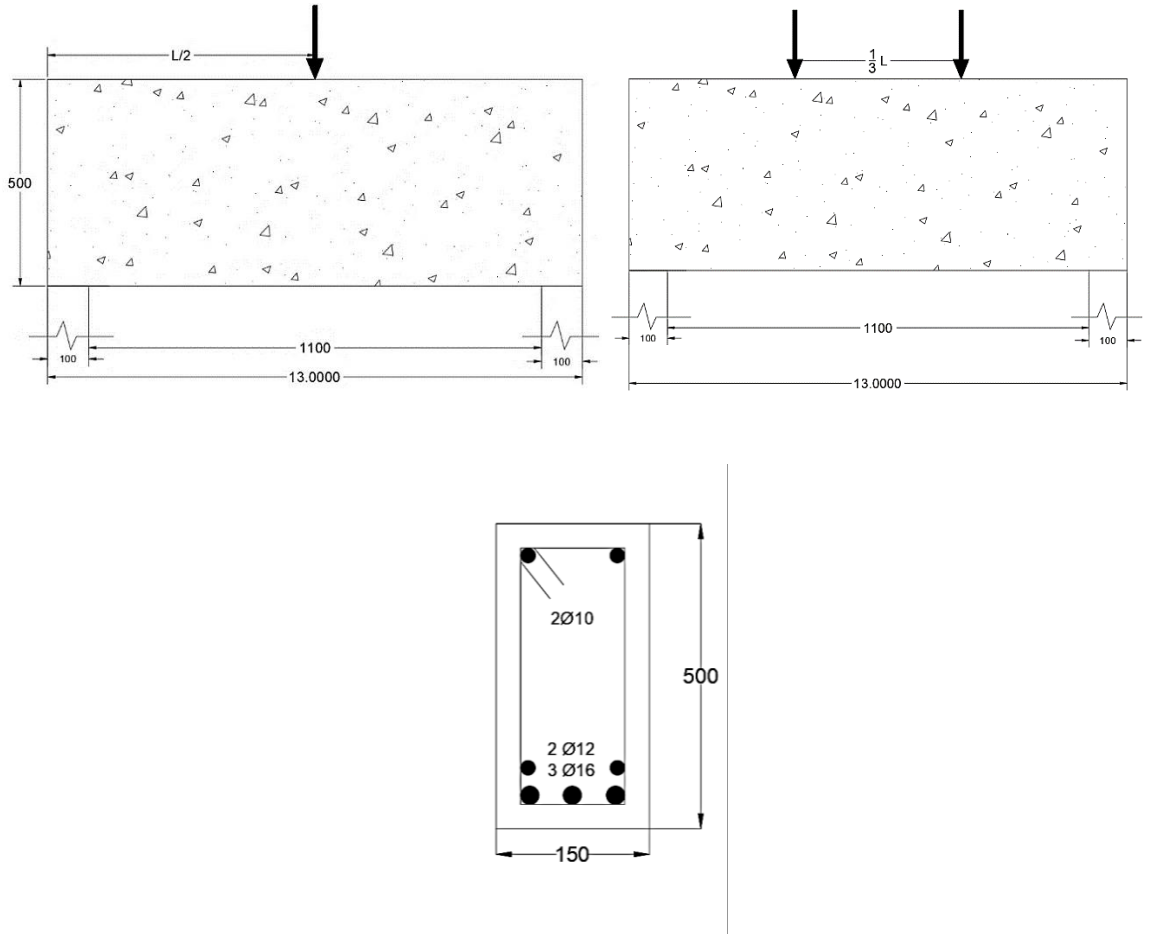

Figure 3- 8 Geometrical details of the R.C. beams.

3.7 Mould Preparation

In the research work, a total of nine moulds were utilized. These moulds were designed to match the dimensions of the fabricated beams, which measured 150 mm x 500 mm x 1300 mm. The moulds were an essential component in the process of casting the concrete beams. To prepare the moulds, they were first cleaned and then coated with oil using a scraper and a steel brush. This oil coating is applied to facilitate the demolding process, ensuring that the concrete beams can be easily removed from the moulds without any damage or sticking. The forms for the beam specimens were created using 20 mm plywood sheets. These plywood sheets were carefully cut and assembled to ensure accurate vertical sides and create 90-degree corners. The plywood was used to form the bottom part of

the mould, as illustrated in Figure 3.9. This configuration allowed for the proper shaping and containment of the concrete during the casting process.

Figure 3- 9 Moulds of the specimens.

3.9 Casting Procedure

In the study, a 100 kg mixer was used to mix the concrete. Before inserting the reinforcement, cage, or casting control specimens, the forms and control moulds were oiled. This oiling process helps to ensure that the concrete does not stick to the forms, allowing for easy demoulding. To maintain the appropriate concrete cover, steel bars were placed inside the forms and securely positioned. These steel bars act as spacers and ensure that the reinforcement is properly embedded within the concrete at the specified depth. All ingredients of the concrete mixture, such as aggregates, cement, and water, were accurately weighed and carefully placed in a clean metal container before mixing. This process ensures the correct proportioning of the materials and helps maintain consistency in the mixture. Figure 3.10 illustrates the casting process, which involved using plywood forms for the moulds and steel forms. The plywood forms were used to shape the main body of the concrete specimens, while steel forms may have been employed for specific areas or features requiring additional support or reinforcement. After the concrete was mixed and cast into the forms,

the forms were left in place for 24 hours to allow the concrete to set. Subsequently, the forms were removed, and the specimens were immersed in water for a curing period of 28 days. Immersion in water is a common method of curing concrete, as it helps maintain proper moisture levels and promotes the development of strength and durability. Additionally, samples were taken from the cast concrete and poured into concrete cubes and cylinders. These samples were used to estimate the concrete properties, such as compressive strength, which is a fundamental characteristic for assessing the quality and performance of the concrete.

Figure 3- 10 fabrication of the experimental specimens.

3.10 Instruments and Test Procedure

In the experimental testing of the fabricated beams, a testing machine with a capacity of 60 tons was utilized. This testing machine is capable of applying controlled loads to the specimens and measuring their response. A dial gauge with a sensitivity of 0.010 mm (10 microns) was employed to evaluate the deflection behavior of the beams. The dial gauge was utilized to measure the deflection or displacement during the loading process. This measurement provides insights into the flexibility and deformation characteristics of the beams, as seen in Figure 3.11. During the loading procedure, both the loading data and displacement were measured at each load increment or step.

Figure 3- 11 Testing of the experimental specimens.

These measurements were recorded to establish the load-displacement relationship and to monitor the response of the beams as the load increased. This data collection helps understand the structural behavior of the beams under different loading conditions. Strain gauges with a precision of one micron were

used to measure the strains experienced by the concrete specimens. These strain gauges are sensitive enough to detect very small changes in strain. The strain gauges were applied to the surface of the concrete specimens, as depicted in Figure (3.11). They were strategically placed to capture the strains and deformations occurring on the surface of the specimens during the loading process. All beams tests were performed at the loading step of 5 kN to provide the optimum testing conditions and prevent the initial failure or crushing of the concrete due to the large step of loading. At the end of each loading step, deflection and strain were recorded. Regarding the crack width, the cracks were remarked with the use of a pen, as revealed in Figure 3.12. All concrete specimens were tested by the flexural Testing Machine. Concerning the test procedure, the test of the specimens was carried out at the age of 28 days after casting. All specimens were cleaned and painted with white paint before testing in order to clarify the propagation of cracks. The concentrated load was applied through a steel load moving plate used to achieve uniform contact. The test stage involved placing the specimen on the testing machine and adjusting it so that the centerline, supports, and line loads were fixed in their correct locations. All the instruments that were needed to complete the testing were then connected. Cracking and load were recorded.

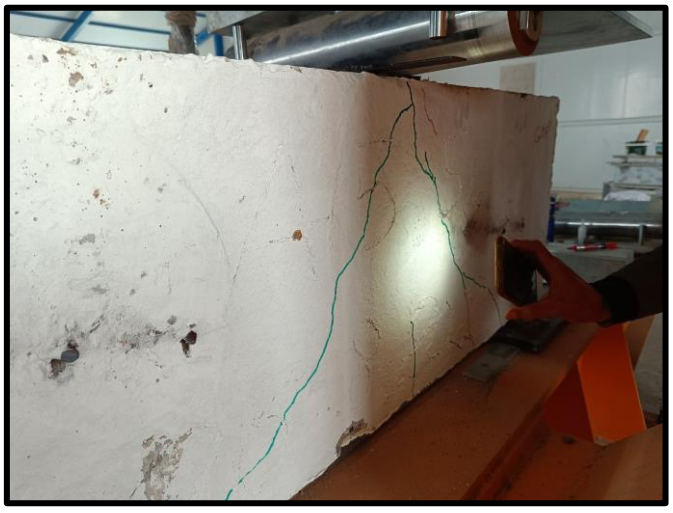

Figure 3- 12 Results recording of the experimental specimens.

CHAPTER FOUR: FINITE ELEMENT FORMULATION AND MATHEMATICAL MODELING

4.1 General

In structural analysis, most problems are complex and accurate solutions to their governing equations are obtained by resorting to numerical methods that enable the researcher to obtain results and solutions for these equations. One of the most important numerical methods for solving complex problems is the finite element method (FEM), which can be used to analyze different types of structural members. Thus, numerical procedures such as FEM are used to obtain approximate solutions to realistic types of problems. FEM is an important technology that provides solutions to different problems in all engineering fields. This work applies nonlinear FEA to RC deep beams subjected to a constant load to study the behavior of these beams [39].

4.2 Nonlinear Finite Element Analysis of Structures

A lot of phenomena in solid mechanics are nonlinear. However, in several applications, using linear formulation will be sufficient to obtain an engineering solution. Otherwise, other problems may require analysis with the nonlinear property to obtain realistic results, such as high deflection and post-yielding. Depending on nonlinear sources, the nonlinear problems involve three types [36]: material nonlinearity, geometric nonlinearity, and both materials and geometric nonlinearity. In the finite element method, the complex structure is first divided (discretized) into a limited number of individual non-overlapping components known as 'elements' over which the variables are interpolated. These elements are connected at many discrete points along their periphery, known as 'nodal points' or 'nodes', as revealed in Figure 4.1 [39]

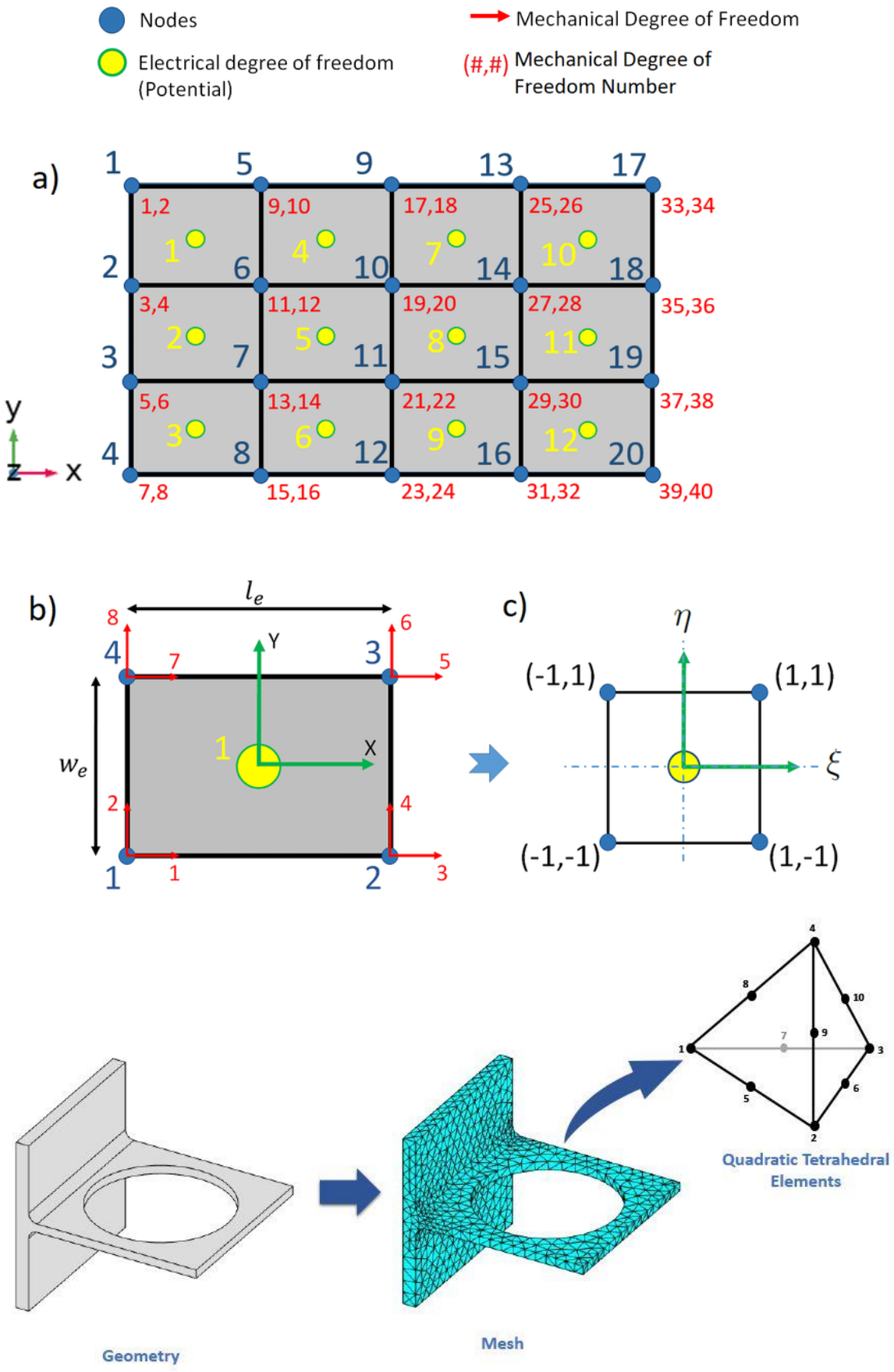

Figure 4- 1 Finite element discretization

The stiffness matrix and applied load vector for each element are computed and then merged to provide a global stiffness matrix and global load vector for the whole structure. In structural problems, the resulting system of simultaneous equations is solved for unknown nodal variables, which are the displacement components [39].

4.3 Basic Steps in Finite Element Method

The basic steps for any problem using finite element analysis to provide a solution are shown below [40]:

a) Pre-processing Stage: This stage includes all processes on elements (creation, discretizing, creating matrices, and assemblage reaching the obtained results). Each step can be detailed as follows:

1) Divide the problem into elements and nodes by producing and discretizing the solution domain into the number of finite elements.
2) Assuming a shape function to define the physical behavior of an element, that is, to provide the element solution, the approximate continuous function is supposed.
3) Develop matrices for each different element.
4) Design and build stiffness matrices regarding inclusion to illustrate the whole problem and construct a general stiffness matrix.
5) Implementation of loading, initial conditions, and boundary conditions on the solution.

b) Solution Phase: To acquire node outcomes, such as displacement at distinct nodes, the resultant algebraic equations are solved.

c) Post-Processing Stage: Obtaining additional results such as stress distribution, values of strains and stresses, shear force, bending moments, etc.

4.4 Material Modeling

4.4.1 Concrete Modeling

A. Plasticity Approach

Many component models have been developed to assess concrete behavior under various stress situations. Some of the principal component models are models based on elasticity and plasticity. In this study, the model based on plasticity is a mathematical expression that gives an elastoplastic response to the stressed material. Concrete crushing concrete is analogous to a law on plasticity in the compression algorithm [41]. This method similarly works based on a rate of Von-Mises independent yielding criterion, which represents a uniaxial stress-stress relationship. The yield term means the value of stress that causes the yield of the material, while the rule of flow after the yield point determines the plastic straining direction. The hardening rule defines the changes in yield surface with a gradual change in yield. Although the followed procedure denotes the concrete straining, the softening in the curve can't be defined adequately by the hardening plasticity theory after the point of peak stress [42].

B. Material Nonlinearity

In solid mechanics, material nonlinearity occurs when the curve of stress and strain, commonly known as the substantial material relation, is no longer linear. As in the basic linear elastic case, the direct proportionality of stress and strain can no longer be assumed. The link may now.be a combined or individual stress function. The main element that describes material behavior is the stress-strain curve. The nonlinearity of the material stress-strain curve is the reason for a nonlinear structural behavior.

Diverse factors, such as loading conditions and the type of the material, may influence the material's stress-strain characteristics. It is important to note that the nonlinearity of the material generally affects its structural behavior, as it directly

affects its resistance to loads and cracks, in addition to its resistance to creep and corrosion. Regarding the behavior of the element after the yield stage, the nonlinearity of the material varies according to the material, as the behavior of the steel material after the yield point is different from concrete, as the steel material continues to resist the loads imposed with a higher strength when compared to the concrete that loses its stiffness faster than steel reaching to the failure [43]. An example of the linearity of the concrete stress-strain curve is shown in Figure 4.2.

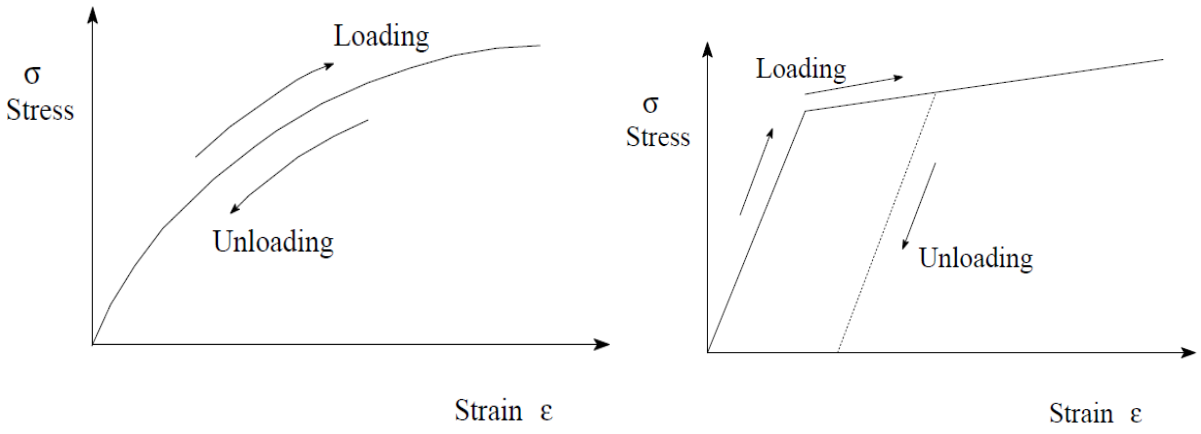

(a) Multilinear curve (b) Bilinear curve

Figure 4- 2 Nonlinear Material Response

C. Multilinear Stress-Strain Relationship

Figure 4.3 illustrates the typical stress-strain response for concrete subjected to uniaxial compression. The concrete behavior is nearly linear to roughly (30 % to 50 %) of the ultimate strength of concrete [44]. The ultimate increase in the strain of the concrete reaches (0.0035), and then the concrete starts crushing, and the curve starts descending until it reaches the rupture point, at which point the concrete will crush completely. High-strength concrete (HSC) is more solid and rigid, but it has low ductility, which makes it very brittle and weak in terms of elasticity. The linear phase of the HSC is higher than that of normal concrete. When the curve reaches its highest peak, there will be a rapid drop, and during this time, the concrete will behave with high brittleness, losing a large part of its

stiffness, as it is completely crushed until the point of the final failure of the concrete [44].

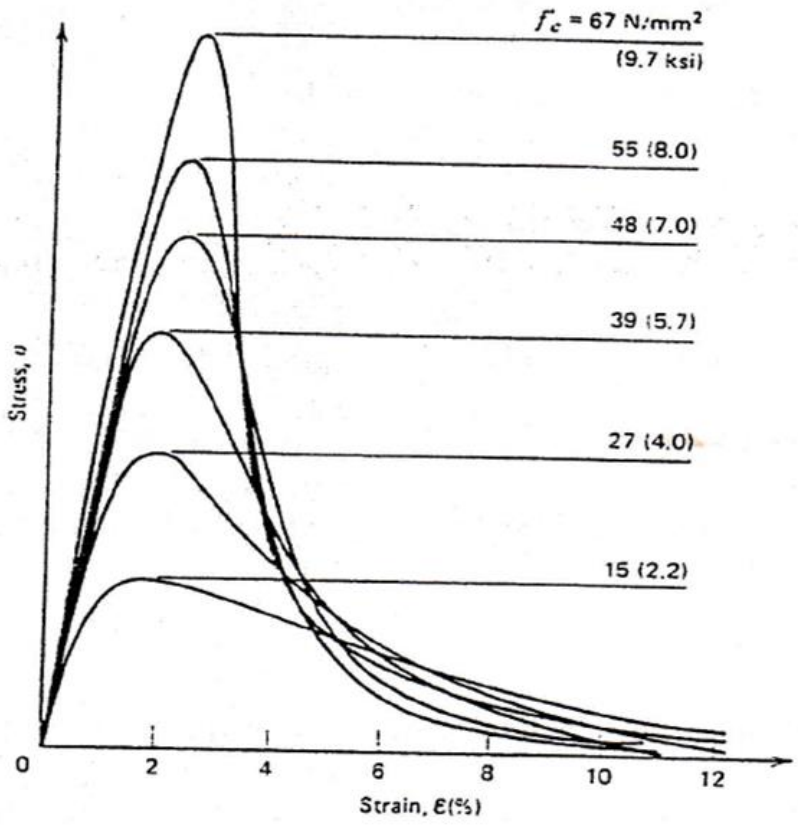

Figure 4- 3 Uniaxial compressive strain curve for concrete with different strength

One of the most important properties of normal concrete and high-strength concrete that must be defined to identify the behavior of concrete in addition to the urgent need for it when defining concrete in the ANSYS program is the Young modulus (E_c**)**, which differs between normal concrete and high strength concrete. The equation for finding the value of the Young modulus (E_c**) IS** given in ACI 318M-19 [45].

$$E_c = 4700\sqrt{f'_c}\ , \qquad (MPa) \qquad \ldots\ldots (4.1)$$

Poisson's ratio for the, which is ranges between (0.15 to 0.22 but in this investigation, a value of (0.2) is chosen for the RC beams analysis [46]. In ANSYS, the concrete behavior for uniaxial compression is defined by a stress-

strain curve with linear and nonlinear phases, starting from the origin, and increases with positive values for stresses and strains. The curve slope correlates to the material's modulus of elasticity, and other segments have slopes lower than the initial slope of the segment. It is worth noting that the ANSYS program does not accept the existence of any descending in the stress-strain curve, as it considers the values that cause a regression in the curve to be a numerical error. The idealized uniaxial stress-strain sketch for concrete specimen can be get as seen in Figure (4.4) and by utilizing these equations as follows [47]:

$$f_c = \varepsilon\ E_c \qquad for \qquad 0 \le \varepsilon \le \varepsilon_1 \qquad \ldots\ldots (4.3)$$

$$f_c = \frac{\varepsilon E_c}{1+\left(\frac{\varepsilon}{\varepsilon_\circ}\right)^2} \qquad for \qquad \varepsilon_1 \le \varepsilon \le \varepsilon_\circ \qquad \ldots\ldots (4.4)$$

$$f_c = f_c^{'} \qquad for \qquad \varepsilon_\circ \le \varepsilon \le \varepsilon_{cu} \qquad \ldots\ldots (4.5)$$

$$\varepsilon_1 = \frac{0.3 f_c^{'}}{E_c} \quad \text{(Hooke's law)} \qquad \ldots\ldots (4.6)$$

$$\varepsilon_\circ = \frac{2 f_c^{'}}{E_c} \qquad \ldots\ldots (4.7)$$

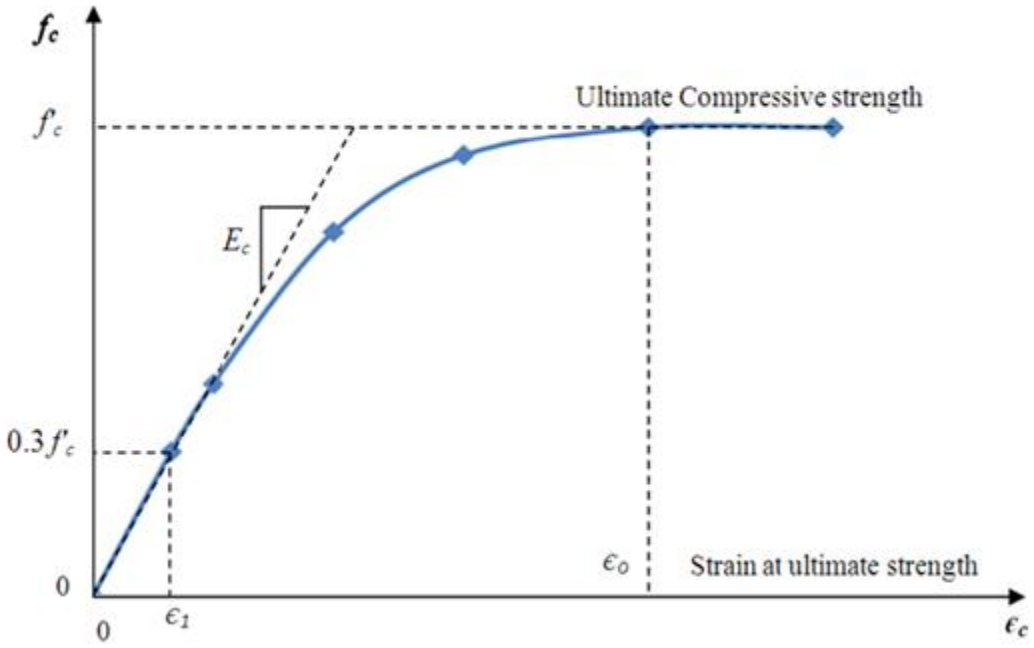

Figure 4- 4 Simplified stress-strain for NSC

D. Cracking Modeling

Cracking affects the internal stress distribution and deflections of concrete members. This phenomenon may either be modeled in FE in two ways, smeared cracking and discrete cracking model. The discrete cracking methodology requires new nodes to occupy the same position, disconnecting or separating concrete element nodes through which the cracking occurs and connected by linked components. This type of modelling is difficult and requires a lot of time, as it needs to renumber the nodes after the appearance of cracks, in addition to the fact that the direction of the cracks is restricted to certain directions [48]. Concerning the smeared crack model, this type of modeling presented by Rashid [49] illustrates this modeling as a changing of the element material property in addition that this model produces cracks without the redefinition of the topology of the finite element. Both models are illustrated in Figure 4.5.

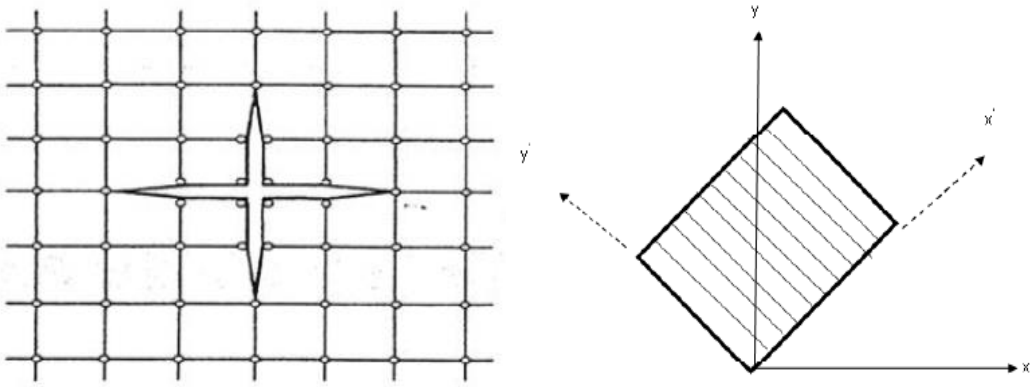

(a) 2D Discrete Crack Model. (b) Smeared Crack Model.

Figure 4- 5 Cracking Modeling

E. Shear Transfer and Tensile Crack Coefficient

Concrete is supposed to behave linearly in tension up to the beginning of cracking where the onset of cracking indicates the onset of hardness loss of concrete. The normal behavior of concrete includes cracking of concrete when it reaches its maximum tensile strength, then the concrete begins to crack and enters the nonlinear stage. When the concrete cracking phase begins, the concrete's stiffness in shear resistance begins to decrease, as the strength of the concrete decreases on the transfer of shear forces between the concrete elements, which causes faster access to failure. The coefficient of transmission of shear forces can be defined by the shear transfer modulus. This coefficient is affected by the type of concrete and the strength of aggregate interlock, in addition to other characteristics such as the reinforcement ratio and size, arrangement of bars, concrete cover depth, and aggregate size. The coefficient of shear transfer (β) represents the circumstances of the face of the crack. βc and βt refer to the coefficients of closed and open cracks [50]. β values often range between 0.0 – 1.0 where 1 represents the presence of rough cracks that allow a complete transfer of shear forces without losing any part of them. While the β value (0) referring to the fine cracks which cannot transfer any shear force through them. There are many investigations for modeling RC structures using varied values of these coefficients [50]. From these studies, βt frequently ranges from 0.05 to 0.65, and

βc varies from 0.25 to 1. Using these coefficients below 0.2 will cause a problem in convergence. There have been some early analyzes to evaluate the impact of βt and βc on the behavior of the model [51]. Concerning the reduction of the stiffness factor, many research studies reviewed the tensile stiffness multiplier factor to simulate the sudden descending in tensile stress as a percentage of the rupture stress. [52], Padmarajaiah, and Ramaswamy [53] used values ranging from 0.45 to 0.95 for prestressed beams in FE for a flexural test. Depending on these studies, and taking into account the good results obtained in the numerical studies by using ANSYS this factor equal to 0.9 [54].

F. Crushing Modeling

When subjected to axial, biaxial, or triaxial stress, the failure of a material can be analysed using finite element analysis. This failure is characterised by a sudden and significant decrease in stiffness. After attaining its maximum strength, the material experiences a linear and rapid decline in stiffness. Crushing simulations frequently entail complex nonlinear behaviour, significant deformations, and material instabilities, resulting in computational difficulties. To guarantee the stability and accuracy of the crushing simulation, it is crucial to carefully choose solution algorithms, time-stepping methodologies, and convergence criteria [55].

G. Reinforcement by Steel Rebar

The concrete beams usually consist of a group of materials, namely concrete, steel rebar, and some additives. The behavior of the concrete beams is a composite behavior of the sum of the behavior of this compound, where the concrete provides strength to the beams to compressive loads, while the steel rebar provides strength to the beams to resist flexural loads. Defining the behavior of these materials is necessary for the program to define the behavior of these elements, where steel behaves in nonlinear behavior under the name of bilinear behavior as presented in Figure 4.6. The first part of the bilinear curve represents the linear

phase of the steel rebar whose slope is referred as the modulus of elasticity (Es). The slope of the second part of the curve is zero, in the application of the rule of elastic perfect plastic. In the present work, the (E_T)strain hardening modulus is presumed to be the same value of yield stress approximately for the longitudinal bar and stirrups. This value was neatly chosen to obtain convergence [56]. Poisson's ratio μ = 0.3 was utilized for the steel reinforcement.

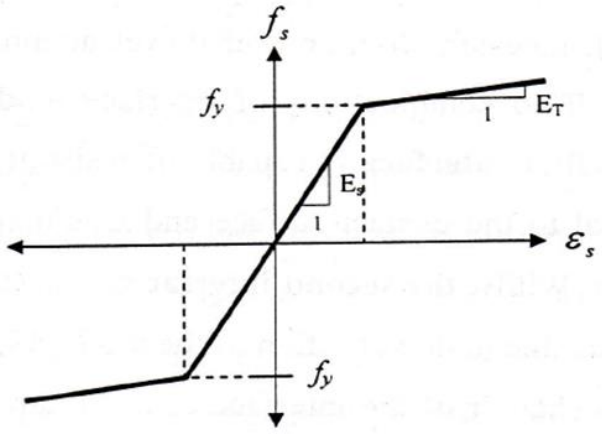

Figure 4- 6 Modeling of reinforcing bars

4.5 ANSYS Computer Program

The computer program ANSYS is a sturdy and interesting engineering finite element package that deals with the theory of finite elements in the analysis and solution of equations may be utilized to solve a lot of structural problems. FEM has become the most common method used to study stress, deformation, and other engineering parameters. FEM uses complicated mathematical equations to accurately approximate how the complex structure reacts to a certain load or condition. FE bundles like ANSYS solve thousands or millions of these equations to find a solution for a model. Handling all these equations be difficult and mostly impossible to solve manually. ANSYS is an inclusive general-purpose FE computer program that contains different elements implemented in the program. ANSYS has the capacity of solving linear and nonlinear problems including the influence of cracking, crushing, yielding of reinforcement, creep… etc. To use ANSYS or any other FEA software smartly, it should that one first fully

understands the underlying basic concepts and limitation of the FEM. In this work, the material parameters that must be taken into consideration to investigate the RC beams behavior that are Young modulus (E_c), compressive strength $f'c$, and the tensile strength (f_t). Also included are young modulus (Es) and steel yielding strength (fy). In addition, the evaluated geometry variables of the beams such as width, depth, and steel rebar [57].

4.6 Nonlinear Solution Techniques

The FE derivation process returns several equations:

$$[K]\{U\} = \{F^a\} \quad \ldots\ldots (4.11)$$

Where;

$[K]$ = the stiffness matrix;

$\{U\}$ = Nodal displacements;

$\{F^a\}$ = applied loads.

Eq. (3.11) calculates the solution of the unknown displacement for linear elastic problems. The stiffness matrix is a function in terms of displacement. In the case of a nonlinear system, the $[K]$ stiffness matrix is a function of the unknown displacement (or its derivatives). There are three techniques for solving the nonlinear Eq. 4.11; the basic technique can be categorized into:

1) The Incremental steps procedure, Figure 4.7 a.
2) Newton procedure (Iterative procedure), Figure (4.7 b).
3) An Incremental- Iterative procedure, Figure (4.7 c).

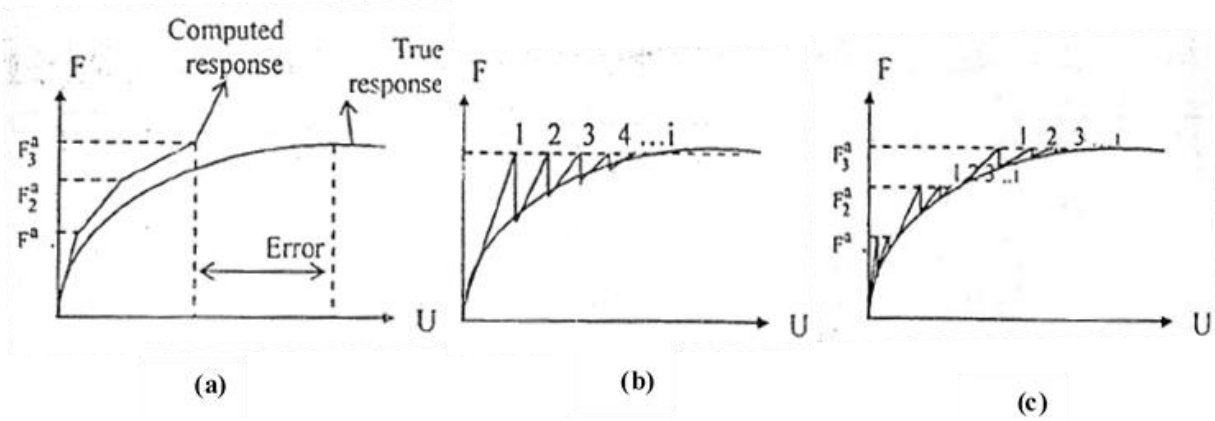

Figure 4- 7 Fundamental methodology for nonlinear equation resolution

4.7 Analysis Termination Criteria

Failure occurs when the body loses its ability to withstand imposed loads as it loses its stiffness completely and is unable to bear any additional loads. This phenomenon is referred in numerical tests by increasing the iterative displacement with continuous growth in the dispersion of energy until it reaches the point where the solution is not converged. The ability of the iteration can be limited by limiting the number of iterative attempts when reaching the non-convergence stage. During the review of several previous studies, it was found that the number of iterations of 250 is the most appropriate value, and what follows is considered to have very little effect. The number and value of iterations depend on the type of problem, the input values, the nonlinearity of the material, as well as the value of the tolerance.

4.8 Convergence Criteria

The iteration is accompanying for every incremental load until convergence is attained. For nonlinear analysis in structural issues, the convergence criteria can be classified into three criteria which the first one is the force criteria which are considered the easiest for solving the problems. The second and third criteria are the displacement and stress ones. The displacement criterion was utilized in this study. The iteration incremental displacements and total displacements are determined by the displacement criteria. When the results are obtained after the

analysis process, the results are checked with the criteria of incremental displacement so that if the values are close and within the permissible limits (tolerance), this solution is considered a convergent solution and takes the following form [59]:

$$\left\|\{\Delta U_i\}\right\| = \left(\max\left|\Delta U_i\right|\right) \le T_n \left(\max\left|\Delta U_i\right|\right) \quad \ldots\ldots (4.12)$$

where, U may equal u, v, w. The norm of the residual forces is checked against the current norm of the applied forces after the individual iteration and takes the following form:

$$\left\|\{R\}\right\| = \left(\sum R_i^2\right)^{0.5} \le T_n \left(\sum F_i^2\right)^{0.5} \quad \ldots\ldots (4.13)$$

where $\{R\}$ is a residual vector:

$$\{R\} = \{F^a\} - \{F^{nr}\} \quad \ldots\ldots (4.14)$$

To control the convergence through an analysis of the model in this work, the modeling of the beams must be correct in a way that ensures that the components are completely connected to each other without overlapping, in addition to coordinating and organizing the process of meshing. One of the factors affecting the occurrence of convergence in the solution in a way that ensures that no nonconvergence is reached is defining the materials correctly and dealing with the behavior of materials strictly, in addition to take care of supports and loads in a strict manner that ensures obtaining a unique solution. Many commands that help the user to get a convergent solution:

1) Using the full new Raphson.
2) Using shear transfer coefficient βt and βc more than 0.2.
3) Tangent modulus for steel reinforcement equal approximately to the yield stress (f_y).
4) The tolerance of the ultimate load is equivalent to (0.005).

5) Increasing the iteration number to 200.

4.9 ANSYS Finite Element Model

4.9.1 SOLID65 Element Description

SOLID65 is utilized to model the solid material with and without rebar which the element is defined by eight nodes having three degrees of freedom at each node: translation in x, y, and z-directions as depicted in Figure (4.8). For example, this ability of solid is utilized to simulate the concrete material with its condition and properties. There is a need to define the failure surface and this is done by using the maximum. compressive and tensile strength. After that, the Young modulus will suffer drop in its value reaching zero in the parallel direction to the principal tensile stress. At the moment, the principal stresses are compressive and located outside the surface of failure. At the same moment of crushing, the modulus of elasticity reached zero besides that the element's ability to resist the applied loads disappear [60]. The most significant feature of SOLID65 is that it can represent the nonlinearity of the material used. SOLID65 has the ability to represent cracks, crush, plastic deformation, and creep. The element is defined by isotropic material properties. The geometry, node position, and coordinate system for SOLID65 are shown in Figure (4.8) [60].

4.9.2 SOLID65 Input Data

This element contains many options that determine the behavior of the material to be represented, including the possibility of including a material as a as a ratio of the solid element volume. Other properties that control the behavior of the solid element which are the shear coefficients (open and close cracks coefficients), cracking stress, crushing stress in uniaxial and biaxial directions, the ambient hydrostatic stress in uniaxial and biaxial directions, in addition to the stiffness multiplier factor. The presence of each element in the analysis programs requires certain inputs to make the program understand the real behavior of this

element, as these inputs directly affect the behavior of element SOLID65 in terms of response to stress and exposure to cracking [60].

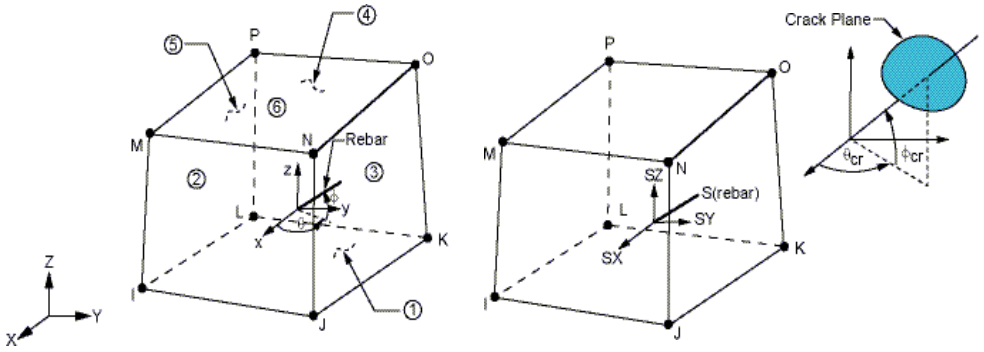

a) SOLID65 geometry b) SOLID65 stress output

Figure 4- 8 SOLID65 element for representing the concrete

4.9.3 LINK180 Element Description

LINK180 is a truss element that has two nodes with three degrees of freedom in each node. This element can be used in a wide range of several engineering problems such as modelling trusses, springs, links, sagging cables, etc. This element is used for uniaxial stress in both compression and tension. This element does not consider bending stress. In the current study, this element was used to model the steel reinforcement, which works as main steel reinforcement and stirrups. A geometry, nodes positions, and coordinate system for LINK180 are presented in Figure 4.9 [60].

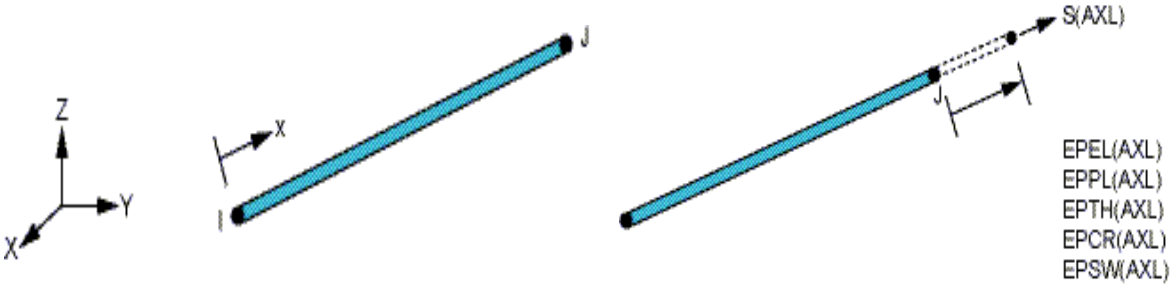

a) LINK 180 geometry b) LINK 180 stress output

Figure 4- 9 LINK180 represents steel reinforcement

Input data for LINK180 are the cross-section area for the used bar, in addition to the initial strain and material properties. There are three ways to model the steel reinforcement in the finite element (especially in ANSYS) which are the discrete model, embedded model, and distributed model (smeared model). Each of these methods is suitable for a specific type of engineering problem.

1) Discrete Representation

This type of representation is considered one of the best and most widely used types to represent all kinds of reinforcing steel, in addition to representing other bars, which includes placing the bars and connecting them to concrete through the node as shown in Figure (4.10 a) It is worth noting that this type is represented with concrete at the same node, meaning that they share one node and the same occupied space. This method provides a perfect match between the displacement of the SOLID65 and the LINK180. This type of modeling is suitable for the engineering problems that deal with analysis of the behavior of steel reinforcement, etc [60].

2) Embedded Representation

The embedded representation is often used with high-order iso-parametric elements. The bar element is constructed by keeping reinforcing steel displacements compatible with an adjacent concrete element as displayed in Figure (4.10 b). When reinforcement is complex, this model is very useful. The reinforcement steel stiffness matrix is evaluated unconnectedly and added to that of the concrete to obtain the inclusive stiffness matrix. The disadvantage of this method is that there are extra degrees of freedom to increase the computational and numerical treatment. This type of modeling is suitable for the engineering problems that deal with analyzing the structural elements that contain a high amount of steel reinforcement and have different positions in the cross section. This method provides the possibility of changing the position of the steel rebar

and adding more steel rebar through additional nodes without resorting to re-modeling the beams.

3) Smeared (Distributed) Representation

This method of modeling supposes that steel reinforcement is distributed uniformly through concrete elements in the defined region of the FE mesh as depicted in Figure (4.10 c). For example, this method is utilized for modeling wire mesh to simulate the occurred cracks, and for large structural members to decrease the number of the used element. Also, where the presence of reinforcement does not have a significant effect on the overall structural behavior. This method is considered one of the best ways to represent the implicit materials inside concrete, such as iron or plastic fibers, as they are added as part of the concrete volume as a result, there is a ‘‘perfect bond” between the concrete core and steel rebar, as presented in Figure 4.10 c. In this work, the discrete model method utilized which reinforcement is constructed by LINK180 at the shared node with SOLID65.

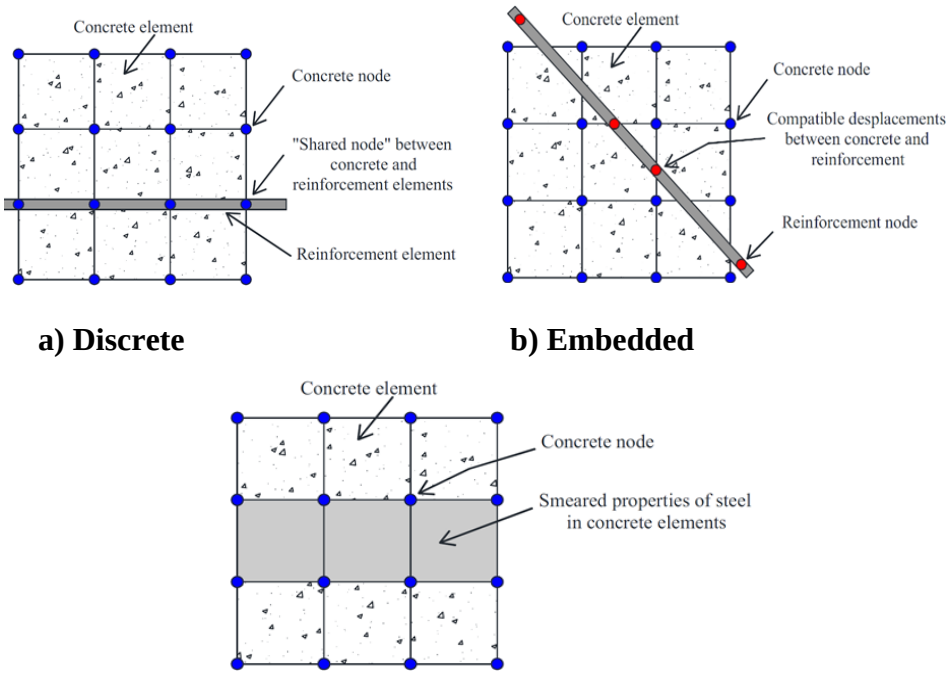

Figure 4- 10 Reinforcement modeling

4.9.4 SOLID185 Element Description

This element contains eight nodes with a displacement in x, y, and z directions at each node. The representation of this element is the same as that of the element SOLID65, but it differs from it in terms of behavior, as SOLID65 has the ability to crack, while this property is not available in the element SOLID185, but it is similar to how the element is drawn during modeling. The presence of this element in this study is necessary represent the steel plate which works on the distribution of stresses and prevents the stress concentration in a specific area as the stress concentration causes early failure and crushing of the concrete element when being in contact with the imposed load. Figure (4.11) shows the shape of this element and the number of nodes [60].

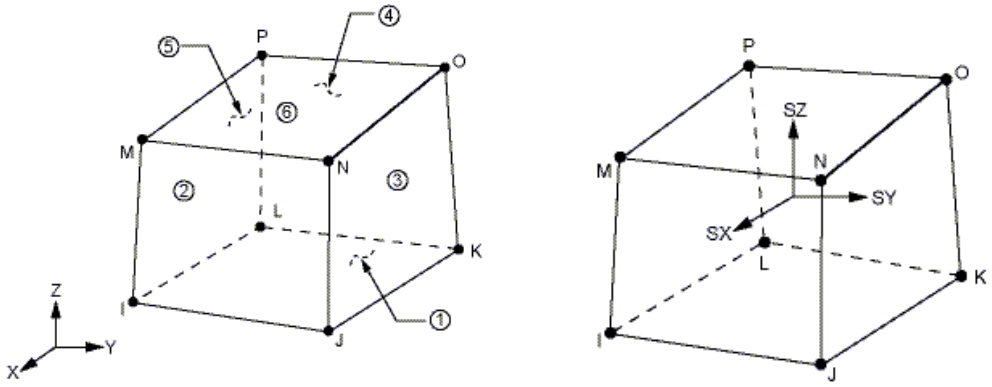

a) SOLID 185 homogeneous structural solid geometry

b) SOLID 185 homogeneous structural solid stress output

Figure 4- 11 SOLID 185 used to model steel plates and supports

4.10 Modeling and Analysis of Deep Beam by ANSYS

In this section, modeling of one specimen is performed. The modeled beams are a RC deep beam reinforced with steel rebar and subjected to static loads. This section included used elements, real constant, material properties, modeling, and boundary conditions. The representation of the concrete beams is done by selecting several elements that represent the behavior of the components of the concrete beams, then defining the properties of these elements, leading to the

modeling of the entire model, then support and loading the model, and analyze and show the results.

4.10.1 Used Elements

For the RC deep beam and rebar, SOLID65, LINK180, and SOLID185, were used to represent the concrete, steel rebar, and steel plate, respectively. Each of these elements represents the real behavior of the beams under shear.

4.10.2 Real Constant

Defining the used elements can be performed by defining the real constant of the used element as seen in Tables 4.1 and 4.2. All materials that need to be defined such as concrete (SOLID65), steel rebar (LINK180), except for the steel plate (SOLID185), which does not need to be defined. For the concrete containing recycled bricks, smeared method was used which the bricks modelled as a volume ratio of concrete.

Table 4- 1 Real constant of concrete (SOLID65).

RCs	**Element**	**Constant**			
			Rebar1	**Rebar2**	**Rebar3**
Concrete	**SOLID65**	**Material No.**	1	1	1
		Vol. Ratio	0	0	0
		Orientation (Theta)	0	0	0
		Orientation (PHI)	0	0	0

Table 4- 2 Real constant of concrete (LINK180)

Steel Reinforcement	**Cross-sectional Area (mm^2)**
6 mm rebar	28
10 mm rebar	78.5

4.10.3 Material Properties

ANSYS element needs some properties for proper entities which are termed "linear isotropic, multilinear isotropic, and bilinear material" for different materials (Concrete, steel rebar, steel plate). The properties of the material are defined by defining the behavior of the material. For example, concrete is defined by entering the linear and the nonlinear parts of the stress-strain curve with the value EX and PRXY, which represent the elastic modulus of the material. PRXY is the Poisson ratio (μ) which was assumed to be 0.2 for concrete and 0.3 for steel. The option of concrete plasticity is added, which is concerned with defining the shear transfer coefficients in open and closed cracks, in addition to entering the values of the compressive and tensile strength of concrete. Steel reinforcement, it is defined using the isotropic bilinear curve option. Steel plate is also known as a non-deformable isotropic linear material.

4.10.4 Modeling and Meshing

A three-dimension model of the concrete structure is built using ANSYS. Modeling of tSteel Plateams in the Cartesian coordinate system is created with several elements about 8124. All modeled specimens in this work have several elements (8000-9000). The process involved creating concrete, steel reinforcement, and steel plates. Creating the model was done by generating the first node and utilizing the copying feature to complement the beam modeling. Then, the concrete element was created by using command prompt line input in each region and the copying feature again. The concrete beams was modeled using a special concrete element SOLID 65. In the current work, modeling the reinforcement by Link 180 is assumed to be discrete modeling throughout the element. The bond between the concrete and steel bars, and concrete is assumed to be a perfect bonding between them, as shown in Figure 4.12.

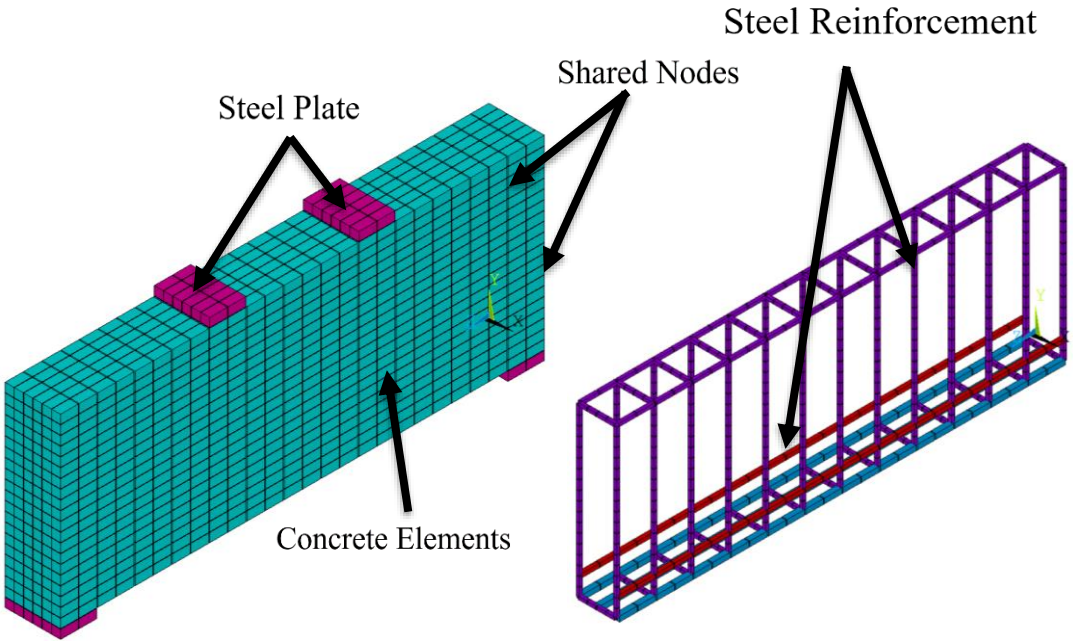

Figure 4- 12 Mesh and elements of the analyzed model.

4.10.5 Boundary Conditions and Loading

It has been found that the simulation of the applied load and the supports has a significant effect on the results of the finite element analysis. A bearing steel plate has been used to distribute the applied load on an area to get a unique solution and to avoid the stresses concentration on some element attached directly to the loading and support zones. To ensure that the model acts the same way as the experimental beams, the boundary conditions needed to be applied at points the supports exist as depicted in Figure 4.13. The boundary conditions are: The concrete beams was supported by hinge at the end of the beams with no displacement in two directions at each edge. A load was applied on the steel plate over the beam directly. The distribution of the applied load on the nodes is that the load is divided on the nodes number as seen in Figure 4.13.

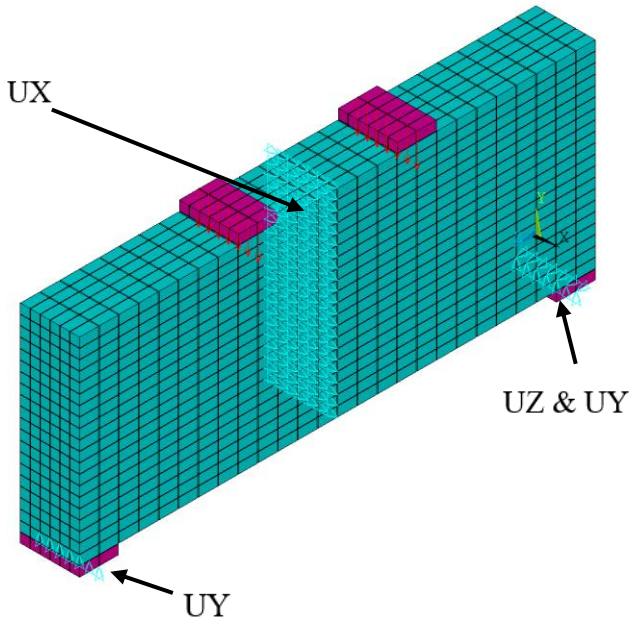

Figure 4- 13 Boundary conditions of the analyzed beams.

4.10.6 Analysis Type

There are several methods of analysis (such as the Full Newton-Raphson method, modified Newton-Raphson method, initial stiffness, and the unsymmetric Newton method) as each of these methods fits a specific analytical problem. Small displacement choice was chosen which means that the large deformations are neglected. Large deformation choice chosen where there is a large displacement such as the bucking deformation as occurring in slender columns. Regarding the applying loads, time increment choice was chosen with a time step size equal to (1). The equation solver was the sparse direct which the best solver for this type of analysis. Concerning the convergence criteria which included select the displacement option with tolerance not exceeded (0.05).

4.11 Parametric Study

For the numerical invesitagation, a parametric study was performed to investigate the effect of several parameters on thew shear behavior of the concrete deep beams made with recycled bricks. The study variables divided the thirteen beams into three series. The first series is a numerical deep beam specimens fabricated and tested to investigate the spacing of shear reinforcement of recycled

bricks the deep beam tested under one-point load as seen in Table 5.1. The second and third series included modeling of ten deep beams by ANSYS APDL to investigate the effect of recycled bricks layers in relation with a/d.

Table 4 -3 Parametric study models.

Beam Status/Var.		Beam ID	Beam Dim.	a/d	Grading Size	Loading Points
Numerical Shear Beams	Shear reinforcement	GA-5-0	150 x 500	2	20	One-point load
		GA-5-15	150 x 500	2	20	One-point load
		GA-5-20	150 x 500	2	20	One-point load
	RBC Thickness	GA-5CM	150 x 500	2	20	One-point load
		GA-10CM	150 x 500	2	20	One-point load
		GA-20CM	150 x 500	2	20	One-point load
		GA-30CM	150 x 500	2	20	One-point load
		GA-40CM	150 x 500	2	20	One-point load
	RBC Thickness	GC-5CM	150 x 500	1	20	Two-point load
		GC-10CM	150 x 500	1	20	Two-point load
		GC-20CM	150 x 500	1	20	Two-point load
		GC-30CM	150 x 500	1	20	Two-point load
		GC-40CM	150 x 500	1	20	Two-point load

CHAPTER FIVE: RESULTS & DISCUSSION

5.1 General

This chapter describes the results of the 22 concrete deep beams tested experimentally and numerically under monotonic loads. Deep beams behavior and failure modes are discussed. The behavior of the deep beams made with recycled bricks is compared with that of the conventional specimens. A study is carried out to explore the effect of many parameters which are expected to affect the behavior of such members. First crack load, ultimate load, displacement, stiffness, ductility, energy absorption, cracks pattern and failure mode, and stress distribution are considered to explore the performance of these specimens. The effect of the various parameters which are expected to affect the shear behavior of such beams is also investigated. These parameters are; replacement ratio, thickness of recycled bricks layers, a/d ratio, beside shear reinforcement.

5.2 General Behavior of Deep Beams

5.2.1 Experimental Shear Beams

The shear behavior investigation revealed testing of two series divided into three groups for each one. The first series is an experimental deep beam specimens fabricated and tested to investigate the replacement ratio, grading size of recycled bricks beside the a/d ratio which the deep beam tested under one-two point loads as seen in Table 5.1. The second series included modeling of thirteen deep beams by ANSYS APDL to investigate the effect of shear reinforcement, a/d, and recycled bricks layers thickness on deep beam shear strength. First group of first series involved testing of nine RC deep beams experimentally fabricated with several replacement ratio of RB and a/d ratio. These beams tested to the failure point under static loads. The results exhibited that the cracking load ranged between (233-441) kN. Also, the outcomes demonstrated that obtained strengths results ranged between (366 – 571) kN with displacement ranged between (4.83-

6.67) mm as shown in Table (5-1). The variance in the ultimate load carrying capacity was due to the changing in the replacement ratio of aggregate by recycled bricks, shear span to depth ratio (a/d), in addition to the recycled bricks grading size. It should be noted that the tested specimens used the (B-CBAC-HCL) mixture for the fabrication of the RC deep beams.

A. Effect of Replacement Ratio.

In the experimental study, three groups of parametric beams were investigated to understand the shear behavior. The replacement ratio, referring to the proportion of a material being replaced by another, directly influenced the shear strength capacity of the reinforced concrete deep beams. For the normal concrete beams with a zero-replacement ratio (beams GA-N, GB-N, and GC-N), the cracking load values were found to be 394 kN, 441 kN, and 423 kN, respectively, as shown in Table 5.1. The ultimate strength exhibited by these beams was 522 kN, 571 kN, and 537 kN, respectively. When the replacement ratio was increased to 5% and 10% for beams GA-5 and GA-10 respectively, there was a reduction in both the cracking and ultimate load capacities. The cracking load decreased from 394 kN to 344 kN and 264 kN when the replacement ratio increased from 0% to 5% and 10% for beams GA-5 and GA-10, respectively. Similarly, the ultimate load capacity decreased as the replacement ratio increased. The shear strength of beams GA-N, GA-5, and GA-10 decreased by 10.4% and 29.9%, respectively, when the replacement ratios were increased to 5% and 10% respectively. These results indicate that as the replacement ratio increased, the shear strength capacity of the beams decreased due to the negative effect of recycled bricks on the bond between the concrete particles. The cracking load and ultimate load exhibited a downward trend with increasing replacement ratios as revealed in Figure 5.1 a and b.

Tabel 5-1 Test results of concrete deep beams.

Beam Status/Var.		Beam ID	Repl. ratio	a/d	Grading	Pcr (kN)	Pu (kN)	Pcr/Pu	Deflection mm	D.I	Energy absorption (kN.mm)
Experimental Shear Beams	Grading Size (19—20) mm	GA-N	0%	2	20	394	522	75.48%	6.230	2.09	920.48
		GA-5	5%	2	20	344	467.6	73.57%	6.110	1.91	788.19
		GA-10	10%	2	20	264	366	72.13%	4.830	1.89	478.17
	Grading Size (10—12) mm	GB-N	0%	2	12	441	566	76.50%	6.670	2.14	1083.04
		GB-5	5%	2	12	360	521	69.10%	6.540	1.99	882.90
		GB-10	10%	2	12	271	444	61.04%	6.490	1.71	659.55
	Shear to depth ratio	GC-N	0%	1	20	423	537	78.77%	4.880	2.75	774.09
		GC-5	5%	1	20	355	483	73.50%	5.130	2.35	682.93
		GC-10	10%	1	20	233	392	59.44%	5.440	1.80	475.32

I.S: Initial Stiffness kN/mm
D.I: Unitless

For the second group (GB-N, GB-5, and GB-10) which fabricated with less grading size of recycled bricks, the cracking load decreased by 18.4% and 38.5% for these beams respectively as revealed in Figure c. When the replacement ratio increased to 5% and 10% for beams (GB-N, GB-5, and GB-10), the ultimate load decreased. This decrease in load resulted in a reduction of shear strength by 8.8% and 23.3% respectively, as shown in Figure d. For beams with two-point loads (GC-N, GC-5, and GC-10), the replacement ratio reduced the cracking load by (16% and 45%) while the ultimate shear strength reduced by 10.1% and 27% when the replacement ratio increased which the increase to 5% and 10% respectively as revealed in Figure 5.1 e and f. The inclusion of recycled bricks as a partial substitute for coarse materials in concrete deep beams can affect both the cracking load and the ultimate shear strength of the beams.

Several factors contribute to the reduction in these properties which the recycled bricks have different mechanical properties compared to conventional coarse aggregates which exhibited lower strength, higher porosity, or variations in particle shape and size distribution. These differences resulted in reduced bond strength between the recycled brick particles and the surrounding concrete matrix, leading to a decrease in the cracking load and ultimate shear strength. The presence of recycled bricks in the concrete mix weakens the overall composite material which the recycled bricks have lower strength or higher porosity, that act as weak points within the concrete matrix. Also, the recycled bricks and the surrounding concrete may have an incompatible interface due to differences in material properties. This interface, known as the interfacial transition zone, prone to cracking and debonding. The presence of recycled bricks exacerbated the formation and propagation of cracks within this zone, which reduced the cracking load and shear strength of the deep beam. Lastly, the particle packing and grading of the recycled bricks differ from that of conventional coarse aggregates. Poor particle packing led to voids or gaps within the concrete mix, which weaken the overall structural integrity. in the cracking load and ultimate shear strength of the deep beams.

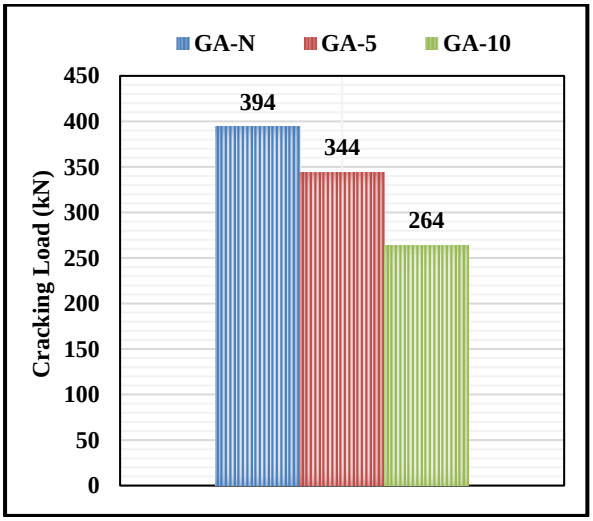

(a)

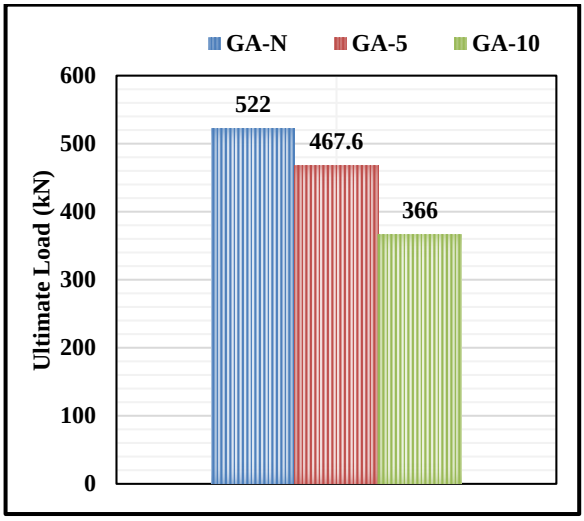

(b)

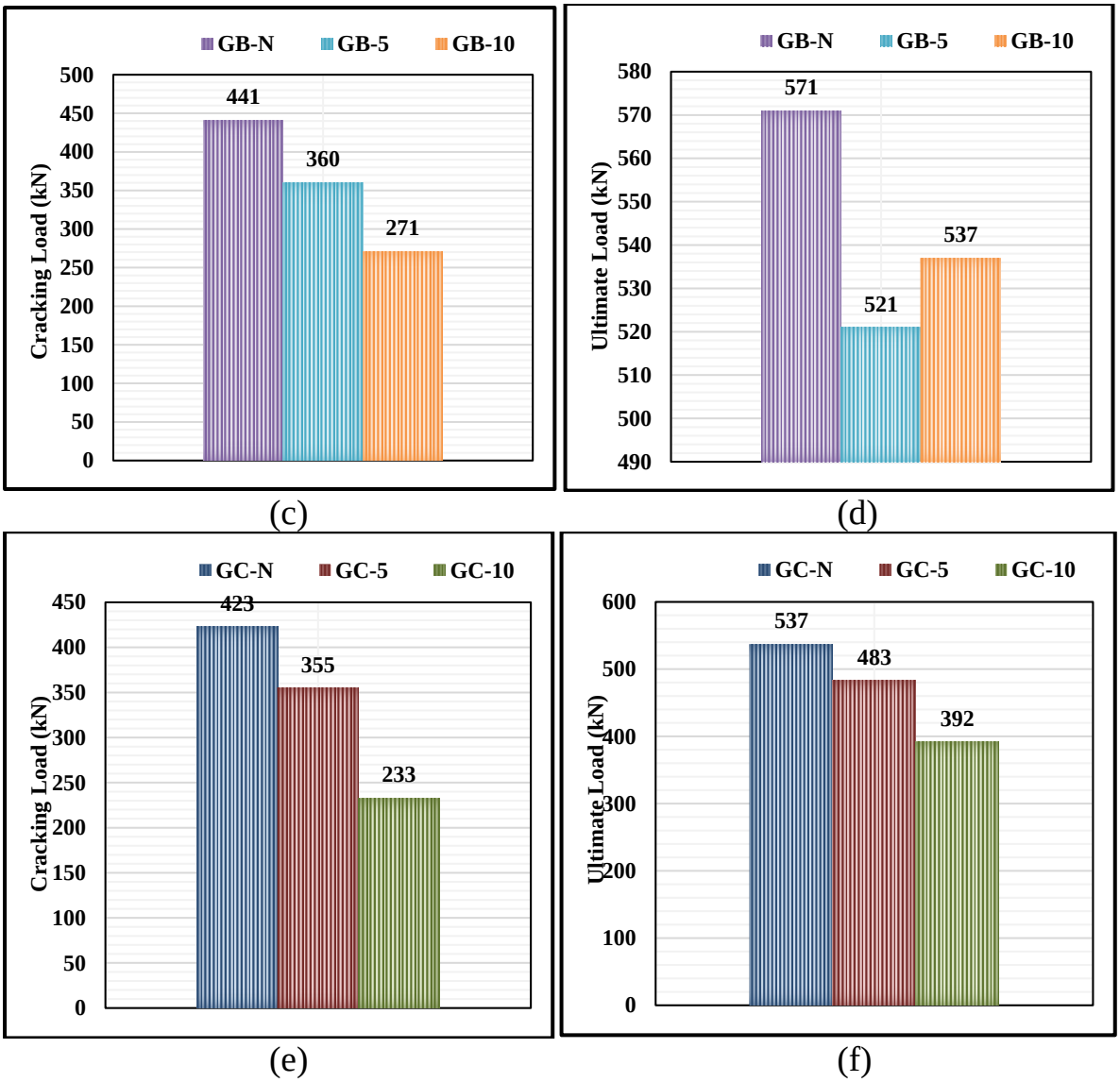

Figure 5- 1 Tested beams results.

The presence of these voids promoted crack initiation and propagation, resulting in a decrease in cracking load and ultimate shear strength. Although of curing the bricks, Recycled bricks might contain contaminants or residual substances that can have adverse effects on the concrete matrix. These contaminants affected the hydration process, leading to reduced strength and durability of the concrete. Regarding the maximum deflection, the replacement ratio reduced the maximum deflection which the reduction occurred for the 10% of replacement ratio higher than 5% as demonstrated in Figs. 5.2, 5.3, and 5.4 which was due to several reasons such as bonding between recycled bricks and

concrete matrix, particle packing and grading, and inhomogeneity and interface effects. Regarding the bonding between recycled bricks and concrete matrix.

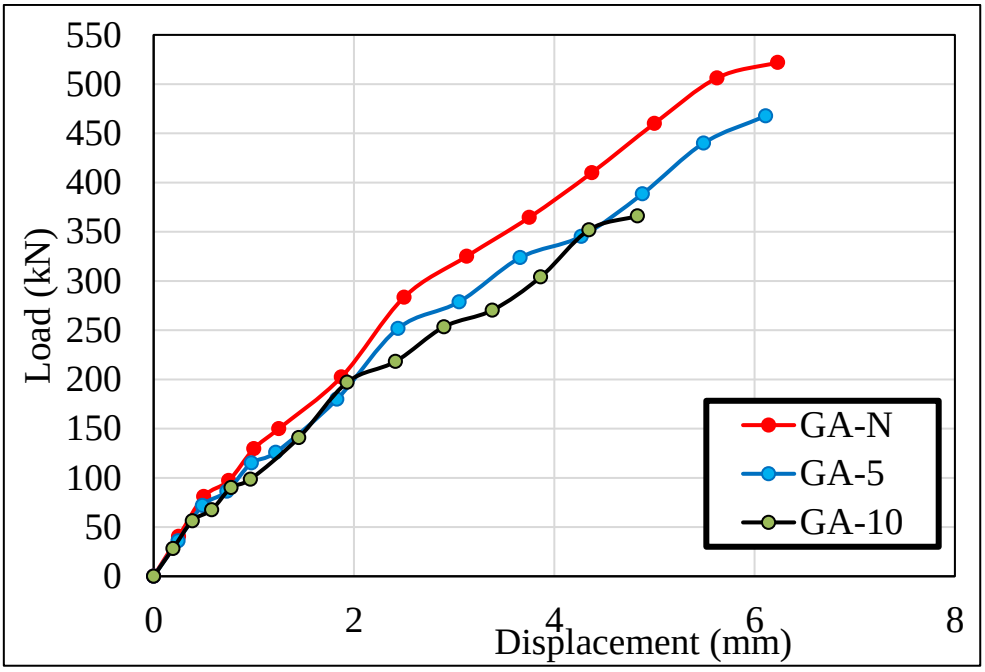

Figure 5- 2 . load deflection results of GA-series.

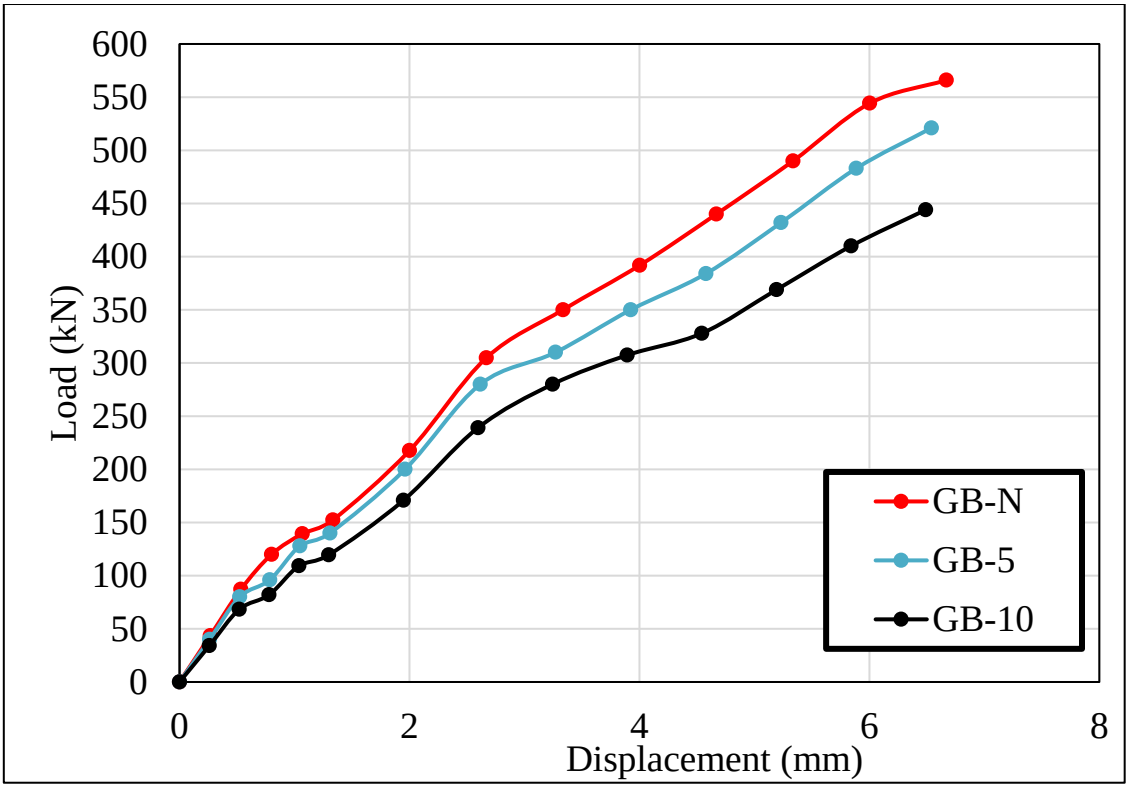

Figure 5- 3 load deflection results of GB- series.

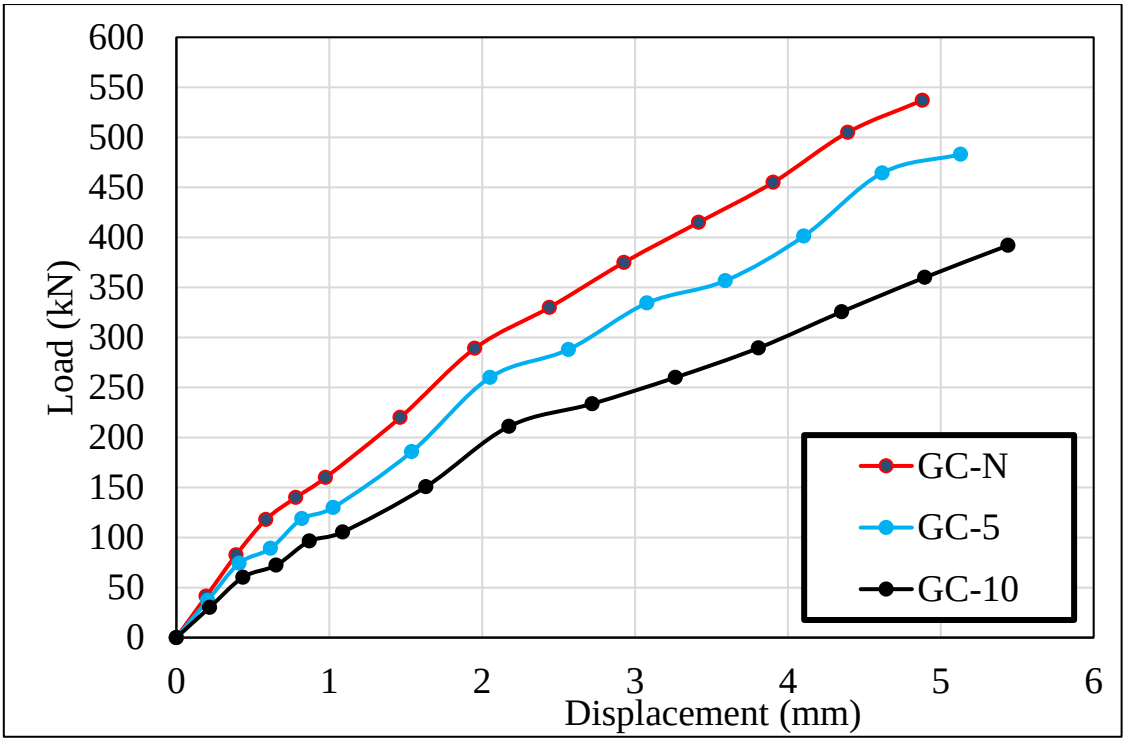

Figure 5- 4 load deflection results of GC- series.

B. Effect of Grading Size of RB.

Figs. 5.5 and 5.6 illustrate the grading size effect on the load displacement curve of recycled concrete deep beams. The grading size of recycled bricks affected the shear strength of deep beams when used as a partial alternative to coarse aggregates. By comparing between the deep beams with different grading size, it is found that the beams with grading size of 19-20 mm led to decrease in the cracking and ultimate load. But this decrement is variable in term of the cracking load and ultimate load carrying capacity which the increase of replacement ratio from zero to 5% an 10% caused a decrement in by 13% and 33% for beams (GA-5 and GA-10) respectively.

While for beams with less grading size of RB the reduction in the cracking load reduced hugely with 18.5% and 38.5% for beams (GB-5 and GB-10) respectively. which this index means that the reducing the grading size of RB affected hugely the cracking load. This phenomenon is different in term of the ultimate load which reducing the grading size led to a less reduction in the ultimate shear strength of the concrete deep beams. The reduction in the ultimate

load for beams (GA-5 and GA-10) were 10.4% and 28.9% respectively higher than the reduction of beams (GB-5 and GB-10) which the reduction in the ultimate shear strength were 8.75% and 22.3% respectively. The comparison between the beams (GA-5 and GB-5) showed that the load displacement curve in term of the cracking load, ultimate strength, and deflection as exhibited in Figs. 5.5 and 5.6.

The cracking load of beam (GA-5) was 344 kN while the beam (GB-5) showed a cracking load of 366 which is higher than last one by 4.65%. the ultimate load and maximum displacement showed that the shear strength of the model (GA-5) was 467.6 kN which is less than (GB-5) by 10.3% while the difference in the deflection was by 7% as exhibited in Figure 5.5. Regarding the higher percentage of replacement ratio, the effect of the grading size on the replacement ratio of 10% was significant.

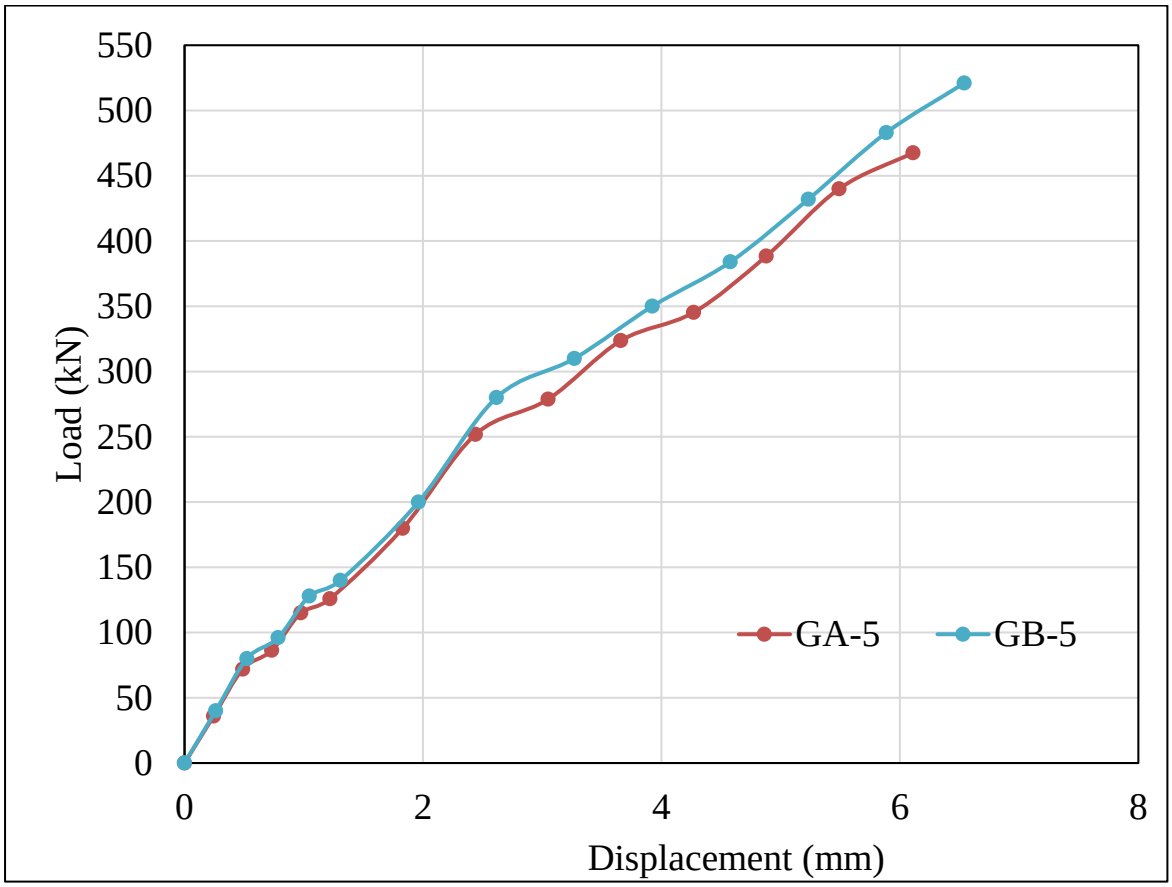

Figure 5- 5 load deflection results of GA-5 and GB-5.

The comparison between the beams (GA-10 and GB-10) showed that the cracking load of beam (GA-10) was 264 kN while the beam (GB-10) showed a cracking load of 271 which is higher than last one by 2.65%. The ultimate load and maximum displacement showed that the shear strength of the model (GA-10) was 366 kN which is less than (GB-10) by 17.5% while the difference in the deflection was by 34.4% as exhibited in Figure 5.6. The effect of the grading size on the shear strength of the deep beam was due to several reasons which one of them is interlocking and shear transfer, the grading size of recycled bricks influences the interlocking and shear transfer mechanism within the deep beam. Smaller-sized recycled bricks generally provide more interlocking and shear transfer between the bricks and the surrounding concrete matrix. This improved interlocking can enhance the shear strength of the deep beam. The grading size of recycled bricks affects the particle packing and void content within the concrete mix. Optimal particle packing with minimal voids is desirable to maximize the shear strength of the deep beam. A well-graded mix with a range of brick sizes achieve better particle packing and reduce voids, resulting in improved shear strength. Also, the important point of this phenomenon is the shear plane development which the grading size of recycled bricks affect the development of the shear plane within the deep beam. A well-graded mix with a suitable range of brick sizes can promote multiple potential shear planes, which can distribute the shear forces more effectively. This distribution of shear forces contributed to improved shear strength. Also, the grading size of recycled bricks impact the compactness and density of the concrete mix. Smaller-sized recycled bricks can fill the voids between larger bricks, resulting in a denser and more compact concrete matrix. A denser mix generally exhibits higher shear strength.

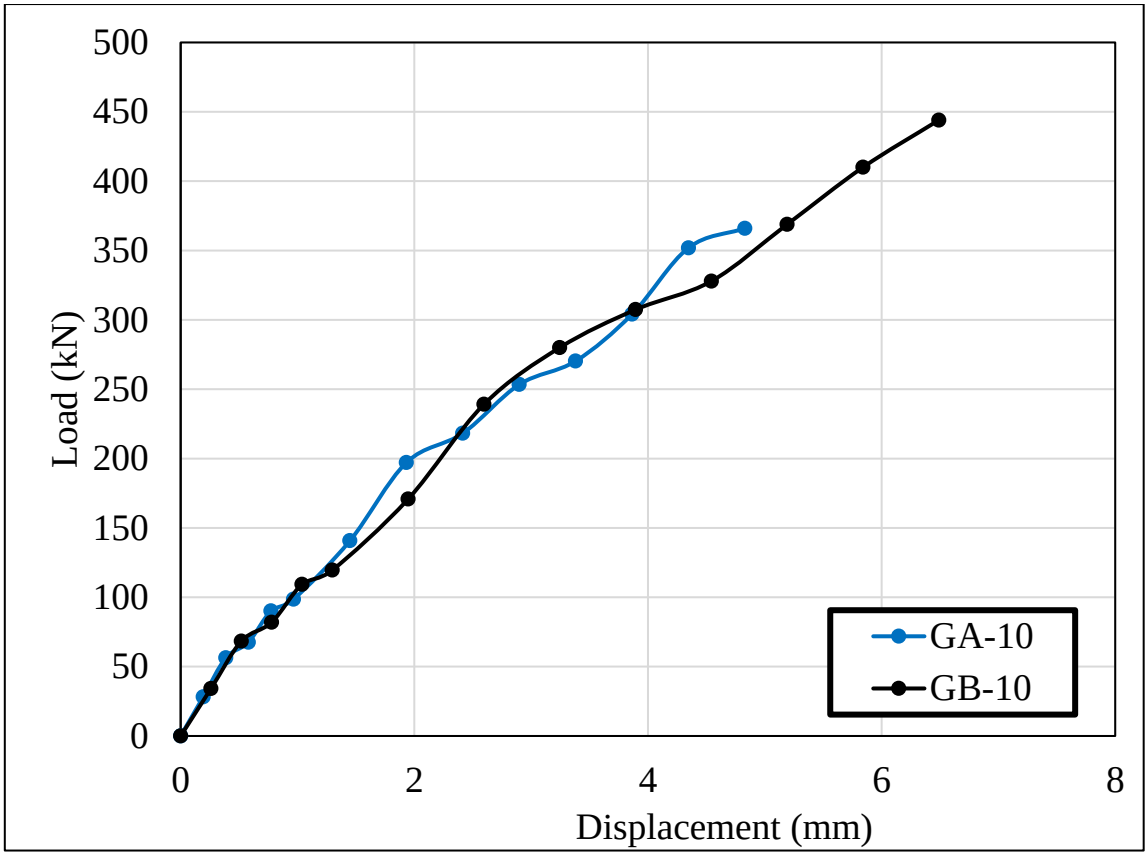

Figure 5- 6 load deflection results of GA-10 and GB-10)

C. Effect of Shear to Span Ratio a/d.

Regarding the effect of the a/d ratio, the reduction of a/d (for two-point load instead of one point load) for the same grading size of the recycled bricks showed that the cracking load was enhanced and revealed higher increment in comparison with the a/d of 2. The comparison between the models with normal concrete (GA-N and GC-N) revealed a distinct variation in the cracking load which the higher a/d ratio which of 394 kN was appeared in the normal concrete deep beam with high a/d ratio that increased to 423 kN when the one-point load replaced with two-point-load at the same properties. The ultimate shear strength for the same beam showed that the concrete was less than cracking one which the ultimate load carrying capacity reached to 537 kN when was 522 kN for the normal concrete deep beams. The displacement of this beam varied hugely which the replacement of the one-point load to two-point load decreased the maximum displacement from 6.23 mm to 4.88 mm with a decrement ratio of 21.7% as seen in Figure 5.7.

for the recycled concrete deep beams (GA-5 and GC-5), the cracking load for these beams were 344 kN and 355 kN respectively with a variation of 3.2%. The ultimate load was comparable which the variation between the both beams were 3.3%. The displacement of these beams was different which the displacement of one point load was 6.11 mm which reduced to 5.13 with a variation of 16% approximately when the a/d changed (Figure 5.8). For the recycled concrete deep beams (GA-10 and GC-10), the cracking load for these beams were 264 kN and 233 kN respectively with a variation of 13.3%. The ultimate load was comparable which the variation between the both beams were 7.1%. The displacement of these beams was different which the displacement of one point load was 4.83 mm which increased to 5.44 with a variation of 12.6% approximately when the a/d changed. The displacement of such beams with higher percentage of recycled bricks showed distinct outcome which at higher percentage of recycled bricks the displacement of the GA-10 was higher than those of GC-10 which the higher percentage of recycled brick reduced the bond between the concrete particles so the increase of shear path in concrete beam led to debonding of the concrete deep beam particles as seen in Figure 5.9.

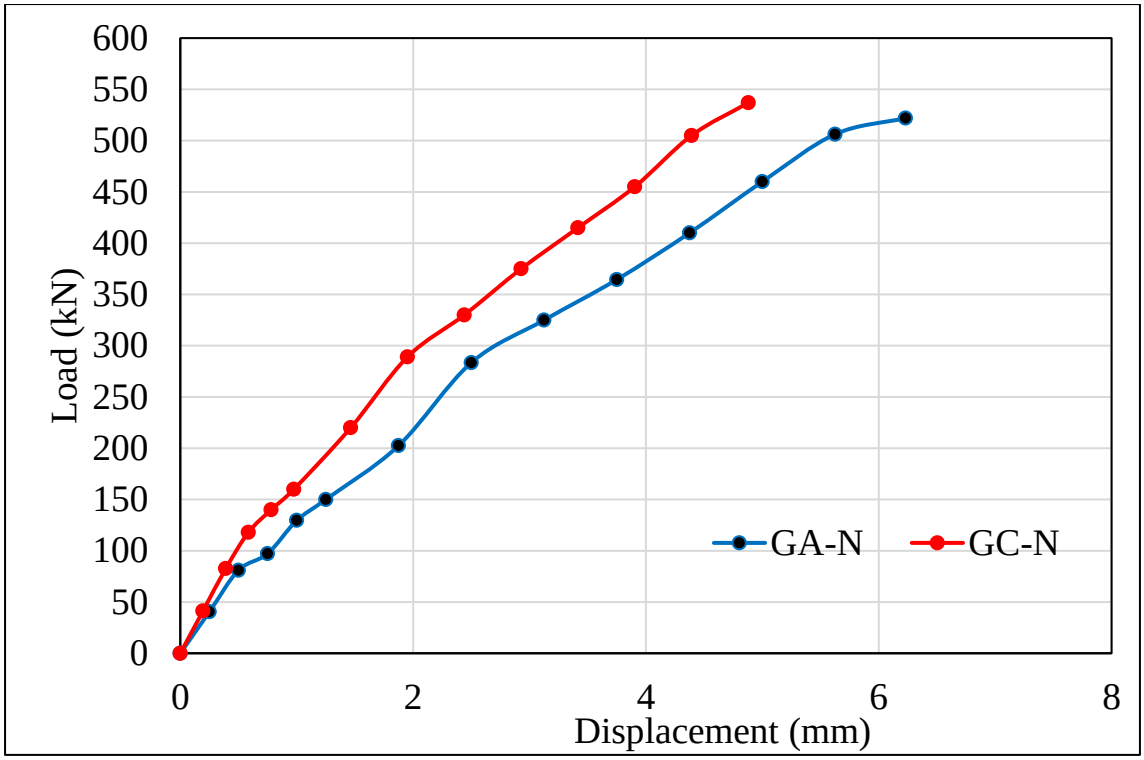

Figure 5- 7 load deflection results of GA-N and GC-N.

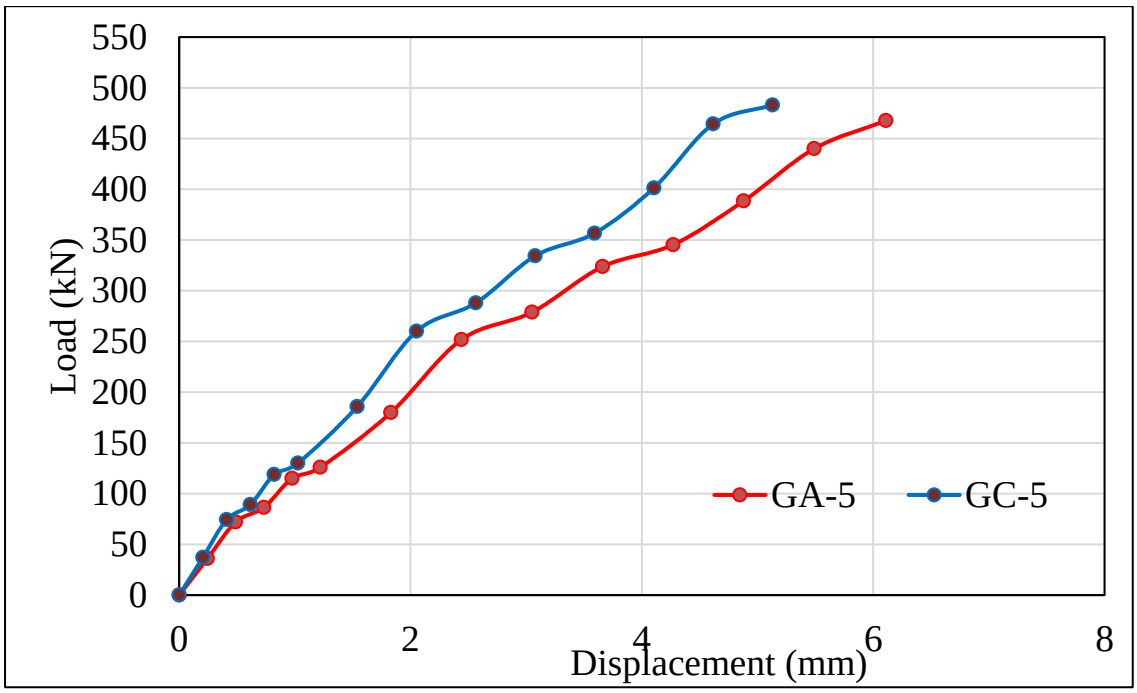

Figure 5- 8 load deflection results of GA-5 and GC-5)

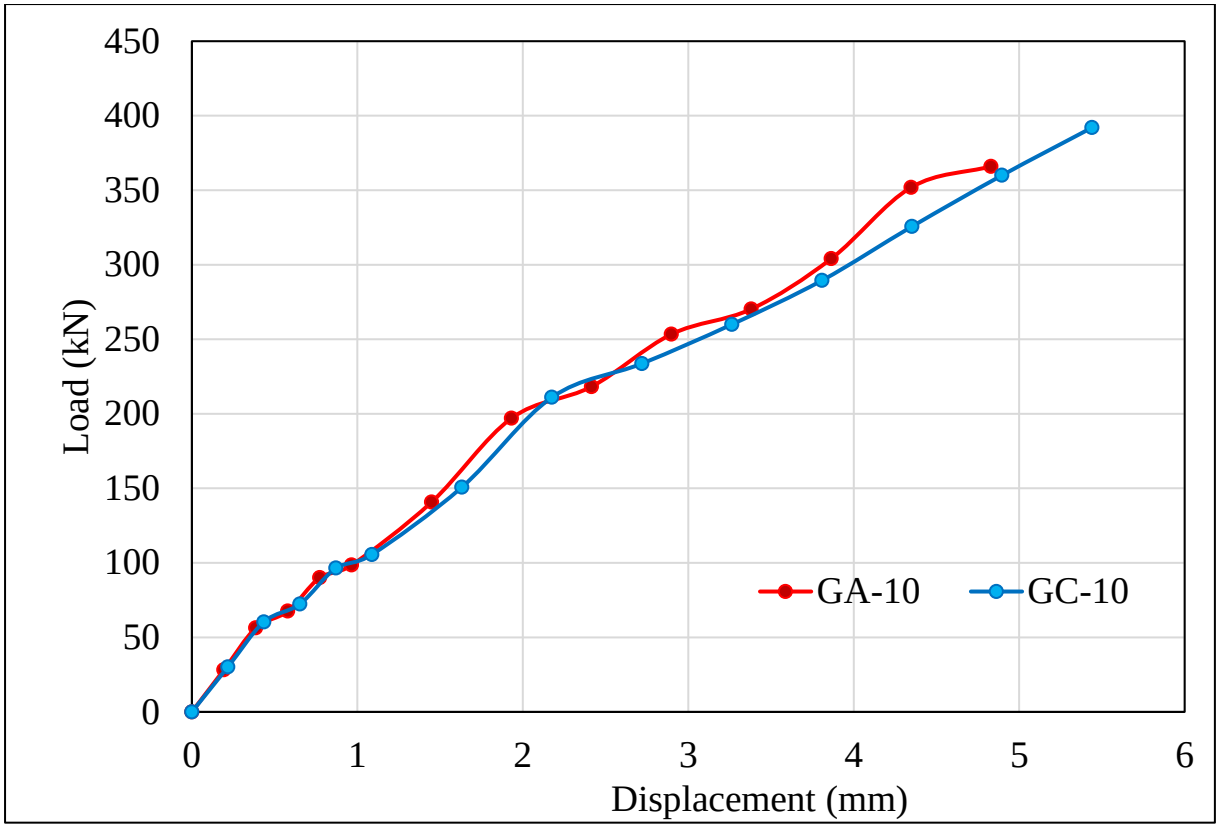

Figure 5- 9 load deflection results of GA-10 and GC-10.

D. Ductility of Deep beams.

Concrete ductility index refers to the material's ability to undergo to undergo substantial deformation without experiencing sudden failure. Ductile concrete structures can exhibit visible deformations, such as cracking and bending under shear loads. Among the affected variable on the ductility, the presence of recycled bricks, can greatly affect the ductility of concrete. Which contributes to reduce the control and distribute cracking, causing sudden failure. This measurement of ductility is obtained by calculating the ratio of the ultimate deflection (Δu) to the yield deflection (Δy) [60]. While the energy absorption can be measured by the area under the load deflection curve. Figures 5.10 to 5.13 shows results of ductility index and energy absorption of deep beams. It is important to note the using recycled bricks material led to decrease the ductility of the structural member. Control beam GA-N has the higher ductility than the other beams. The beam (GA-5) has less ductility than the control beam because it is made of

recycled bricks material, which is characterized by less ductility because it contains recycled material missed their properties during the using. The ductility index of beams GA-5 and GA-10 was (1.91, and 1.89) respectively, and the percentage of decrease in ductility for both beams were comparable (9.5%) when compared with the control one. The Deep beams with smaller grading size (GB-N, GB-5, and GB-10) offered higher ductility when compared with beams GA-series beams. which the ductility increment ratio value was (2.4%, 7%, and 20.1) % respectively. Comparing the deep beams with two-point load with opposite them (two-point load) demonstrated that the ductility increased by 31.6% for the normal concrete deep beams and this ductility decreased by 14.4% and 34.5% when the replacement ratio increased to 5% and 10% respectively as demonstrated in Figure 5.11.

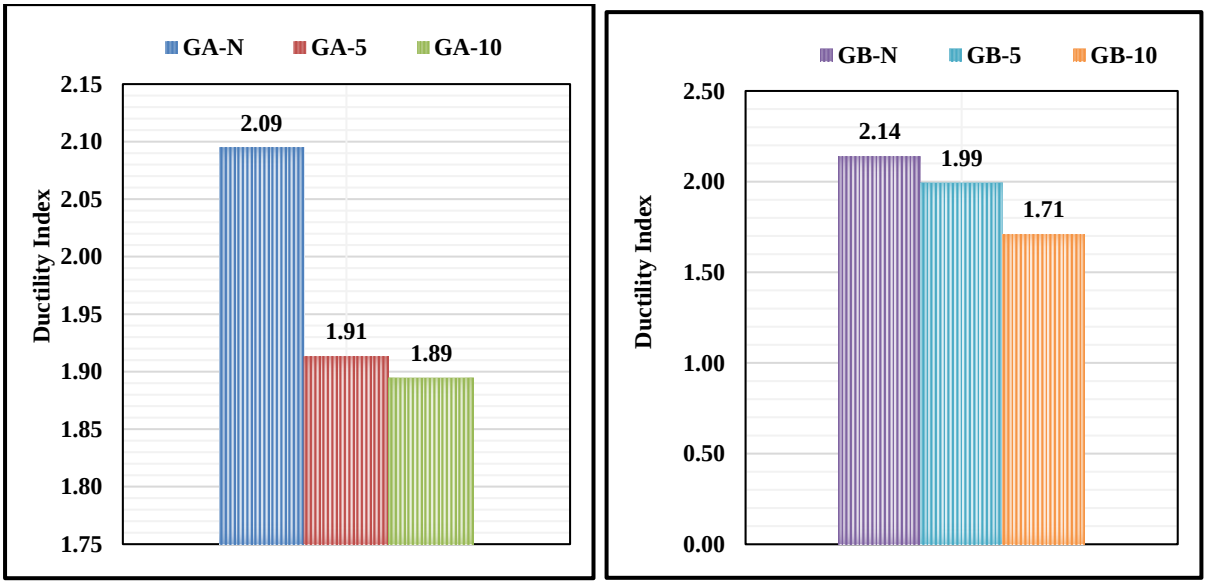

Figure 5- 10 Ductility index of Deep beams.

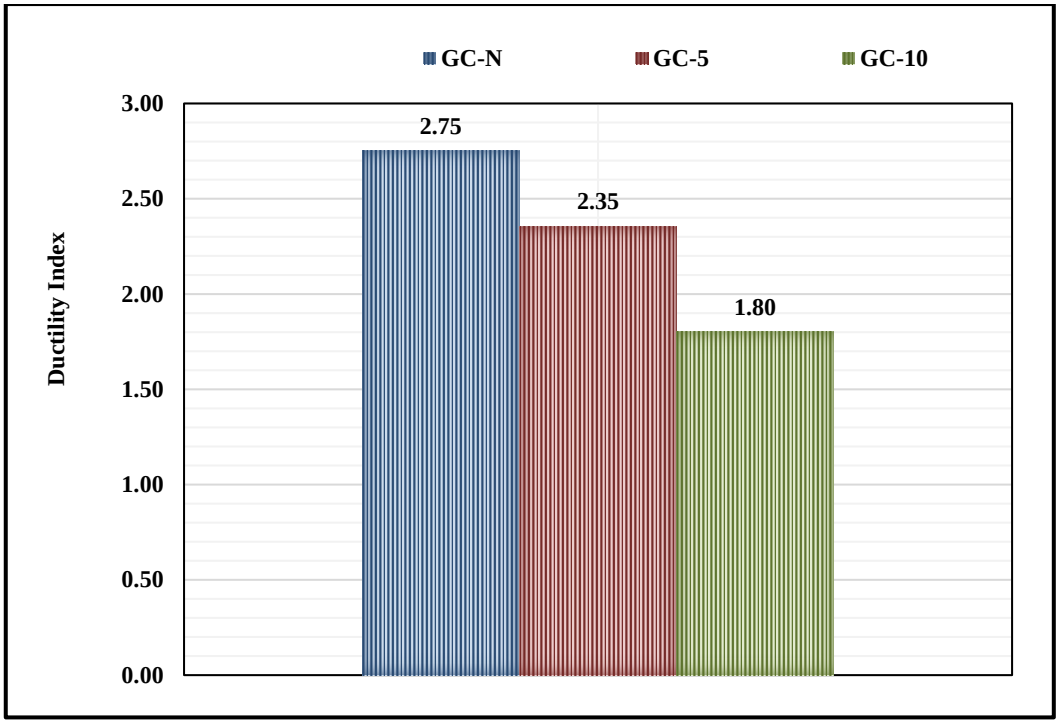

Figure 5- 11 Ductility index of Deep beams.

E. Energy Absorption Capacity of Deep beams.

Regarding the energy absorption, the concrete deep beam affected by the replacement ratio of recycled bricks which higher drop in the energy absorption were observed. Control beam GA-N has the higher energy than the other beams which scored of 920.48 kN.mm which reduced after addition of recycled bricks into the concrete mixture. The beam (GA-5) has less energy absorption than the control beam because it is made of recycled bricks material, which is characterized by less energy absorption because it contains recycled material missed their properties during the previous using. The energy absorption of beams GA-5 and GA-10 was (788.2, and 478.2) kN.mm respectively, and the percentage of decrease in energy absorption for both beams were (14.4% and 48.1%) when compared with the control one. The Deep beams with smaller grading size (GB-5, and GB-10) offered less energy absorption when compared with beams GA-X beams. which the energy absorption reduction value was (20%, and 40.2%) respectively as demonstrated in Figure 5.12.

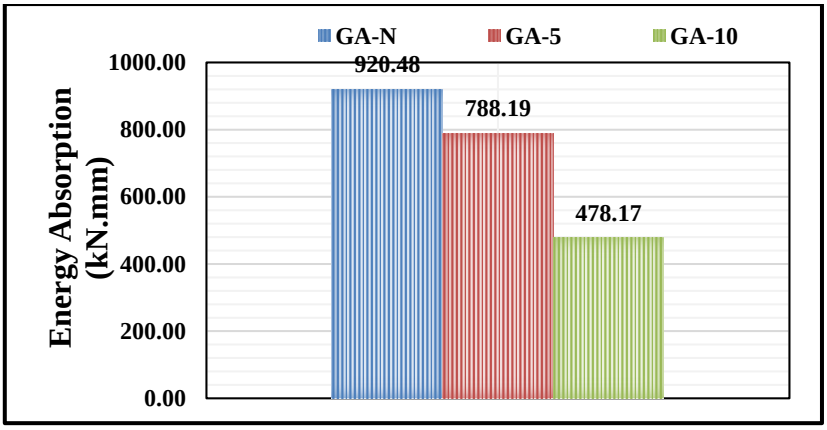

(a) GA-series

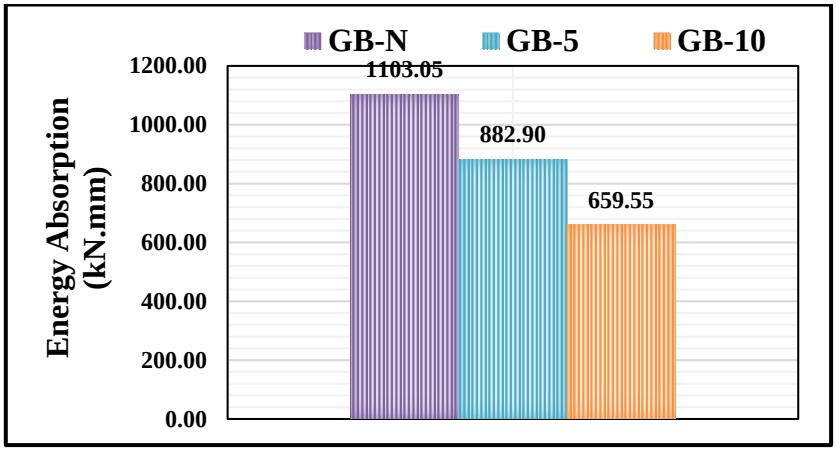

(a) GB-series

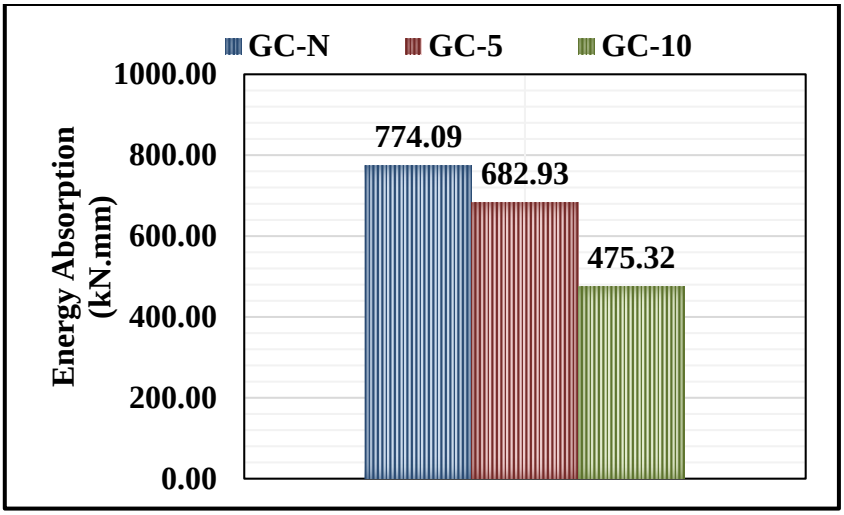

(a) GC-series

Figure 5- 12 Energy absorption of Deep beams.

Comparing the deep beams with two-point load with opposite them (two-point load) demonstrated that the energy absorption decreased by 15.9% for the

normal concrete deep beams and this energy absorption decreased by 11.8% and 38.6% when the replacement ratio increased to 5% and 10% respectively as demonstrated in Figure 5.12.

G. Cracking and Failure Mode

Figure 5.14 shows the crack characteristics and failure mode for each beam tested. The cracking mode of the tested beams revealed a variable behavior of failure related to the beam type which the RBC beams showed a different failure mode than NC beams. Cracking in shear deep beams can occur with or without the use of recycled bricks. In normal concrete deep beams, cracking primarily occurs due to shear forces exceeding the capacity of the beam. These beams have a large depth-to-span ratio, which makes them prone to shear failure. The cracking mode in shear deep beams without recycled bricks is similar to conventional deep beams. When subjected to shear forces, the primary mode of cracking in shear deep beams is diagonal tension. As the shear force increases, diagonal cracks start to develop in the beam, propagate from the point of maximum shear. These cracks typically form at an angle of 45 degrees to the axis of the beam and propagate towards the supports. The cracks reduce the stiffness and resistance to shear forces, led to a decrease in the load-carrying capacity of the beam. Therefore, crack control is essential to maintain the structural integrity of shear deep beams. Regarding the RBC beams, when recycled bricks are used in deep beams, the cracking mode can be influenced by the properties of the recycled bricks. Recycled bricks are typically obtained from demolished structures or waste materials and may have different characteristics compared to conventional bricks. These variations affected the cracking behavior of deep beams with recycled bricks. The recycled bricks possess inferior strength or bonding properties, which led to early failure and cracking in the beams. The weaker bricks not able to resist the shear forces effectively, resulting in premature cracking and reduced load-carrying capacity. Additionally, appropriate

reinforcement detailing, such as shear reinforcement, can be provided to enhance the overall structural integrity and prevent excessive cracking.

(a) GA-N

(b) GA-5

(c) GA-10

(d) GB-N

(e) GB-5

(f) GB-10

(g) GC-N

(h) GC-5

(i) GC-10

Figure 5- 13 Cracks pattern for beams.

5.3 Theoretical Study (Finite Element Study)

A. Verification

In the current study, the structural behavior of simply supported deep beams is simulated depending on available experimental tests. Thirteen deep beams based on experimental tests are used. The results of numerical analysis alongside the experimental ones for specimens (GA-N to GC-10) that used for the verification purpose in terms of load-deflection curve, ultimate load, maximum deflection, and crack patterns are presented in Tables (5.1) to (5.2), and Figure (5.14). Figure (5.14) shows that the predicted behavior concerning the load deflection curves is almost identical to the experimental results. The values of ultimate load are shown in Table (5.1). It can be observed that the values ratio of experimental to numerical ultimate load are between (97%) to (108%). Table (5.2), also gives the experimental and numerical values of the maximum deflection. The ratio of experimental to theoretical values of deflection are acceptable but with ratios less than load values matching due to the nature of concrete and bricks material which tend to be brittle material. Because of the simplification and assumption of the employed FEM, it seems no way to obtain crack propagation as accurately as the experimental test. This may be due to the difference between the condition of the theoretical and experimental tests.

Tabel 5-2 Verification results include the failure load.

Beam Status/Var.		Beam ID	$Vu, ANS.$ (kN)	$Vu, Exp.$ (kN)	$\frac{Vu, Exp}{Vu, ANS.}$
Experimental Shear Beams	Grading Size (19—20) mm	GA-N	542	522	103.83%
		GA-5	491	467.6	105.00%
		GA-10	379	366	103.55%
	Grading Size (10—12) mm	GB-N	612	566	108.13%
		GB-5	515	521	98.85%
		GB-10	431	444	97.07%

	Shear to depth ratio	GC-N	556	537	103.54%
		GC-5	496	483	102.69%
		GC-10	424	392	108.16%

Table 5.3: Verification results include maximum deflection.

Beam Status/Var.		Beam ID	Δ, N, (mm)	Δ, Exp, (mm)	$\frac{\Delta, ANS}{\Delta, Exp.}$
Experimental Shear Beams	Grading Size (19—20) mm	GA-N	5.64	6.230	90.55%
		GA-5	5.14	6.110	84.06%
		GA-10	4.67	4.830	96.69%
	Grading Size (10—12) mm	GB-N	5.36	6.670	80.36%
		GB-5	4.99	6.540	76.35%
		GB-10	7.42	6.490	114.27%
	Shear to depth ratio	GC-N	5.51	4.880	112.99%
		GC-5	4.71	5.130	91.81%
		GC-10	4.59	5.440	84.38%

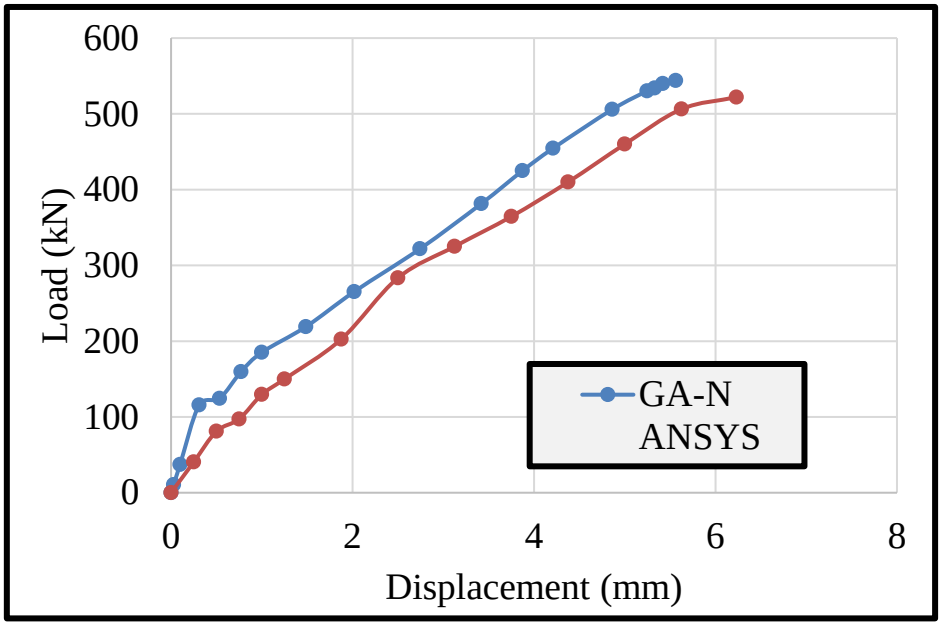

(a) Numerical and experimental beam (2L1).

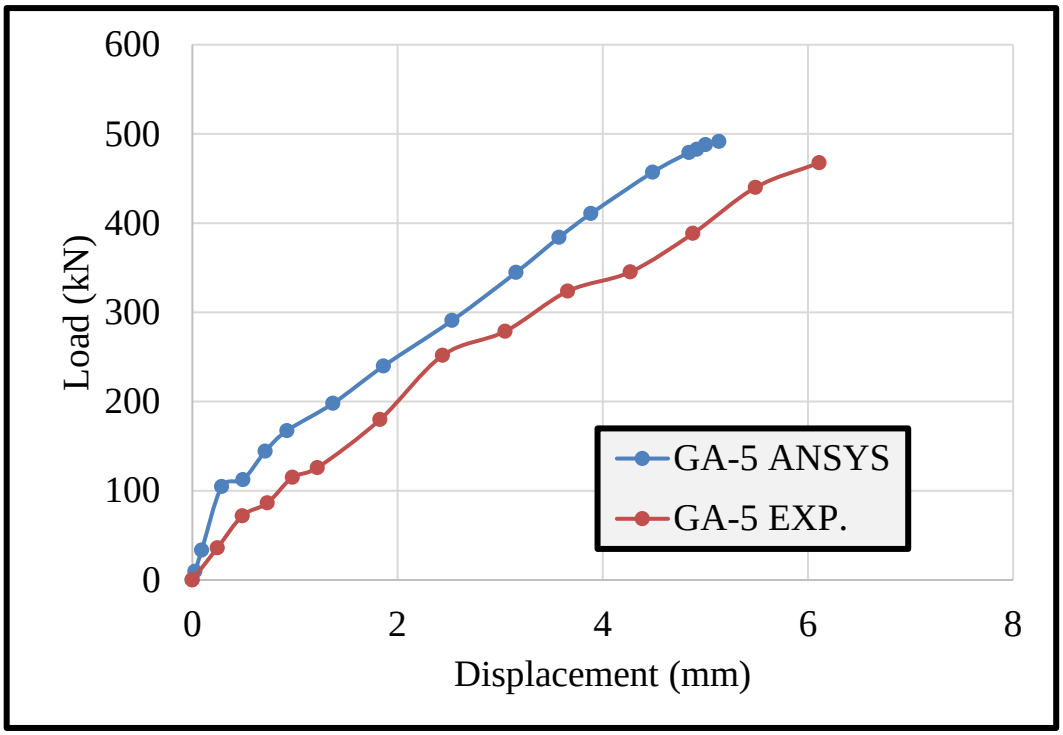

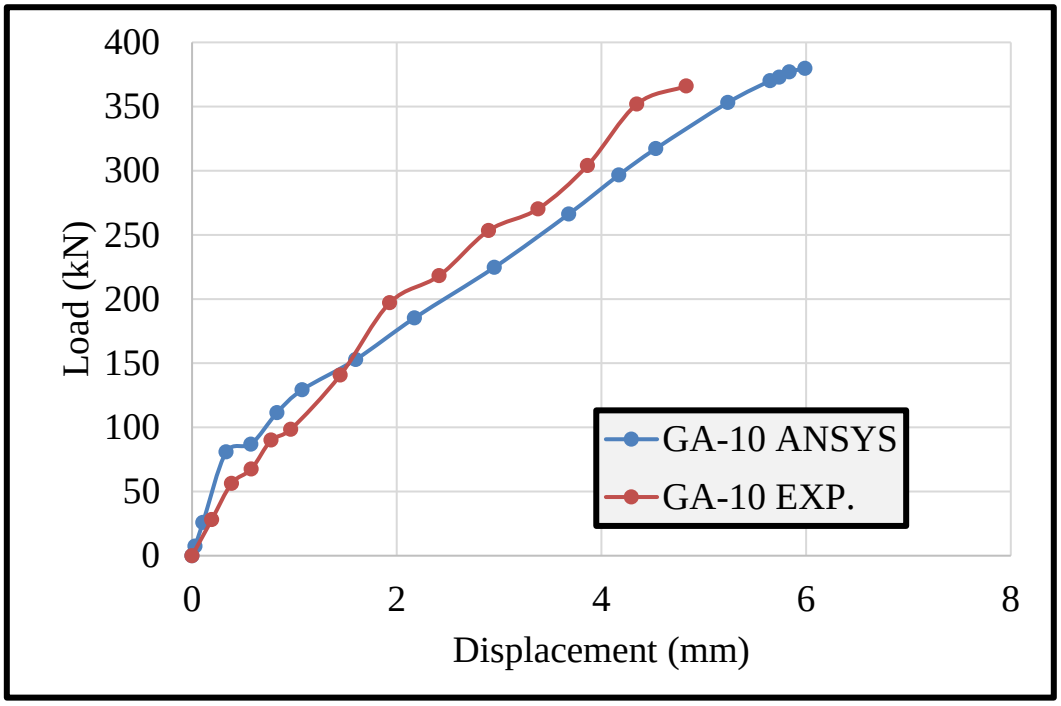

Figure 5- 14 Verification relationship.

But the major reason is the nature of the concrete material. It must be noted that the obtained cracks from numerical test is larger than one exists in the experimental test, and sometimes it was extended to areas where cracking were not physically observed. Extensive cracks are predicted by the FE modeling because the greater intensity of stress at the nodes. The greater intensity obtained

for the numerical cracking may be due to the cracking modeling used, in which material degradation is distributed over all the volume of the element. Also, assuming perfect bond between among the used elements causes high stress concentrations in the concrete elements.

B. Parametric Study

B.1 Effect of Shear Reinforcement Ratio

The shear behavior investigation revealed testing of three series divided into three groups for each one as seen in Table 5.4. The second and third series included modeling of ten deep beams by ANSYS APDL to investigate the effect of recycled bricks layers in relation with a/d.

Table 5-4 Effect of Shear Reinforcement Ratio

Beam Status/Var.		Beam ID	a/d	Grading	Pcr (kN)	Pu (kN)	Pcr/Pu	Deflection mm	D.I	Energy absorption (kN.mm)
Numerical Shear Beams	Shear reinforcement	GA-5-0	2	20	87	335	25.97%	3.440	1.90	112.23
		GA-5-15	2	20	301	427	70.49%	3.870	2.76	436.83
		GA-5-20	2	20	263	406	64.78%	4.030	2.52	397.46
	RBC Thickness (a/d=2)	GA-5CM	2	20	381	514	74.12%	5.860	2.19	837.25
		GA-10CM	2	20	370.3	503	73.62%	5.850	2.15	812.35
		GA-20CM	2	20	366	491	74.54%	5.710	2.15	783.70
		GA-30CM	2	20	365	484	75.41%	5.740	2.11	785.66
		GA-40CM	2	20	341	481	70.89%	5.790	2.08	740.40
	RBC Thickness (a/d=2)	GC-5CM	1	20	382	515	74.17%	4.922	2.62	705.13
		GC-10CM	1	20	376	509	73.87%	4.914	2.59	692.87
		GC-20CM	1	20	355	495	71.72%	4.796	2.58	638.52
		GC-30CM	1	20	311.67	490	63.61%	4.822	2.54	563.53
		GC-40CM	1	20	291.3	489	59.57%	4.864	2.51	531.29

The simulated beams showed a cracking load with a range of (87-382) kN for shear plain concrete deep beam and reinforced one which the shear plain concrete deep beam revealed a lower cracking load strength among the simulated beam. In term of the ultimate load and maximum displacement, the ultimate strength showed higher values with range of (335-515) kN and maximum displacement of (3.44 -5.86) mm as seen in Fig 5.15. the variation in the outcomes was due to the used variables which the hybridization of concrete deep beam with layers of recycled bricks enhanced the shear behavior of the simulated deep beams. The first series of experiments involved the testing of three numerically fabricated RC deep beams with varying transverse steel reinforcement ratios. These beams were subjected to static loads until failure. The results revealed that the cracking load ranged between 87 kN and 301 kN. Furthermore, the obtained strength results varied between 335 kN and 427 kN, with displacements ranging from 3.44 mm to 4.03 mm, as presented in Table 5.1. The variability in the ultimate load carrying capacity of the beams can be attributed to several factors. Firstly, the changing transverse steel reinforcement ratio played a significant role in influencing the strength and behavior of the beams. Additionally, the shear span to depth ratio (a/d) and the RB constant ratio also contributed to the observed variations in load-carrying capacity. The beam with recycled bricks of 5% and without shear reinforcement (GA-5-) revealed that a lower cracking load of 87 kN which addition of shear reinforcement enhanced the cracking by more than three times.

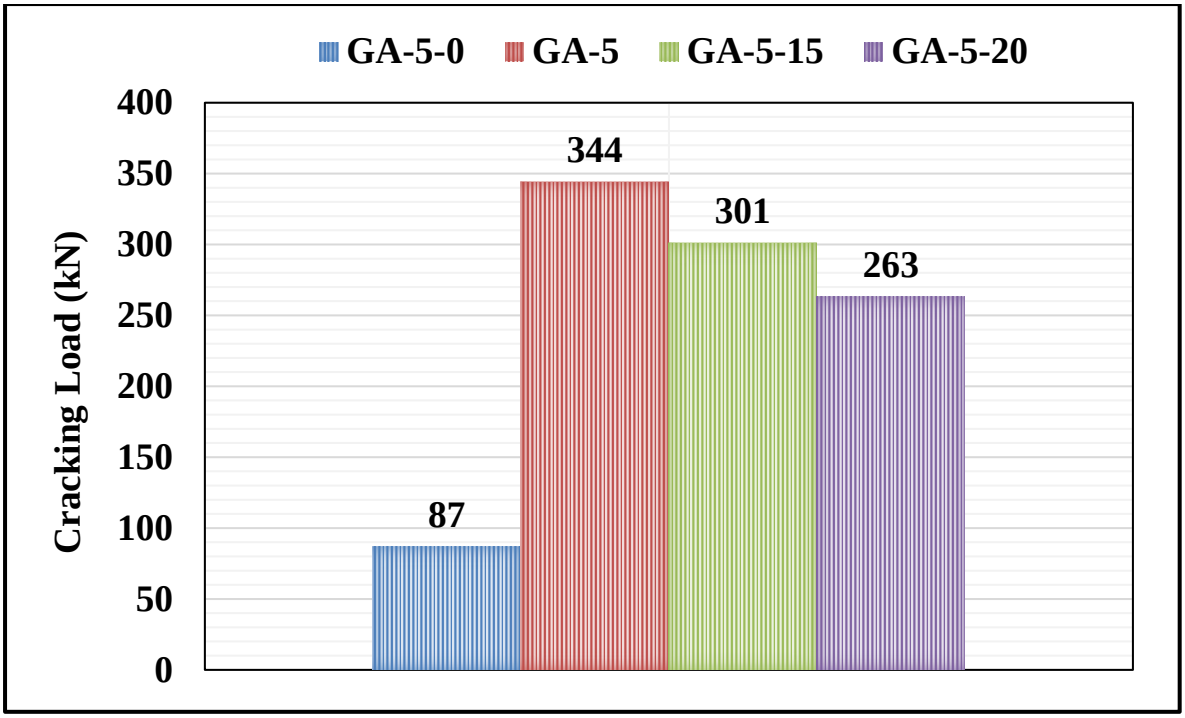

Figure 5- 15 load deflection curve of GA-5 and GA-5-0.

Regarding the ultimate shear strength, Reinforcing the shear regions by steel rebar enhanced the ultimate strength which placing the shear stirrups @ 10, 15, and 20 cm revealed an enhancement in the ultimate shear strength by 39.6%, 27.46%, and 21.2% respectively when compared with the shear plain concrete deep beam (GA-5-0). concerning the displacement, Reinforcing the shear regions by steel rebar enhanced the maximum displacement which placing the shear stirrups @ 10, 15, and 20 cm revealed an enhancement in the maximum displacement by 77.6%, 12.5%, and 17.2% for models (GA-5, GA-5-15, GA-5-20) respectively when compared with the shear plain concrete deep beam (GA-5-0) as seen in Figure 5.16. These findings highlighted the importance of proper selection and design of transverse steel reinforcement in RC deep beams. The results indicated that increasing the transverse reinforcement ratio led to higher cracking loads and ultimate strength beside the maximum displacement. It also suggests that optimizing the shear span to depth ratio and considering the RB constant ratio can further enhance the performance of RC deep beams.

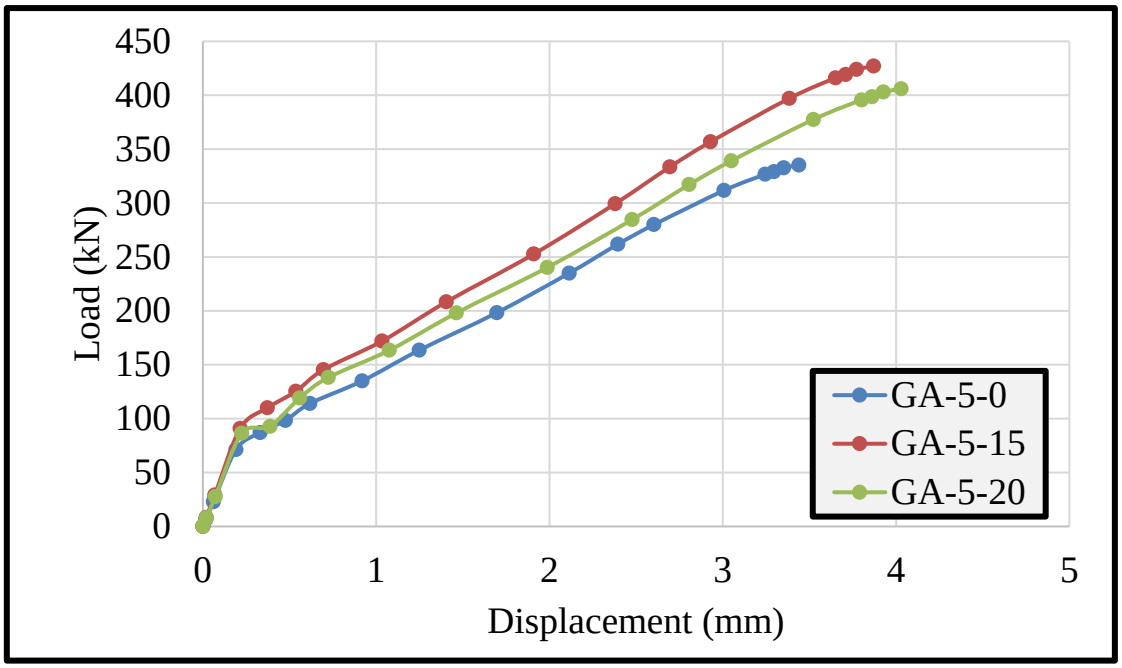

Figure 5- 16 load deflection curve of numerical group

C. Effect of Recycled Bricks Layer

The second series of experiments involved the testing of three numerically fabricated RC deep beams with varying the thickness of the recycled bricks in concrete deep beam. The beams hybridized with 5, 10, 20, 30, and 40 cm recycled bricks layers from the top of the cross section. These beams were subjected to static loads until failure. For the beams with a/d of 2, The results revealed that the cracking load ranged between 341 kN and 381 kN. Furthermore, the obtained strength results varied between 481 kN and 514 kN, with displacements ranging from 5.71 mm to 5.86 mm, as presented in Table 5.1. The variability in the ultimate load carrying capacity of the beams can be attributed to several factors. Firstly, the changing recycled bricks thickness which played a significant role in influencing the strength and behavior of the beams. Additionally, the shear span to depth ratio (a/d) and the RB constant ratio also contributed to the observed variations in load-carrying capacity. The beam with recycled bricks of 5% and with higher thickness of recycled bricks layer (GA-40CM) revealed that a lower cracking load of 341 kN as seen in Figure 5.17.

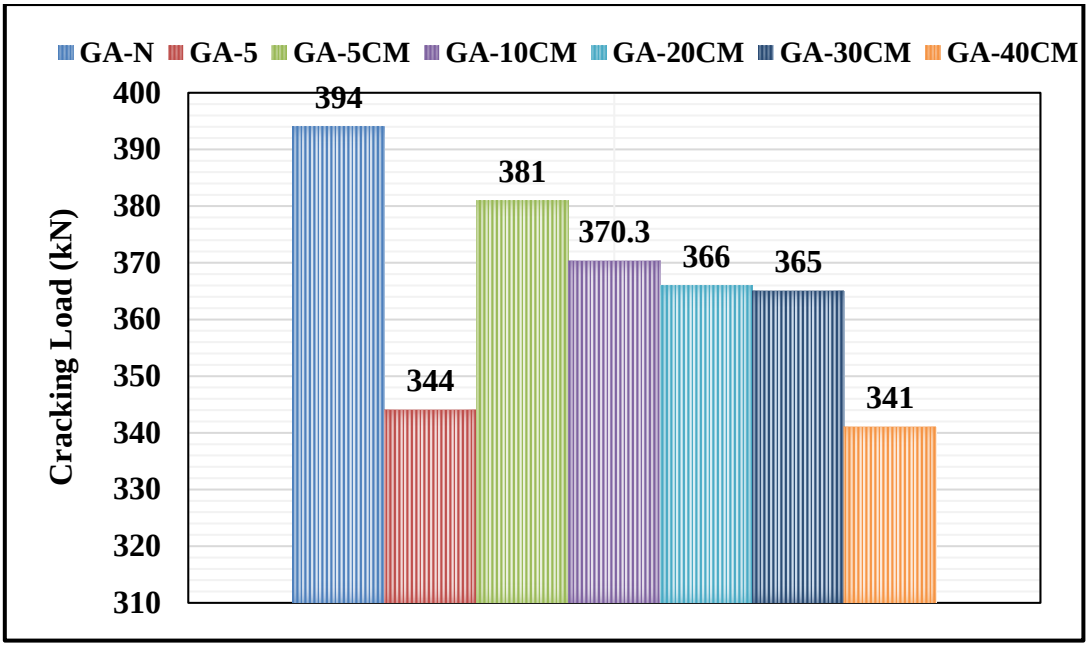

Figure 5- 17 load deflection curve of GA numerical series.

The incorporation of recycled bricks in hybridized cross-section regions had an impact on the ultimate shear strength and maximum displacement of the deep beams. The results showed that as the recycled bricks were placed in the cross-section regions at different thicknesses (5 cm, 10 cm, 20 cm, 30 cm, and 40 cm), there was a reduction in the ultimate shear strength compared to the conventional concrete deep beam (GA-N). The decrement in the ultimate shear strength ranged from 1.5% for a placement length of 5 cm to 7.9% for a placement length of 40 cm. Regarding the maximum displacement, the hybridization of the cross-section regions by recycled bricks also influenced the displacement behavior. When compared to the conventional concrete deep beam (GA-N), the placement of recycled bricks at different lengths (5 cm, 10 cm, 20 cm, 30 cm, and 40 cm) resulted in comparable displacement values. This indicates that the presence of recycled bricks did not significantly affect the maximum displacement of the deep beams. These findings proposed that the addition of recycled bricks in the cross-section regions of deep beams led to a slight reduction in the ultimate shear strength. However, it does not have a significant impact on the maximum displacement behavior as seen in Figure 5.18.

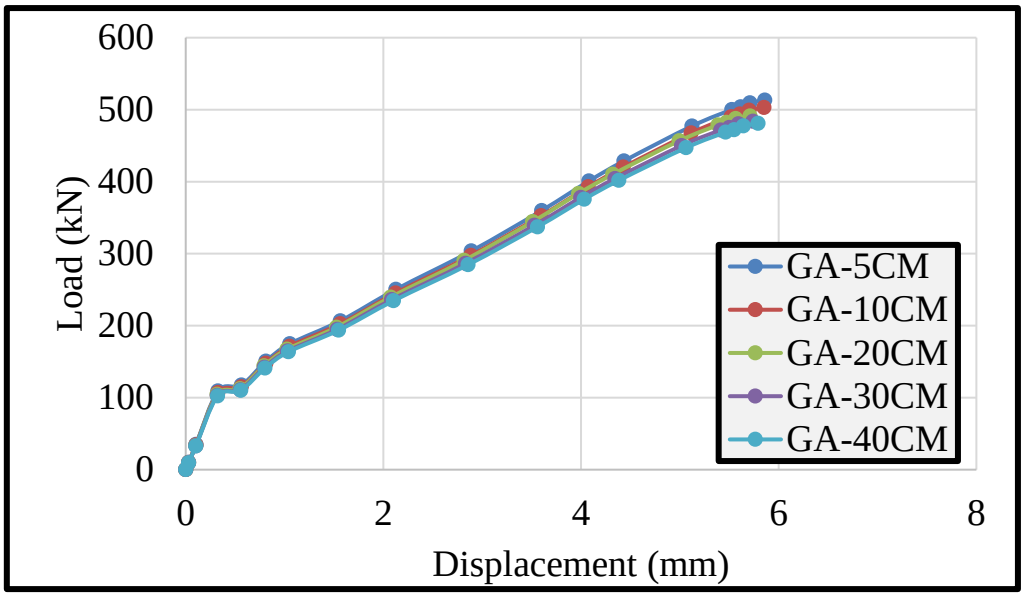

Figure 5- 18 load-displacement curve numerical series.

In the case of beams subjected to two-point loads with a shear span to depth ratio (a/d) of 1, the hybridization of the cross-section regions with recycled bricks had an impact on the ultimate strength and maximum displacement. The results indicated that as the recycled bricks were placed in the cross-section regions at different lengths (5 cm, 10 cm, 20 cm, 30 cm, and 40 cm), there was a reduction in the ultimate shear strength compared to the conventional concrete deep beam (GA-N). The decrement in the ultimate shear strength ranged from 4.1% for a placement length of 5 cm to 9% for a placement length of 40 cm. Regarding the maximum displacement, the hybridization of the cross-section regions with recycled bricks also influenced the displacement behavior. When compared to the conventional concrete deep beam (GC-N), the placement of recycled bricks at different lengths (5 cm, 10 cm, 20 cm, 30 cm, and 40 cm) resulted in comparable displacement values. This proposed that the presence of recycled bricks did not significantly affect the maximum displacement of the deep beams. These findings highlighted that the addition of recycled bricks in the cross-section regions of deep beams subjected to two-point loads may lead to a reduction in the ultimate shear strength. However, it has a limited effect on the maximum displacement behavior as seen in Figure 5.19.

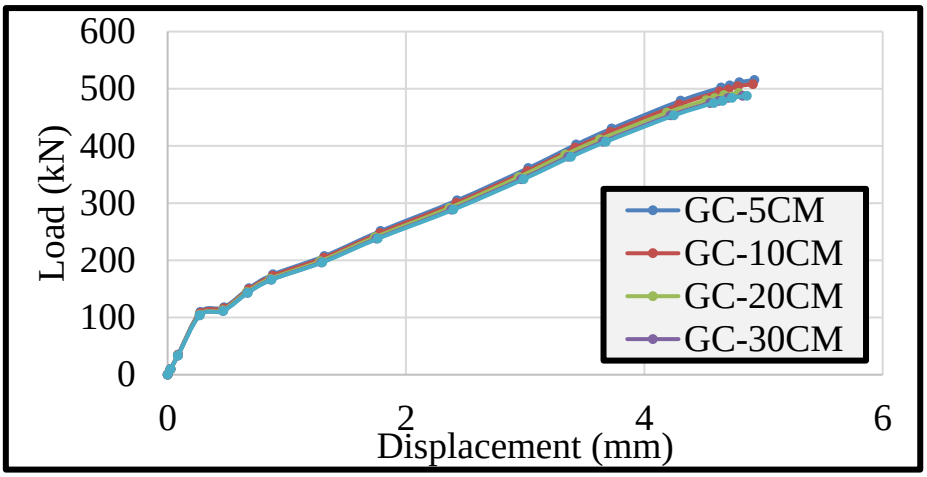

Figure 5- 19 load-displacement curve numerical series.

D. Ductility Index

Regarding the ductility of the first numerical series, the addition of stirrups and as expected lead to increase the ductility but for the concrete beam with recycled bricks revealed a distinct behavior. The change of transverse steel reinforcement in the deep beams made with recycled bricks of 5% showed a different behavior in contrast with conventional concrete which the plain concrete deep beams showed a ductility of 1.9 which increased to 2.09, and 2.76, and 2.52 when the beam reinforced with stirrups @15 and 20 cm for beams (GA-5-0, GA-5-15, and GA-5-20) respectively as demonstrated in Figure 5.20.

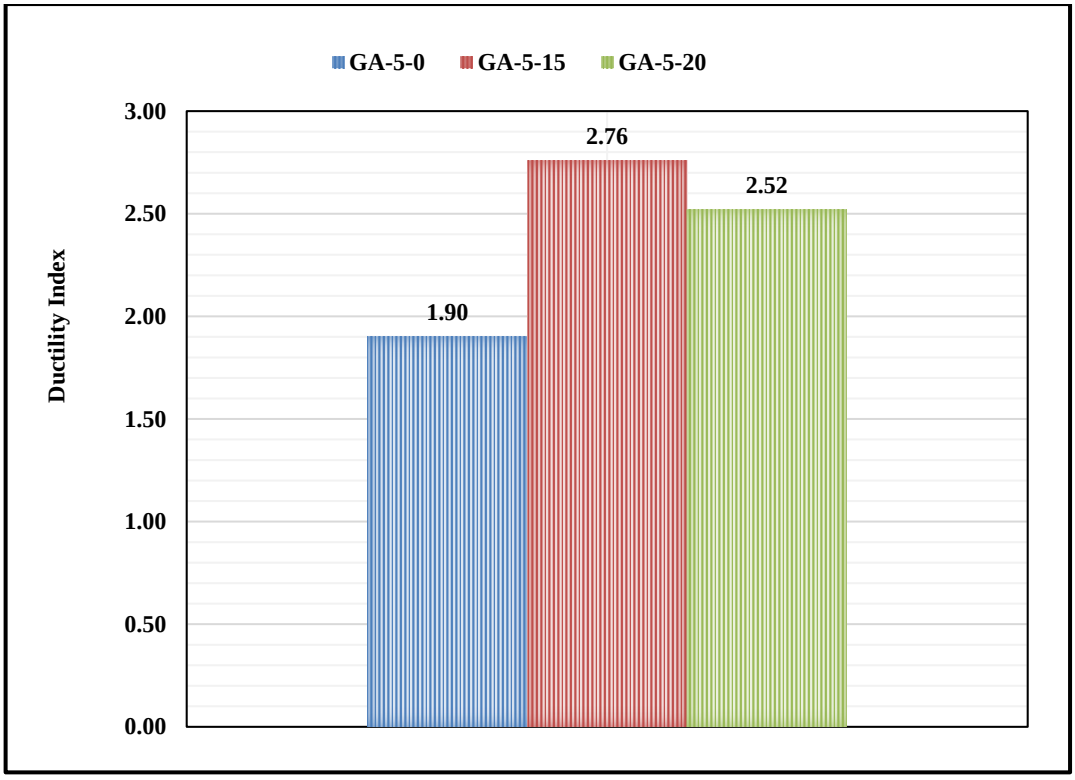

Figure 5- 20 Ductility index of numerical series.

Regarding the ductility of the second numerical series, the addition of recycled material and as expected lead to decrease the ductility but for the concrete beam with recycled bricks revealed a distinct behavior. The hybridization of concrete deep beams with 5, 10, 20, 30, and 40 cm recycled bricks layers from the top of the cross section the deep beams made with recycled bricks of 5% showed a different behavior in contrast with conventional concrete which the concrete deep beams with 5 cm layer of recycled bricks showed a ductility of 2.19 which increased the thickness of recycled bricks thickness to 10, 20, 30, and 40 cm decreased the ductility slightly which offered a reduction by 1.9%, 1.9%, 3.8%, 5.2% for models GA-5CM, GA-10CM, GA-20CM, GA-30CM, and GA-40CM respectively as demonstrated in Figure 5.21. Regarding the ductility of the third numerical series, the hybridization of concrete deep beams with 5, 10, 20, 30, and 40 cm recycled bricks layers from the top of the cross section the deep beams made with recycled bricks of 5% showed a different behavior in contrast with conventional concrete which the concrete deep beams

with 5 cm layer of recycled bricks showed a ductility of 2.62 which increased the thickness of recycled bricks thickness to 10, 20, 30, and 40 cm decreased the ductility slightly which offered a reduction by 1.2%, 1.5%, 3.1%, 4% for models GC-5CM, GC-10CM, GC-20CM, GC-30CM, and GC-40CM respectively as demonstrated in Figure 5.22.

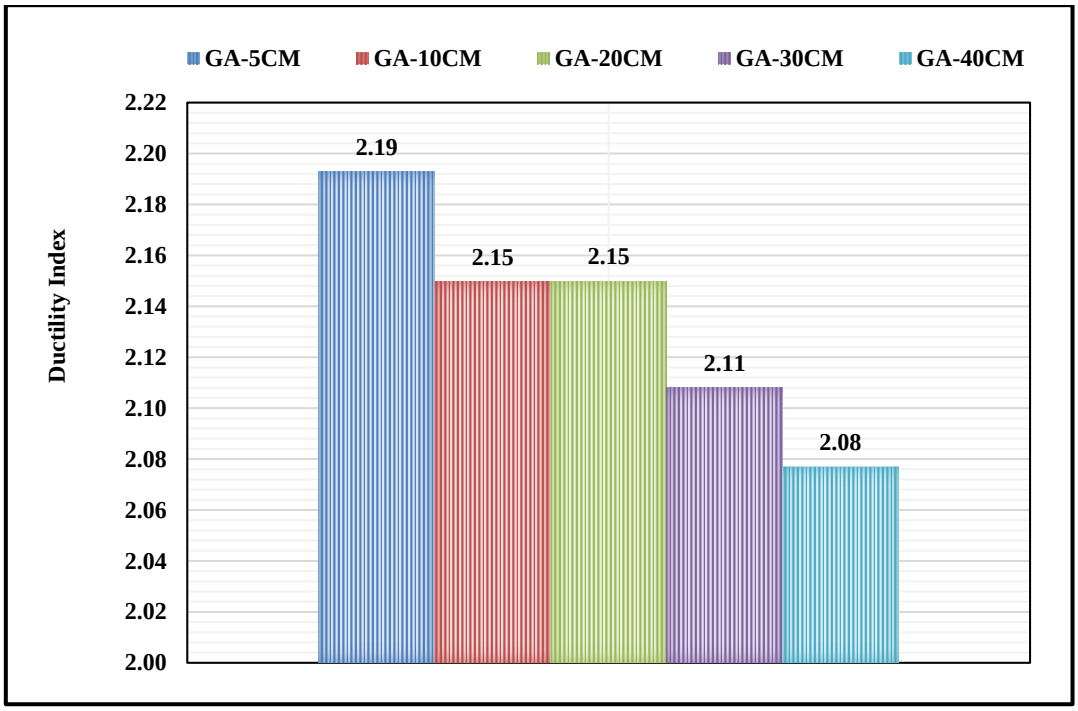

Figure 5- 21 Ductility index of numerical series.

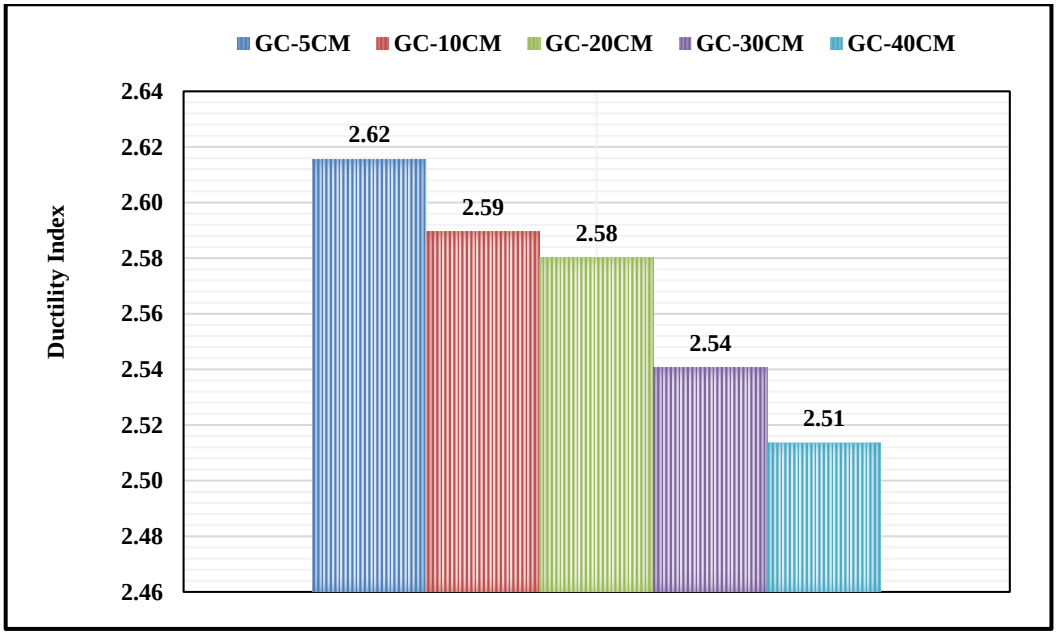

Figure 5- 22 Ductility index of numerical series.

F. Energy Absorption Capacity

Stirrups, as predicted, increased energy absorption in the first numerical series, but a concrete beam reinforced with recycled bricks exhibited unusual behaviour. For deep beams reinforced with stirrups @10, 15, and 20 cm for beams (GA-5-0, GA-5-15, and GA-5-20), respectively, the energy absorption increased from 112.23 for plain concrete deep beams to 788.2, 436.83, and 397 for deep beams made with 5% recycled bricks. This contrasts with conventional concrete, as shown in Figure 5.23. Regarding the ductility of the second numerical series, the hybridization of concrete deep beams with 5, 10, 20, 30, and 40 cm recycled bricks layers from the top of the cross section the deep beams made with recycled bricks of 5% showed a different behavior in contrast with conventional concrete which the normal concrete deep beams without recycled bricks (GA-5) showed an energy absorption of 920.48 which increased the thickness of recycled bricks thickness to 10, 20, 30, and 40 cm decreased the stiffness slightly which offered a reduction by 9.1%, 11.8%, 14.9%, 14.65, 19.6% for models GA-5CM, GA-10CM, GA-20CM, GA-30CM, and GA-40CM respectively as demonstrated in Figure 5.24.

Regarding the energy absorption of the third numerical series, the hybridization of concrete deep beams with 5, 10, 20, 30, and 40 cm recycled bricks layers from the top of the cross section the deep beams made with recycled bricks of 5% showed a different behavior in contrast with conventional concrete which the concrete deep beams with 5 cm layer of recycled bricks showed a stiffness of 2.62 which increased the thickness of recycled bricks thickness to 10, 20, 30, and 40 cm decreased the energy absorption slightly which offered a reduction by 1.2%, 1.5%, 3.1%, 4% for models GC-5CM, GC-10CM, GC-20CM, GC-30CM, and GC-40CM respectively as demonstrated in Figure 5.25.

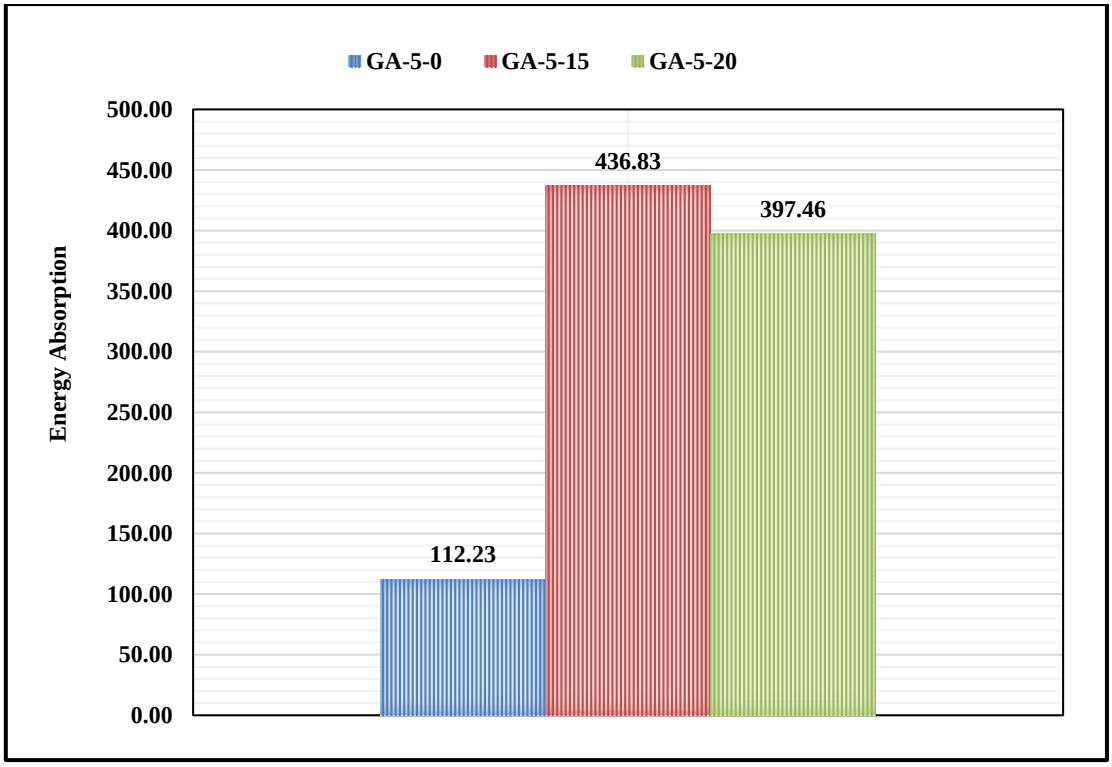

Figure 5- 23 Energy absorption of numerical series.

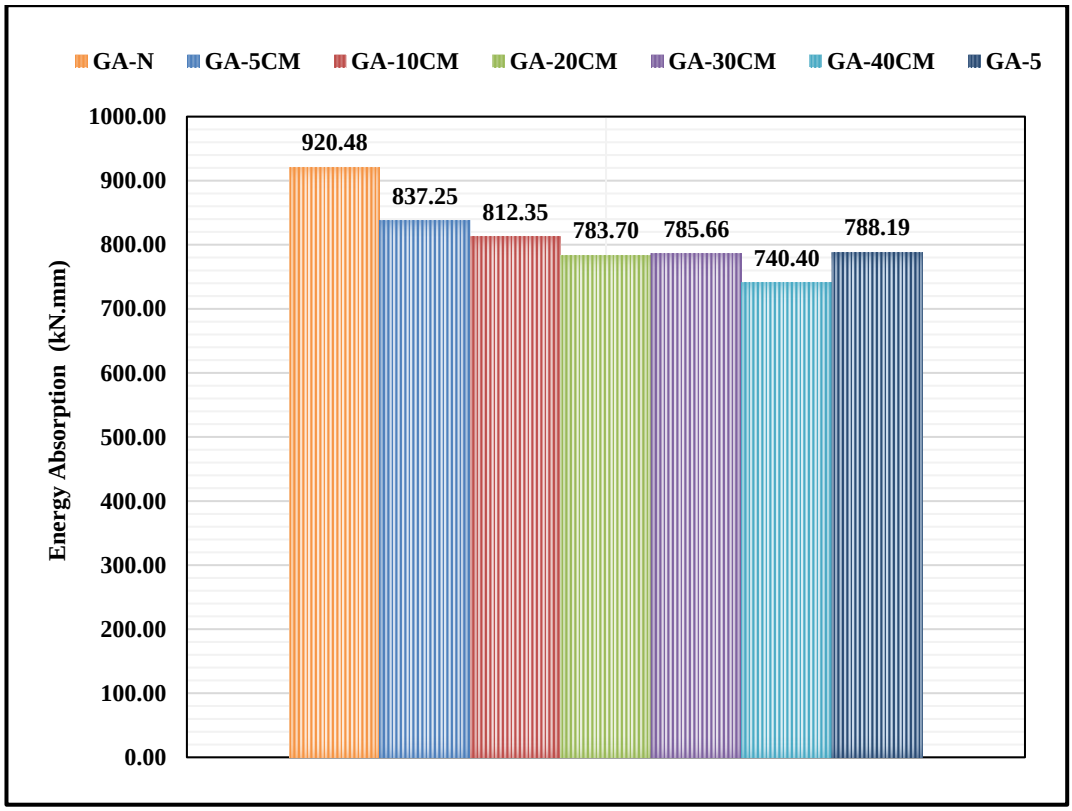

Figure 5- 24 Energy absorption of numerical series.

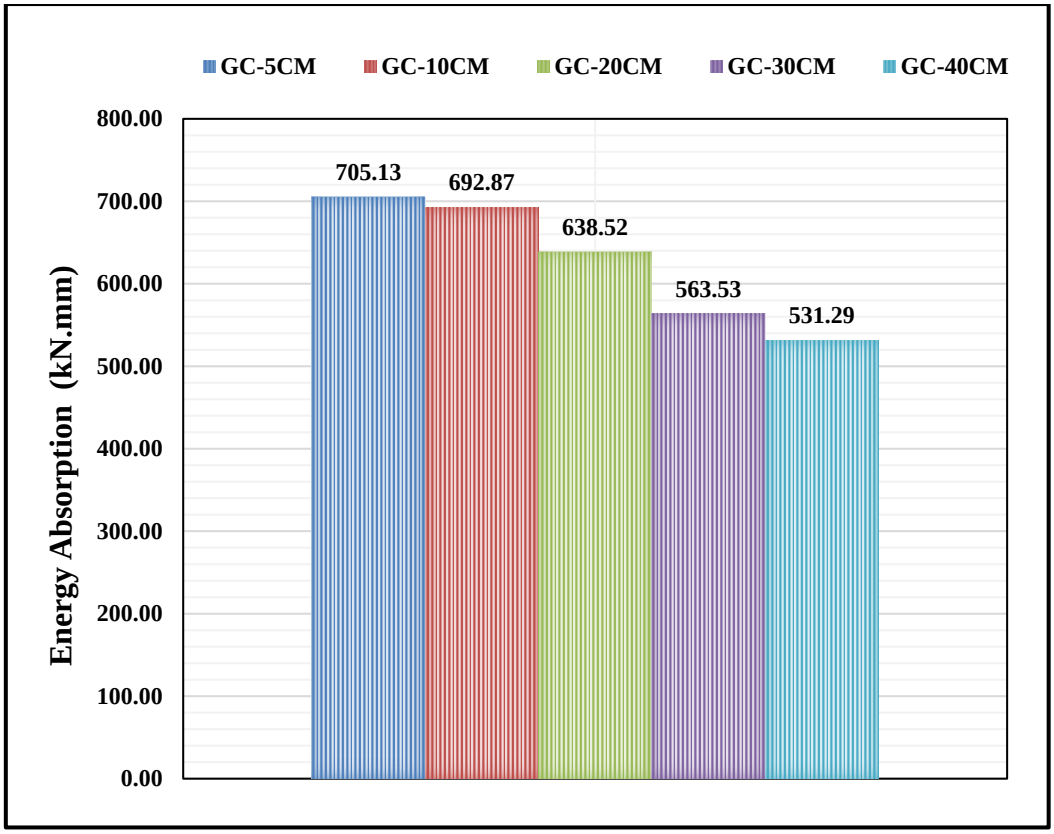

Figure 5- 25 Energy absorption of numerical series.

G. Cracking Pattern, Shear Stress and Strains

The shear stress path contours of deep beams provide a visual representation of how shear stresses are distributed and transmitted within the beam's cross-section. These contours explain the flow and transfer of shear forces through different regions of the beam. In a deep beam, the shear stress path contours typically exhibit a complex pattern due to the presence of multiple load paths and load transfer mechanisms. The contours illustrate the varying magnitudes and directions of shear stresses at different locations within the beam. Typically, near the point of application of the load, the shear stress path contours show high shear stress concentrations. As the shear forces travel towards the supports, the contours may spread out and form a wider distribution. This is often observed in the mid-span region of the beam. Regarding the control deep beam made with normal concrete showed that the cracks started at the shear zones and extended to the loading region for both ends. Shear dominated failure was occurred for all concrete deep beams. Concerning the parametric beams, the recycled bricks

layers affected the crack pattern and stress distribution for deep beams as revealed in figure below.

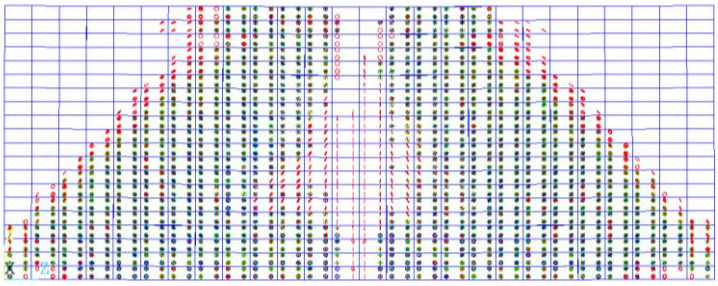

Cracking Pattern

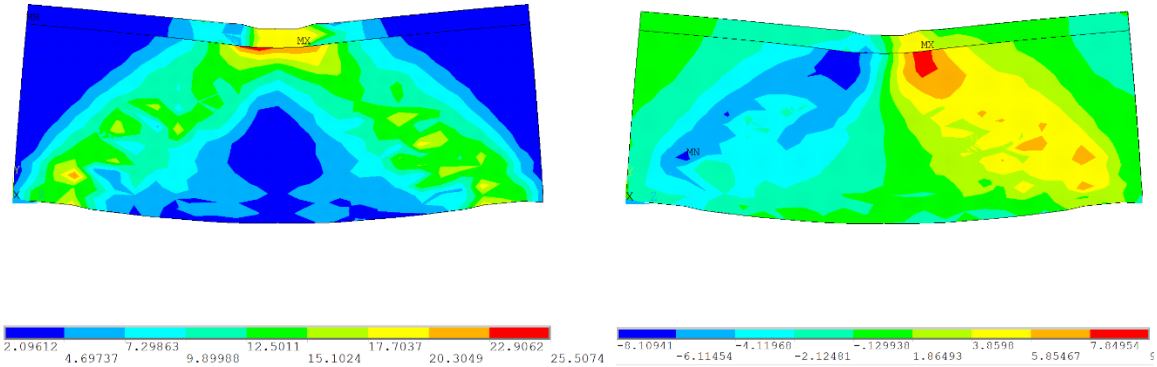

Stress intensity Shear Stress

1. GA-5CM

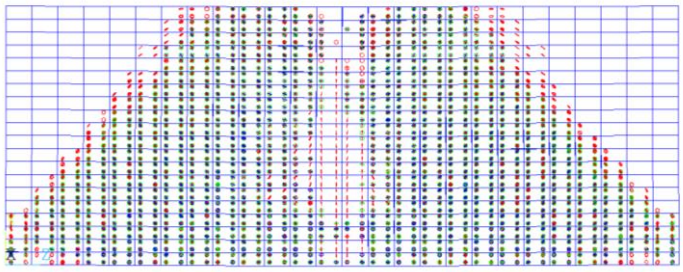

(a) Cracking Pattern

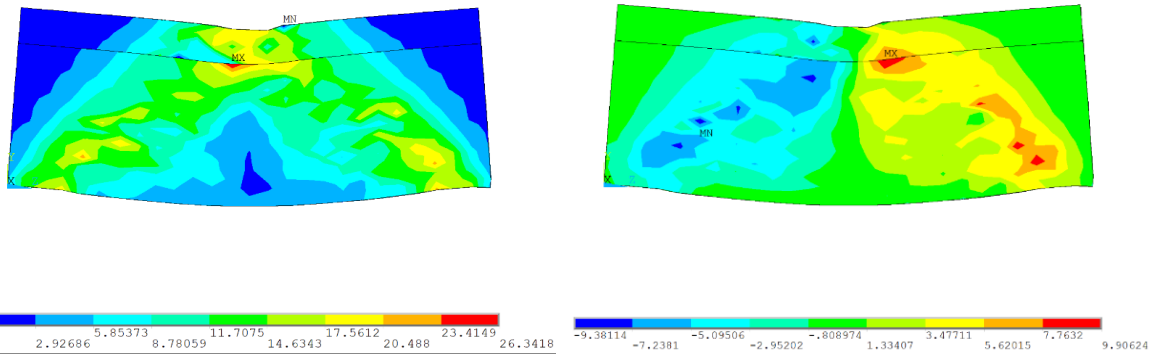

Stress intensity Shear Stress

2. GA-10CM

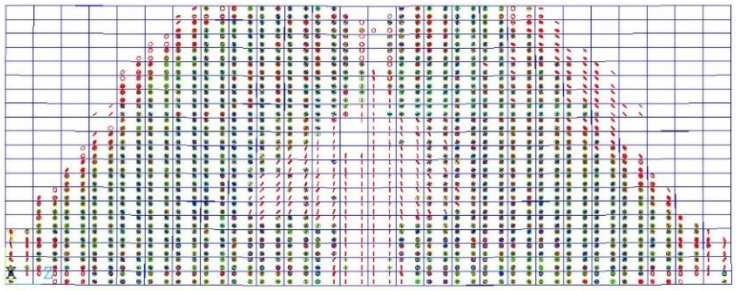

Cracking Pattern

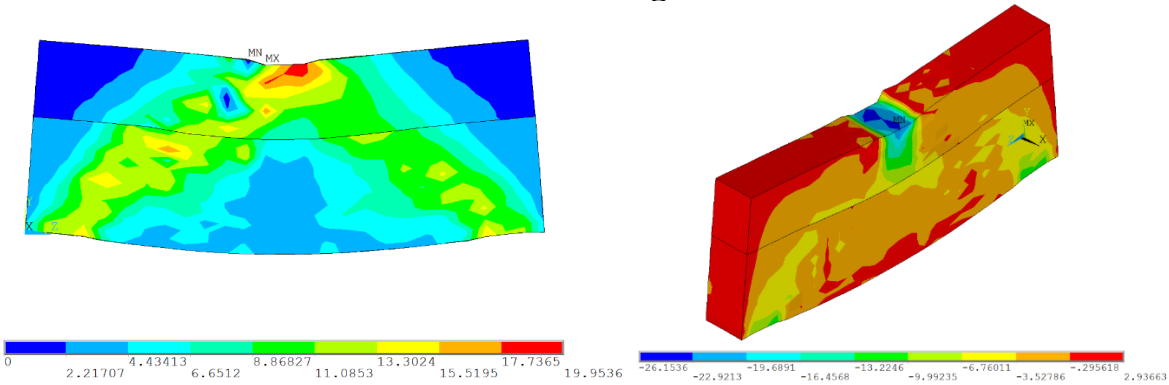

Stress intensity Shear Stress

3. GA-20CM

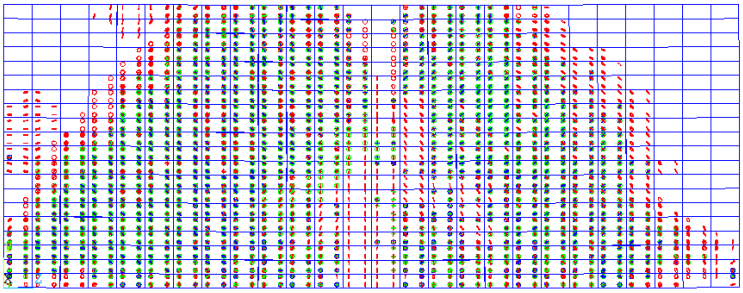

Cracking Pattern

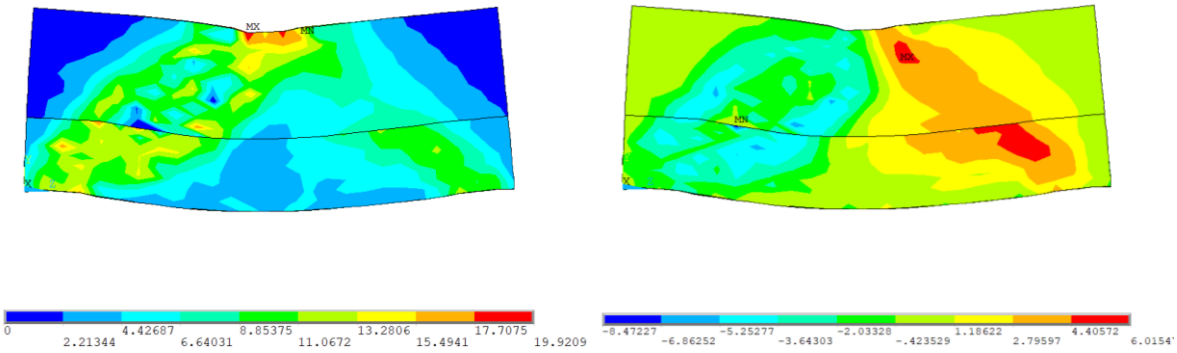

Stress intensity Shear Stress

4. GA-30CM

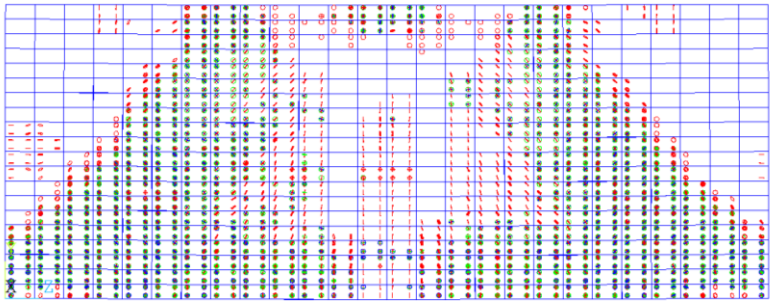

(b) Cracking Pattern

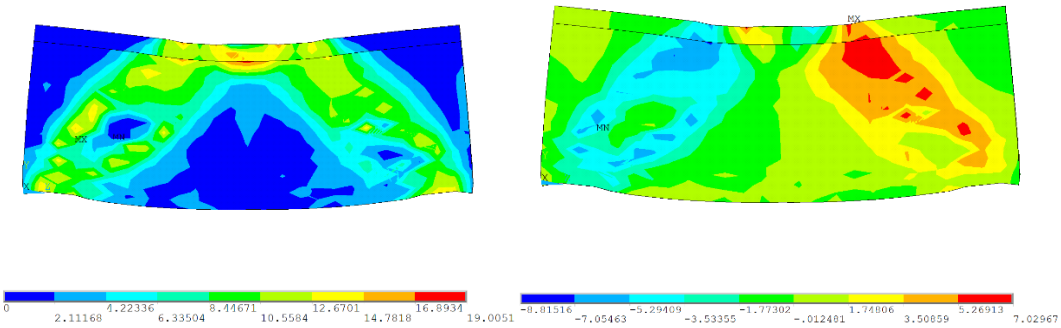

Stress intensity Shear Stress

5. GC-5CM

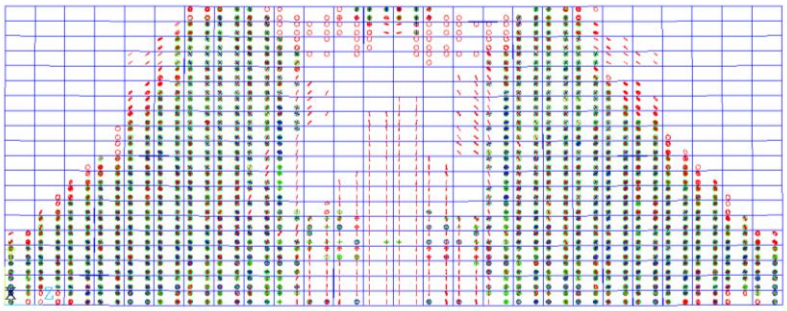

Cracking Pattern

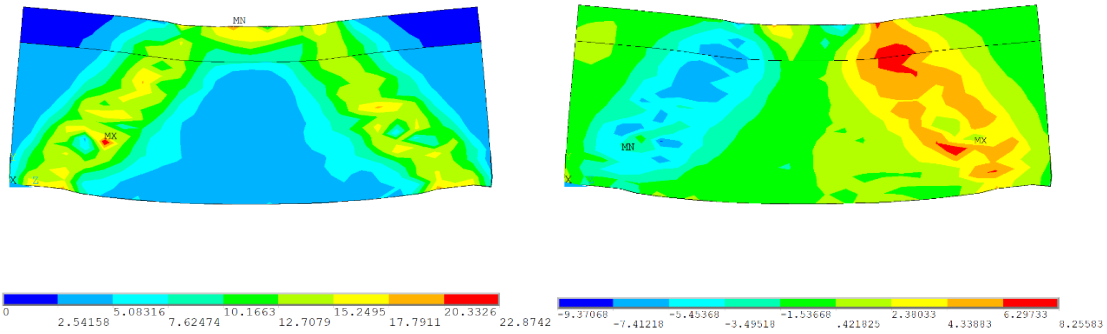

Stress intensity Shear Stress

6. GC-10CM

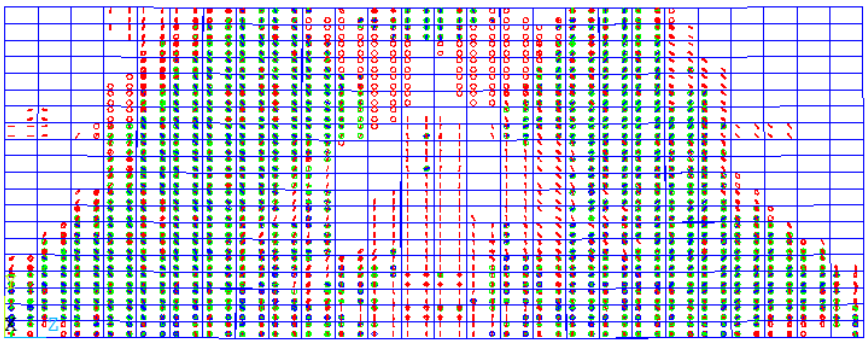

Cracking Pattern

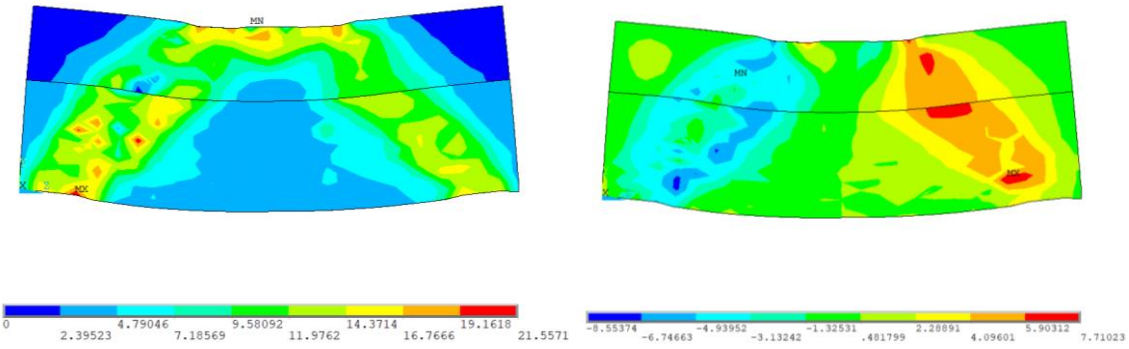

Stress intensity Shear Stress

7. GC-20CM

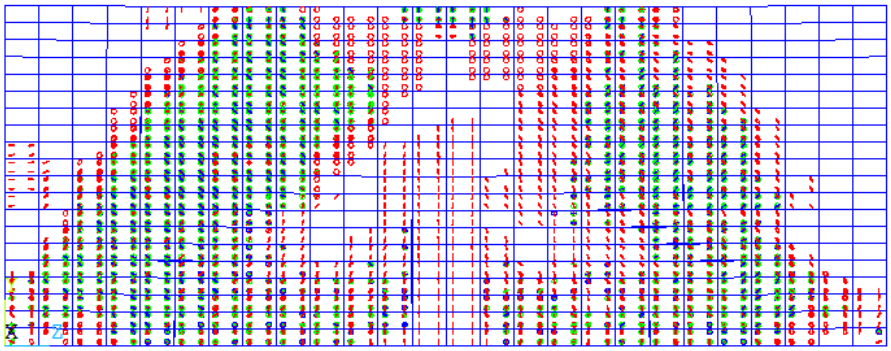

Cracking Pattern

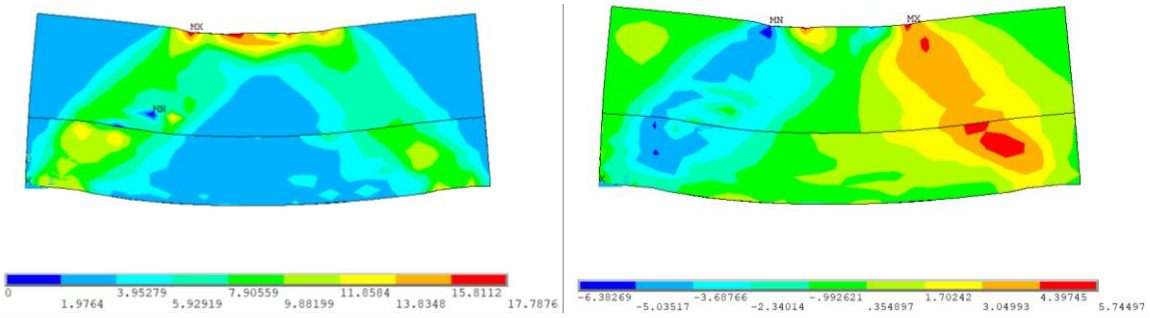

Stress intensity Shear Stress

8. GC-30CM

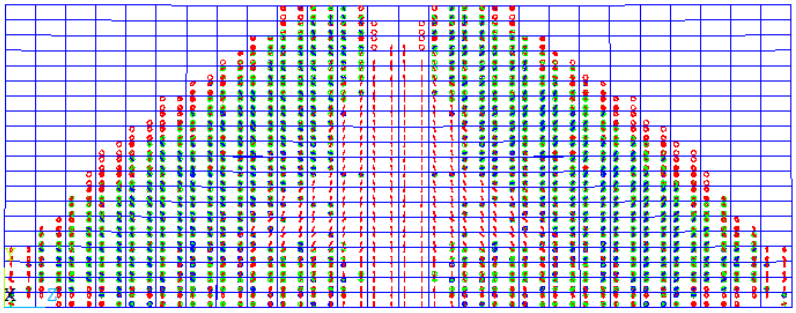

Cracking Pattern

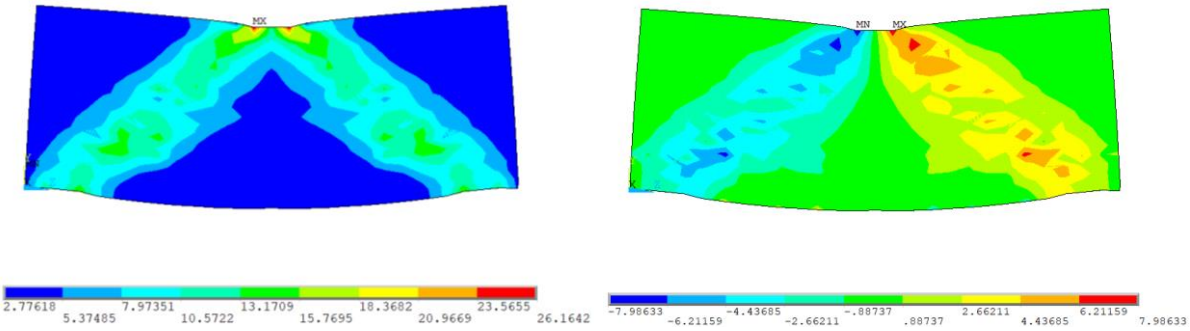

Stress intensity Shear Stress

9. GA-5-0

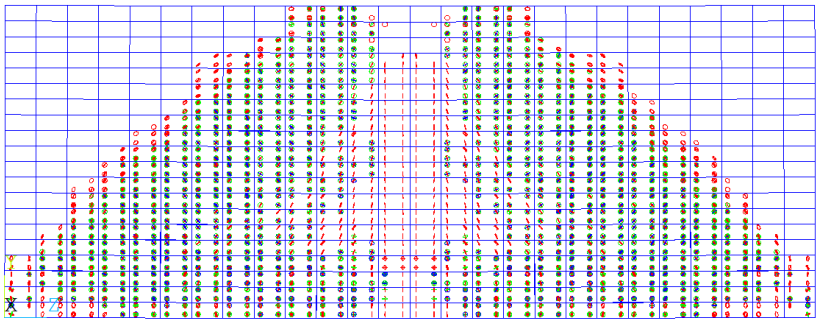

Cracking Pattern

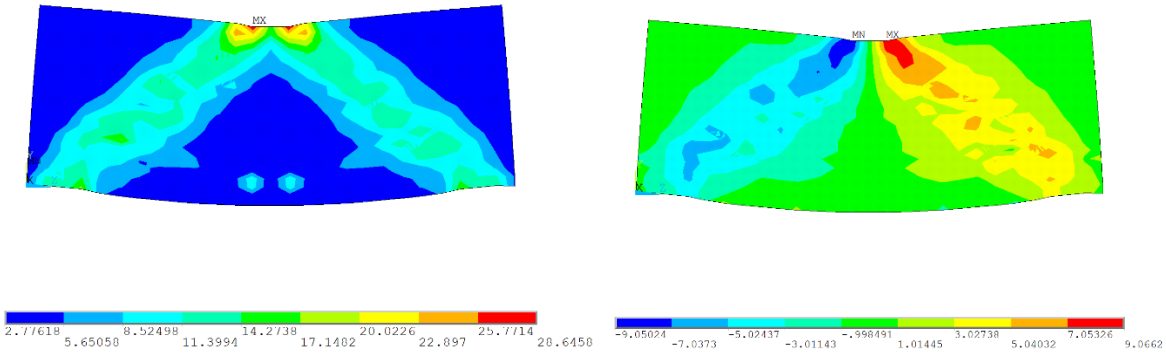

Stress intensity Shear Stress

10. GA-5-10

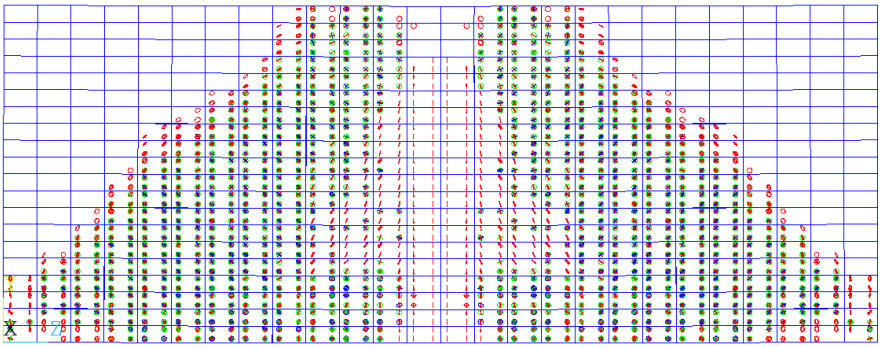

Cracking Pattern

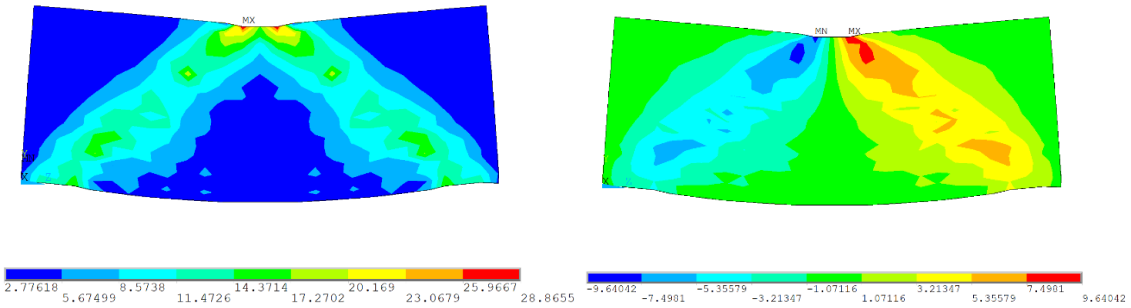

Stress intensity Shear Stress

11. GA-5-20

Figure 5- 26 Failure mode and stress distribution for numerical beams.

CHAPTER SIX: CONCLUSIONS AND RECOMMENDATIONS

6.1 Conclusions

This section summarizes the key findings and conclusions from the experimental and numerical investigation on the behavior of RC deep beams. The study focuses on the shear behavior of deep beams made of recycled bricks concrete with recycled bricks. Through the experimental study, various factors influencing the shear behavior of recycled concrete deep beams at failure have been identified and analyzed. This section provides a concise overview of the significant factors that affect the behavior of deep beams.:

1) Natural concrete deep beams exhibit a linearity of 75%. While the average linearity of the concrete deep beams made with recycled bricks of 62%.
2) The crushed bricks' presence in concrete mixtures has a notable impact on cracking load, ultimate load, and deflection of the deep beams.
3) Increasing the replacement ratio from zero percent to 5% and 10% resulted in a reduction in both the cracking and ultimate load capacities. These results indicated that as the replacement ratio increased, the shear strength capacity of the beams decreased. The cracking load and ultimate load exhibited a downward trend with increasing replacement ratios.
4) For smaller grading sizes, Increasing the replacement ratio resulted in a reduction in both the cracking and ultimate load capacities but the reduction in the cracking and ultimate strength were higher than those of larger grading sizes. The grading size of recycled bricks affects the shear strength of deep beams when used as a partial alternative to coarse aggregates. By comparing the deep beams with different grading sizes, it is found that the beams with grading sizes of 19-20 mm led to a decrease in the cracking and

ultimate load by an average value of 13% and 33% while beams with less grading size of RB the reduction in the cracking load reduced hugely with 18.5% and 38.5%.

5) For the shear span to depth ratio effect, the influence of shear span to depth ratio for recycled concrete beams was significant the displacement of this beam varied hugely and the replacement of the one-point load to two-point load decreased the maximum displacement of 21.7%. For the recycled concrete deep beams, the cracking and ultimate load showed a variation of (3-7%) only. The displacement of these beams was different and the displacement of one point load was 16%.
6) Regarding energy absorption, the concrete deep beam was affected by the replacement ratio of recycled bricks, and a higher drop in energy absorption was observed. The control beam has a higher energy than the recycled bricks concrete beams which is reduced after the addition of recycled bricks into the concrete mixture with (14.4% and 48.1%). The Deep beams with smaller grading sizes (GB-5, and GB-10) offered less energy absorption when compared with beams GA- series beams. which the energy absorption reduction value was (20%, and 40.2%) respectively.
7) Normal concrete deep beam has higher ductility than recycled brick concrete beams which the CBA deep beams characterized by less ductility. The ductility index of beams made with recycled bricks concrete revealed a decrease in ductility (9.5%) when compared with the conventional concrete beam. The Deep beams with smaller grading sizes offered higher ductility when compared with conventional concrete beams. Comparing the deep beams with two-point loads opposite them (two-point load) demonstrated that the ductility increased by 31.6% for the normal concrete deep beams and this ductility decreased by 14.4% and 34.5% when the replacement ratio increased to 5% and 10% respectively.

6.2 Recommendation for Future Works

Extra investigation to understand the basic behavior of RC deep beams is required. The following suggestions are recommended:

1) Studying the seismic behavior of deep beams with different proportion of crushed bricks.
2) Shear behavior of deep beams under cyclic loading.

APPENDIX: FINITE ELEMENT MODELING

A. Stress strain relationship

For the concrete modeling, the stress strain curves were defined according to the ACI code 318 M-19 [45]. Figure A1 and Tables A1, A2, and A3 illustrate the stress strain curve of the normal and recycled bricks concrete with different replacement ratio that used in the simulation of the concrete deep beams. It should be noted that used mixtures were the recycled bricks concrete treated with HCL (B-CBAC-HCL).

Table A 1 Stress strain values of normal strength concrete with compressive strength of 54 MPa

Strain	Stress
0.0001	3.451319
0.00025	8.582294
0.0005	16.84385
0.00075	24.50268
0.001	31.34485
0.00125	37.23871
0.0015	42.13357
0.00175	46.04693
0.002	49.0459
0.0025	52.70442
0.0035	54.03333

Table A 2 Stress strain values of recycled bricks concrete with replacement ratio of 5% with compressive strength of 50.4 MPa.

Strain	Stress
0.0001	3.333017
0.00025	8.284934
0.0005	16.23852
0.00075	23.57215
0.001	30.07164
0.00125	35.61139
0.0015	40.15116
0.00175	43.72049
0.002	46.3976
0.0025	49.51036
0.0035	50.4

Table A 3 Stress strain values of recycled bricks concrete with replacement ratio of 10% with compressive strength of 43.33 MPa

Stress	Strain
3.089981	0.0001
7.673675	0.00025
14.99194	0.0005
21.65222	0.00075
27.44193	0.001
32.25174	0.00125
36.0668	0.0015
38.94403	0.00175
40.98532	0.002
43.05447	0.0025
43.33333	0.0035

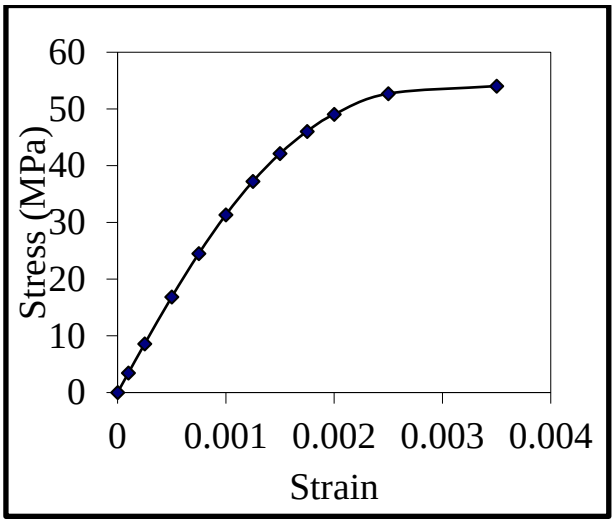

(a) NSC

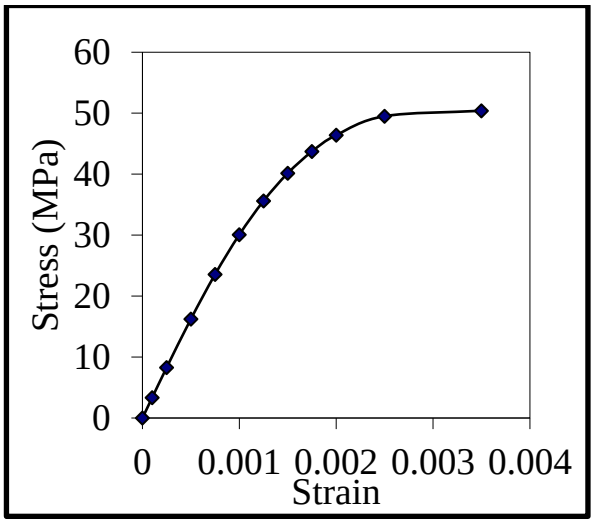

(b) Recycled bricks concrete (5%)

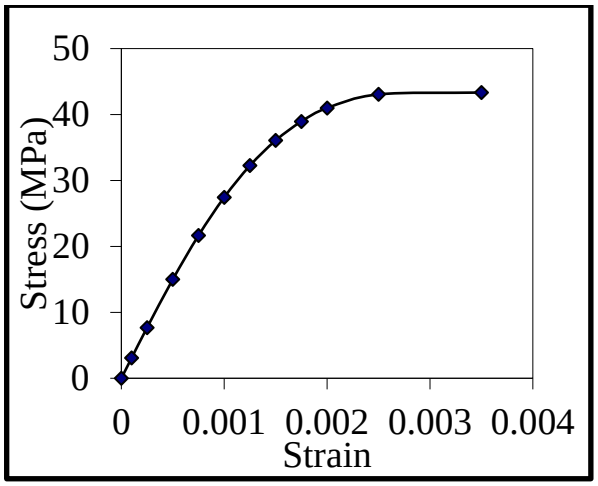

(c) Recycled bricks concrete (10%)

Figure A 1 Stress-Strain relationships of concrete deep beams.

REFERENCES

1) EPA, U. "Sustainable management of construction and demolition materials." (2017).
2) Movassaghi R., “Durability of Reinforced Concrete Incorporating Recycled Concrete as Aggregate (RCA)” M.Sc. Thesis, College of Engineering, University of Waterloo, Canada, 2006.
3) Jeffery S., and Kamal H. Khayat, (2014), "Recycled Concrete Aggregate (RCA) for Infrastructure Elements", Missouri University of Science and Technology.
4) Al-Musawi T. H. A. " Shear Strength of Indirectly Loaded Reinforced Concrete Beams Cast with Self-Compacting Concrete Containing Recycled Concrete as Coarse Aggregate", Ph.D. Thesis, Faculty of Engineering, University of Basrah, Nov., 2020.
5) Paul, s. C., babafemi, a. J., anggraini, v., & rahman, m. M. (2018). Properties of normal and recycled brick aggregates for production of medium range (25–30 mpa) structural strength concrete. Buildings, 8(5), 72.
6) Nixon pj. Recycled concrete as an aggregate for concrete – a review. 37-drc committee; 1976. P. 371–8.
7) Hasaba s et al. Drying shrinkage and durability of concrete made of recycled concrete aggregates. Jpn concrete int 1981;3:55–60.
8) Jeffery S., and Kamal H. Khayat, (2014), "Recycled Concrete Aggregate (RCA) for Infrastructure Elements", Missouri University of Science and Technology.
9) Revilla-Cuesta, V., Fiol, F., Perumal, P., Ortega-López, V., & Manso, J. M. (2022). Using recycled aggregate concrete at a precast-concrete plant: A multi-criteria company-oriented feasibility study. Journal of Cleaner Production, 373, 133873.

10) Teijón-López-Zuazo, E., Vega-Zamanillo, Á., Calzada-Pérez, M. Á., & Robles-Miguel, Á. (2020). Use of recycled aggregates made from construction and demolition waste in sustainable road base layers. Sustainability, 12(16), 6663.
11) Debieb, F., & Kenai, S. (2008). The use of coarse and fine crushed bricks as aggregate in concrete. Construction and building materials, 22(5), 886-893.
12) Khan, S. A. (2005). Evaluation of Mechanical Properties of Recycled Aggregate Concrete.
13) Yang, J., Du, Q., & Bao, Y. (2011). Concrete with recycled concrete aggregate and crushed clay bricks. Construction and Building Materials, 25(4), 1935-1945.
14) Kumar, N., Saxena, A. K., Soni, G., & Qureshi, F. Analysis of Concrete Made from Recycled Bricks, 2017.
15) Mohammed, T. U., Hasnat, A., Awal, M. A., & Bosunia, S. Z. (2015). Recycling of brick aggregate concrete as coarse aggregate. Journal of Materials in Civil Engineering, 27(7), B4014005.
16) Zhu, L., & Zhu, Z. (2020). Reuse of clay brick waste in mortar and concrete. Advances in Materials Science and Engineering, 2020.
17) Abbas, Z. K., & Abd, S. K. (2021). Study of using of recycled brick waste (RBW) to produce environmentally friendly concrete: A review. Journal of Engineering, 27(11), 1-14.
18) Monawar, A., & Alawi, M. H. (2021). Demolition waste of bricks as recycled aggregates in concrete mix and energy impact. Journal of Al-Azhar University Engineering Sector, 16(60), 495-504.
19) Rasheed, L. S., Ridha Mahmmod, L. M., Alaa Abed Alameer, S., & Thamer Abdulrasool, A. (2021). Behavior of concrete beams internally cured with clay brick waste. Pollack Periodica, 16(1), 32-37.

20) Janotka, I., Martauz, P., & Bačuvčík, M. (2021). Design of concrete made with recycled brick waste and its environmental performance. Minerals, 11(5), 463.
21) Ali, Y. M. (2022). Effect of silica fume on the behavior of lightweight RC beams made from crushed bricks.
22) Alam, M. A., & Ahmad, S. I. (2023). Experimental Torsional Capacity of Plain Concrete Beams Made from Crushed Clay Brick and Recycled Brick Concrete as Coarse Aggregate. Advances in Civil Engineering, 2023.
23) Fung-Kew Kong and SusantoTeng, "Web Reinforcement Effects on Lightweight Concrete Deep beams," Journal Proceedings, V. 68, PP. 514-520, 1971.
24) Fung-Kew Kong and SusantoTeng , "Effect of Embedment Length of Tension Reinforcement on the Behavior of Lightweight Concrete Deep Beams," Structural Journal, V. 93, PP. 21-29, 1996.
25) Keun-Hyeok Yang, "Tests on Lightweight Concrete Deep Beam," Structural Journal, V. 107, PP. 663-670,2010.
26) YasarHanifi Gedik and Hikaru Nakamura, "Evaluation of three-dimensional effects in short deep beams using a rigid-body-spring-mode," Department of Civil Engineering, Nagoya University, Chikusa-ku, Nagoya 464-8603, Japan, 2011.
27) Deewan, M. "Behavior of different types of reinforced concrete deep beams strengthened with CFRP sheets", thesis, university of Basra, 2012.
28) Khudhair, J. A., & Alhussein, T. H. (2020). Shear Strength of Directly and Indirectly Loaded Rectangular Self-Compacted Reinforced Concrete Deep Beams Containing Recycled Concrete as Coarse Aggregate. Anbar Journal of Engineering Sciences, 11(2).

29) Kachouh, N., El-Maaddawy, T., El-Hassan, H., & El-Ariss, B. (2022). Shear response of recycled aggregates concrete deep beams containing steel fibers and web openings. Sustainability, 14(2), 945.

30) Sagheer, A. M., & Tabsh, S. W. (2022). Shear Strength of Concrete Beams without Stirrups Made with Recycled Coarse Aggregate. Buildings, 13(1), 75.

31) ASTM C191-08. Standard test methods for time of setting of hydraulic cement by Vicat needle; 2008.

32) IQS 5/2019 “Iraqi Standards for portland cement, 2019.

33) ASTM. 2006. Standard Test Method for Sieve Analysis of Fine and Coarse Aggregates, ASTM C136, Annual Book of American Society for Testing Materials Standards, Vol. C 04.02.

34) ASTM C494/C494M-1999a, “Standard Specification for Chemical Admixtures for Concrete”, Vol. 4.2, 1999, 9p.

35) EFNARC. (2005). “The European Guidelines for Self-Compacting Concrete Specification, Production and Use.” English ed. Norfolk, UK: European Federation for Specialist Construction Chemicals and Concrete Systems.

36) ASTM A615/A615M-13, "Standard Specification of Deformed and Plain Carbon Steel Bars for Concrete Reinforcement", (ASTM A615M-13), ASTM International West Conshohocken. (2013).

37) ASTM C496/C496M-04, Standard Test Method for Splitting Tensile “Strength of Cylindrical Concrete Specimens, 2004, pp. 1-5.

38) ASTM C78-09, Standard Test Method for Flexural Strength of Concrete (Using Simple Beam with Third-Point Loading), 2009.
39) Dobrzański, L.A., Pusz, A., Nowak, A.J., and Górniak, M., "Application of FEM for Solving Various Issues in Material Engineering", Journal of Achievements in Materials and Manufacturing Engineering, Vol.42, Issue 12, pp.134-141, 2010,
40) Moaveni, S., "Finite Element Analysis Theory and Application with ANSYS", Prentice Hall, Upper Saddle River, New Jersey 07458, 1999.
41) Kwak, H., and Filippou, F.C., "Finite Element Analysis of Reinforced Concrete Structures Under Monotonic Load", Department of Civil Engineering / University of California / Berkeley / California, USA, Report No. UCB SEMM-90/14, November, 1990.
42) Wischers, G., "Application of Effects of Compressive Loads on Concrete", Betontechnische Berichte, No.2 and 3, Duesseldorf, Germany, 1978.
43) Zienkiewicz, O.C., "The Finite Element Method", 3rd Ed., McGraw-Hill Book Company, New York, 1977.
44) Guide to Quality Control and Testing of High-Strength Concrete Reported by ACI Committee 363.2R-92.
45) ACI CODE-318-19(22): Building Code Requirements for Structural Concrete and Commentary (Reapproved 2022)
46) Hsu, L.S., and Hsu, C.T.T., "Complete Stress-Strain Behaviour of High-Strength Concrete under Compression", Magazine of Concrete Research (ASCE Journal), Vol.46, No.169, pp.301-312, 1994.
47) Desayi, P., and Krishnan, S., "Equation for the Stress-Strain Curve of Concrete", Journal of the American Concrete Institute, Vol.61, No.3, pp.345-350, March, 1964.
48) Chen, W.F., "Plasticity in Reinforced Concrete", McGraw-Hill, 1982.
49) Rashid, Y.R., "Analysis of Prestress Concrete Pressure Vessels", Nuclear Engineering and Design, Vol.7, No.4, pp.334-344, 1968.

50) Hawileh, R.A., Rahman, A., and Tabatabai, H., "Nonlinear Finite Element Analysis and Modeling of Precast Hybrid Beam–Column Connection Subjected to Cyclic Loads", Applied Mathematical Modelling, Vol. 34, pp. 2562-2583, 2010.

51) Hawileh, R.A., Abdalla, J.A., and Tanarslan, M.H., "Modeling of Nonlinear Response of RC Shear Deficient T-Beam Subjected to Cyclic Loading", Computers and Concrete, Vol.10, No.4, pp. 413–428, 2012.

52) European Committee for Standardization (CEN), Eurocode 3, "Design of Steel Structures", Part 1.1: General Rules and Rules for Building, DD ENV, EC3, 1993.

53) Padmarajaiah, S.K., and Ramaswamy, A.A., "Finite Element Assessment of Flexural Strength of Prestressed Concrete Beams with Fiber Reinforcement", Cement Concrete Composite, Vol.41, pp.24-229, 2002.

54) Al-Sahlawi, Y.M.Y., "Strengthening of Self Compacting Reinforced Concrete T-Deep Beams with Opening by CFRP Sheet", M.Sc. Thesis, College of Engineering, University of Kufa, Iraq, 2018.

55) Wolanski, A.J., "Flexural Behavior of Reinforced and Prestressed Concrete Beams Using Finite Element Analysis", M.Sc. Thesis, University of Marquette, 2004.

56) Kachlakev, D., Miller, T., Yim. S., Chansawat, K., Potisuk, T., "Finite Element Modeling of Reinforced Concrete Structures Strengthened with FRP Laminates", Report SPR 316, California Polytechnic State University, San Luis Obispo, 2001.

57) ANSYS Manual, Version (13), USA, 2011.

58) Al-Tai, S., "Nonlinear behavior of Reinforced Concrete T- beam strengthened with CFRP subjected to shear", M.Sc. Thesis, College of Engineering, University of Babylon, 2007.

59) Banzant, Z.P., "Comment on Orthotropic Models for Concrete and Geomaterials", Journal of Engineering Mechanics Division, ASCE, Vol.106, No. 3, pp. 849-865, 1983.
60) Stolarski, T., Nakasone, Y., & Yoshimoto, S. (2018). Engineering analysis with ANSYS software. Butterworth-Heinemann.
61) M. J. Priestley and R. Park, "Strength and ductility of concrete bridge columns under seismic loading," *Structural Journal,* vol. 84, no. 1, pp. 61-76, 1987.
62) T. Sullivan, G. Calvi, and M. Priestley, "Initial stiffness versus secant stiffness in displacement-based design," in *13th World Conference of Earthquake Engineering (WCEE)*, 2004, vol. 65, no. 2888, pp. 581-626

الخلاصة

تقدم هذه الأطروحة تحرياً شاملاً في سلوك القص للعتبات الخرسانية المسلحة العميقة. تتناول الدراسة تأثير استخدام الطابوق المعاد تدويره مع الخرسانة العادية كبديل جزئي للركام الخشن. تم إجراء اختبارات تجريبية وعددية لتحليل العوامل المؤثرة على سلوك هذه العتبات عند الفشل. تم إجراء فحوص مختبرية على تسعة عتبات لمعرفة تأثير العوامل المختلفة على سلوك العتبات العميقة. تم تقسيم العينات التجريبية إلى ثلاث مجموعات من العتبات مصممة للفشل في القص مع استخدام متغيرات مختلفة. شملت المتغيرات الرئيسية نسبة الاستبدال للركام-الطابوق، وحجم التدرج، ونسبة المسافة بين مسافة القص إلى العمق الفعال (a/d). أظهرت نتائج التحليل ما يلي: بالنسبة للسلسلة الأولى، عندما زادت نسبة الاستبدال إلى 5٪ و 10٪، كان هناك انخفاض في كل من مقاومة العتبات للتشقق والمقاومة القصوى بنسبة 10.4٪ و 29.9٪ على التوالي. أشارت هذه النتائج إلى أنه مع زيادة نسبة الاستبدال، انخفضت مقاومة القص للعتبات. فيما يتعلق بالهطول ، قللت نسبة الاستبدال من الهطول حيث كان الانخفاض أعلى بالنسبة للعتبات بنسبة 10٪ استبدال أكثر من 5٪ لعدة أسباب مثل ضعف قوى الربط بين الطابوق المعاد تدويره والخرسانة ، وعدم التجانس بين مكونات الخلطة الخرسانية. بينما بالنسبة للعتبات ذات حجم التدرج الأقل للركام المعاد تدويره، انخفض مقاومة للتشقق بشكل كبير بنسبة 18.5٪ و 38.5٪ للعتبات بنسبة 5٪ و 10٪ من الطابوق المعاد تدويره . كان الانخفاض في المقاومة القصوى لنفس هذه العتبات 10.4٪ و 28.9٪ على التوالي. فيما يتعلق بتأثير نسبة مسافة القص إلى العمق الفعال ، فإن الانخفاض فيها (بالنسبة للحمل المسلط على نقطتين بدلاً من حمل ذو نقطة واحدة) لنفس حجم تدرج الطابوق المعاد تدويره أظهر أن مقاومة العتبة للتشقق تم تحسينه بشكل واضح. فيما يتعلق بالهطول فان هذه العتبات تأثرت بشكل كبير عند تغيير عدد نقاط التحميل والذي قلل الهطول من 6.23 ملم إلى 4.88 ملم بنسبة انخفاض قدرها 21.7٪.

الجزء الثاني تضمن التحليل العددي لسلوك العتبات العميقة على أساس النتائج المستخرجة من الجانب العملي . تم استخدام نتائج اختبار العتبات من التجارب العملية لمحاكاة العتبات العميقة نظريا. بالمقارنة مع التجارب المختبرية، فقد كانت منحنيات الحمل - الهطول للعينات العملية والنظرية متطابقة جدًا وفقًا لنتائج التحليل العددي. فيما يخص المتغيرات النظرية فان الدراسة النظرية تتكون من ثلاث مجموعات. المجموعة الأولى هي عتبات عميقة تم نمذجتها واختبارها تحت حمل على نقطة واحدة لمعرفة تأثير طبقات الخرسانة الحاوية على طابوق معاد تدويره على العتبات الخرسانية العميقة المصنوعة من الخرسانة العادية. استخدمت المجموعتان الثانية والثالثة عشرة عتبات عميقة لدراسة تأثير وجود الحديد العرضي من حيث المسافة بين قضبان الحديد. أظهرت النتائج العددية أن التسليح العرضي عزز من مقاومة العتبات الخرسانية

العميقة. زادت مقاومة القص العظمى بنسبة 39.6٪ و 27.46٪ و 21.2٪ مقارنة بالعتبة الخرسانية العميقة البسيطة. فيما يتعلق بالنماذج الأخرى فانه تم استخدام اسماك مختلفة للخرسانة الحاوية على طابوق معاد تدويره حيث اظهر تأثيراً واضحاً على مقاومة العتبات للقص وايضا على نسبة الهطول فيها حيث ادى الى انخفاض في مقاومة القص مقارنة بالعتبة الخرسانية العميقة العادية.

جمهورية العراق
وزارة التعليم العالي والبحث العلمي
كلية الهندسة/ جامعة ميسان
قسم الهندسة المدنية

مقاومة القص للعتبات الخرسانية العميقة باستخدام الطابوق المعاد تدويره كركام خشن

رسالة
مقدمة الى كلية الهندسة جامعة ميسان
كجزء من متطلبات نيل درجة الماجستير في الهندسة المدنية / الانشاءات

2024

من قبل
شمس الضحى داخل خلف
بكالوريوس علوم الهندسة المدنية، 2016

المشرف على الأطروحة: الاستاذ المساعد الدكتور سامر محمد جاسب